UNIVERSITY OF CALIFORNIA

Los Angeles

A transient microcircuit underlying critical period plasticity in the visual cortex

A dissertation submitted in partial satisfaction of the

requirements for the degree of Doctor of Philosophy

in Neuroscience

by

Courtney Yaeger

2018

ABSTRACT OF THE DISSERTATION

A transient microcircuit underlying critical period plasticity in the visual cortex

by

Courtney Yaeger

Doctor of Philosophy in Neuroscience

University of California, Los Angeles, 2018

Professor Joshua Trachtenberg, Chair

During so-called critical periods of early postnatal life, sensory experience profoundly and permanently sculpts cortical neural circuitry. After critical period closure, experience-dependent plasticity is dramatically limited, and it is not known what differentiates juvenile and adult plasticity mechanisms. At its core, plasticity is a dendritic phenomenon, and in the cortex, plasticity is determined by changes in sensory input and cortical state. Here we show that dendritic and somatic activity in pyramidal neurons is fundamentally different across critical period closure due to the cholinergic engagement of inhibitory circuitry. At the peak of the critical period, acetylcholine released from the basal forebrain directly excites somatostatin-expressing (SST) interneurons. The resultant inhibition of pyramidal cell dendrites and of fast-spiking, parvalbumin-expressing (PV) inhibitory neurons enhances branch-specific dendritic responses and increases somatic spiking within pyramidal neurons. By adulthood, SST cells lose

cholinergic excitability, and inhibition becomes inverted along the somatodendritic axis, with less SST-mediated dendritic inhibition and more PV-mediated somatic inhibition. When SST cells are optogenetically activated in adult cortex, branch-specific dendritic activity and somatic disinhibition re-emerge. Conversely, suppressing SST cell activity during the critical period prevents the normal development of binocular receptive fields by impairing the experience-dependent maturation of ipsilateral eye inputs. These data reveal a transient circuit through which inhibition and neuromodulation converge to facilitate experience-dependent plasticity by shaping dendritic and somatic activity.

The dissertation of Courtney Yaeger is approved.

Dean Buonomano

Peyman Golshani

Dario Ringach

Larry Zipursky

Joshua Trachtenberg, Committee Chair

University of California, Los Angeles

2018

TABLE OF CONTENTS

Chapter 6: Discussion

LIST OF FIGURES

ACKNOWLEDGEMENTS

None of this would have been possible without the constant support of my advisor and mentor, Dr. Josh Trachtenberg. Thank you for taking me on, teaching me the most cutting-edge methods of neuroscience, and giving me the freedom to explore and fail without judgment. Thank you for training me to “get buckets” and to be fearless in the pursuit of ground truth. Thank you for sharing your ability to see the big picture and recraft it if necessary. Thank you for being transparent about the realities of academic science and for helping me get my first KooKooRoo (or in the least, get it reviewed). Please put me on the waitlist for a Neurolabware microscope in the next ten years.

I am very grateful for my committee and my many other mentors at UCLA. Thank you, Dr. Larry Zipursky, for your grounding perspective (“You know, it doesn’t really matter what you do in grad school…”) and for convincing me I belonged by shaking my hand after my oral qualifying exam. Thank you, Dr. Peyman Golshani, for personally teaching me how to patch, for giving me limitless use of your electrophysiological rig and essentially adopting me into your own lab. Thank you, Dr. Dario Ringach, for showing me the secrets of Scanbox software and for all your help with visual stimuli, optogenetics, and the image processing pipeline. I am a much better programmer and scientist with your work as a reference. Thank you, Dr. Dean Buonomano, not only for your input on this research, your guidance on all things electrophysiology, and your comments on our manuscript, but also for many fun philosophical conversations along the way.

Several other people have been integral to my success in this program. Elaine Tring taught me almost every technique used in this manuscript, and I constantly aspire to attain her level of expertise and to be as good a teacher. I have truly loved being part of the Neural Microcircuits community and have enjoyed the mentorship and wisdom of Dr. Jack Feldman. Thank you, Jack, for investing in me and bringing me into a community that I have learned so much from. Dr. Nick Wisniewski, my statistics instructor and advisor, cares so much about

statistics that it is truly contagious, and his teachings and support have been endlessly valuable. And finally, I learned just as much from my peers as from the faculty above, which is why this program is so wonderful. Special thanks to: Dr. Maite Lazaro, Dr. Michael Einstein, Dr. Jason Moore, Dr. Hua Chai, Dr. Sophie Rengarajan, Dr. Jennifer Tribble, and (future Dr.) Janelle Liu.

To my family: my brother, who taught me to question everything but believe in myself; my sister, who showed me how to fearlessly go my own way; my mother, who instilled in me her love of learning and her grit; and my father, who constantly reminds me what really matters. To my grandfather, who approaches all challenges with humor and who imparted a “can-do” confidence (even if you don’t know what you’re doing) into our family; and to my grandmother, who showed me how to be generous with love and kindness and who was not able to finish her own Ph.D. This is for you.

This manuscript is an elongated version of work co-authored by myself, Dario Ringach, and Josh Trachtenberg. I conducted the experiments, Dario provided the algorithm used for deconvolution and receptive field analyses, and Josh and I analyzed the data and wrote the manuscript. This work was supported by NIH RO1 EY023871, NRSA F31 EY027196, and NRSA T32 NS0582.

VITA

Education

University of California, Los Angeles, expected 2018
Doctoral Candidate, Interdepartmental PhD Program in Neuroscience (NSIDP)

University of Illinois, Urbana-Champaign, 2013
B.S. Individual Plan of Study in Neuroscience

Research Experience

2014-2018 Graduate Student Researcher, UCLA, with Dr. Joshua Trachtenberg
Investigation of cortical circuitry and plasticity across development, using methods in calcium imaging, electrophysiology, optogenetics, and pharmacology.

2011-2013 Research Assistant, University of Illinois, with Dr. Justin Rhodes
Study of neural anatomy, activation, and hormonal release in clownfish during social sex change.

Publications

(2019) **Yaeger, C.E.,** Ringach, D.L., and Trachtenberg, J.T. "A developmentally-restricted inhibitory circuit controlling localized dendritic spiking and critical period plasticity." Under review.

2014 **Yaeger, C.**, Ros, A.M., Cross, V., DeAngelis, R.S., Stobaugh, D.J., and Rhodes, J.S. "Arginine vasotocin signaling is required for behavioral dominance and induction of c-Fos protein in the preoptic area and ventral tegmental area in male *Amphiprion ocellaris*." *Neuroscience*, 267, 205–218.

Grants

2016 Predoctoral Ruth L. Kirschstein National Research Service Award (NRSA): "Enhancing Dendritic Inhibition for the Control of Critical Period Plasticity." F31 EY027196.

2015 NINDS/NIH Training Program for Neural Microcircuits, UCLA: T32-NS058280.

Presentations

Selected oral presentations:

2017 Invited Speaker, 11th Annual Dynamics of Neural Microcircuits Symposium, UCLA: "Inversion of an inhibitory microcircuit at critical period closure."

2017 Selected Speaker, Gordon Research Seminar & Conference on Dendrites: Molecules, Structure, and Function, Lucca, Italy: "Optically probing dendritic inhibition during the visual critical period."

2016 Data Blitz, Neuroscience Interdisciplinary Program Retreat. "How are neural circuits modulated to induce experience-dependent plasticity?"

Selected poster presentations:

2018 Poster Presentation, 12th Annual Dynamics of Neural Microcircuits Symposium, UCLA: **C.E. Yaeger**, D.L. Ringach, and J.T. Trachtenberg. “V1 pyramidal neurons lose dendritic inhibition and somatic disinhibition across critical period closure.”

2016 Poster Presentation, Society for Neuroscience, San Diego: **C.E. Yaeger** and J.T. Trachtenberg. “Cholinergic modulation of an inhibitory microcircuit changes dendritic integration after the visual critical period."

2016 Poster Presentation, 10th Annual Dynamics of Neural Microcircuits Symposium, UCLA: **C.E. Yaeger** and J.T. Trachtenberg. “An inhibitory microcircuit for altering dendritic encoding during the visual critical period.”

2015 Poster Presentation, Society for Neuroscience, Chicago: **C.E. Yaeger**, D.L. Ringach, and J.T. Trachtenberg. “Somatostatin-expressing interneurons in primary visual cortex undergo a developmental switch in neuromodulated excitation.”

Honors and Awards

2014-2018 Achievement Rewards for College Scientists (ARCS) Foundation Award

2016 Best Data Blitz Presentation, NSIDP Retreat

2015 Brain Research Institute Neuroscience Graduate Travel Award

Teaching Experience

Winter, Spring 2015 Teaching Assistant, Lecturer, and Coordinator. Neuroscience 192B: Project Brainstorm, Dr. Ellen Carpenter, Program in Neuroscience

Academic and Community Service

2018 Speaker, public lecture for Brain Power Hub: “The art and science of empathy.”

2017 Volunteer Lab Instructor, UCLA STEM and Fulfillment Fund

2017 Representative, NSIDP Admissions Committee

2016 Speaker, public lecture for Gil’s Sanctuary: “Meeting of the minds: Intersections of art and neuroscience.”

2016 Representative, NSIDP Committee for Curricular Reform

2015 Volunteer, AWiSE EmpowHER STEM Day

2015 Director, UCLA Brain Awareness Week

2015 Mentor, NSIDP Graduate Student Mentoring Program

2015 Contributor, Survive Grad School Essay Project: “Working the Grind in Graduate School: Lessons from a Big Ten Athlete.”

2014 Volunteer, UCLA Exploring Your Universe and Brain Awareness Week

Professional Memberships

Society for Neuroscience (SFN)

UCLA Advancing Women in Science and Engineering (AWiSE)

Chapter 1: Introduction

1.1 Overview

The first postnatal experiences of the conscious cortex dictate the refinement of its final wiring diagram. This time in development forms a “critical period,” because sensory input alone drives the organization of cortical circuitry. It is during this time that passive sensory experience has its largest impact on plasticity. In adulthood, experience-dependent plasticity depends on present stimuli, the context in which they are experienced, and past associations. Sensory experience no longer has the same impact as in development, and adult plasticity is incremental and rapidly reversible in comparison. Understanding the mechanism of critical period plasticity and its closure is a long-standing and unresolved issue in neuroscience.

While it is impossible to overlook the importance of sensory input to the developing cortex, cortical activity is also determined by cortical state (Ringach, 2009). The balance between bottom-up input and top-down modulation dictates the potential for plasticity. The opening of the critical period requires the development and innervation of inhibitory interneurons (Chattopadhyaya et al., 2004; M Fagiolini & Hensch, 2000; Hanover, Huang, Tonegawa, & Stryker, 1999; Lazarus & Huang, 2011) as well as neuromodulatory input (Bear & Singer, 1986; Kasamatsu & Pettigrew, 1976; Kuppermann & Kasamatsu, 1984). It is unknown how inhibition and neuromodulation interact to engage sensory-dependent plasticity, nor how these conditions change with maturation. This thesis aims to advance our understanding of how inhibition and neuromodulation contribute to a biophysical plasticity mechanism specific to the critical period.

1.2 Elevated sensory-dependent plasticity in the developing visual cortex

In the 1960s, Hubel and Wiesel discovered and defined a critical period for the development of the visual system, in which unilateral deprivation of an eye caused permanent damage (Hubel & Wiesel, 1970; Wiesel & Hubel, 1963). By studying kittens deprived of visual

experience in one eye, Hubel and Wiesel found that brief deprivation permanently shifted functional properties of neurons in primary visual cortex (V1) to favor the remaining eye. In contrast, adult responses were impervious to brief deprivation, and the same protocol did not produce an ocular dominance shift. These breakthroughs led to an understanding that visual experience instructs the balance of ipsilateral and contralateral inputs for binocular vision. Hubel and Wiesel's monocular deprivation procedure became the paradigm for understanding the physiological underpinnings of juvenile sensory-dependent plasticity. Among other experience-dependent outcomes of the critical period in mouse V1, here we will focus exclusively on the development of the binocular zone.

Despite anatomical differences from cats and monkeys, the mouse visual system has been useful for elucidating the mechanisms of binocular development. In mice, the critical period for ocular dominance occurs between postnatal day 19 (P19) and 32 (P32), in which 4 days of monocular deprivation produces the largest loss of responses to the deprived eye (Gordon & Stryker, 1996; but see Smith & Trachtenberg, 2007). The critical period for ocular dominance closes gradually; as the animal matures, longer and longer periods of deprivation are needed to produce a shift in neuronal activity, and these shifts are not as pronounced (Lehmann & Löwel, 2008).

At eye opening (approximately P14), thalamocortical inputs are already in place (Cang et al., 2005; Crowley & Katz, 1999; Godement, Salaün, & Imbert, 1984), but differ in strength. Contralateral inputs strongly innervate the cortex, but ipsilateral inputs are significantly weaker. Visual experience drives the balance between these two inputs by maintaining the strength of the contralateral eye and strengthening the ipsilateral input (Crair, Gillespie, & Stryker, 1998). Monocular deprivation degrades the response of the deprived eye, but changes in cortical response depend on which eye has been deprived. Ipsilateral deprivation at the peak of the critical period has no immediate effect on the contralateral input, but longer periods of deprivation eventually degrade contralateral inputs (Crair et al., 1998; Antonini, Fagiolini, &

Stryker, 1999). In contrast, when the contralateral eye is deprived, the ipsilateral inputs strengthen and gain cortical territory (Faguet, Maranhao, Smith, & Trachtenberg, 2009). These findings collectively suggest that the contralateral input develops almost entirely without visual experience, while the ipsilateral input depends on it. The presence of the stronger contralateral input provides resistance to the development of the ipsilateral input, but eventually the two inputs are matched in strength. Therefore, competitive plasticity and maintenance are crucial components of a potential plasticity mechanism.

The main limitation of deprivation studies is that it does not necessarily reflect plasticity mechanisms involved during normal development. Monocular deprivation of the contralateral eye eliminates the competition for the ipsilateral input, allowing it to strengthen to a larger degree than in typically developing mice (Faguet et al., 2009). After eye-opening in normal development, thalamic drive is constant between the two eyes, yet the ipsilateral input is selectively strengthened. One measureable outcome of regular visual input is binocular matching, in which the contralateral and ipsilateral inputs drive the same orientation preference in their shared target. During the critical period, a significant proportion of binocular neurons gain matched orientation preferences between P21 and P28 (B.-S. Wang, Sarnaik, & Cang, 2010). Because critical period plasticity is synonymous with experience, there must be distinct features of cortical processing that distinguish the juvenile from the adult. How normal experience drives cortical circuitry to achieve binocular matching is not understood.

1.3 Inhibition is necessary for critical period plasticity

In the early search for factors that regulate critical periods, the predominant hypothesis was that plasticity incurred because of mismatched inhibition and excitation. Manipulations of brain-derived neurotropic factor (BDNF) --an activity-dependent growth factor involved in synapse formation and plasticity-- led to the discovery that the critical period opens with the advent of GABAergic inhibition and innervation. BDNF overexpression induces a precocious

critical period for ocular dominance, in which the critical period opens and then closes at earlier time points (Hanover et al., 1999; Z J Huang et al., 1999). Similarly, mice lacking GABA-synthesizing enzyme GAD65 do not show ocular dominance changes with monocular deprivation unless rescued by the administration of a GABA-A receptor agonist (Hensch et al., 1998). Other genetic and pharmacological manipulations of GABA can induce or delay the critical period (M Fagiolini & Hensch, 2000; Z Josh Huang, 2009).

To understand how inhibition shapes plasticity rules of excitatory cells, it is imperative to understand the physiology, connectivity, and engagement of GABAergic circuitry. Neurons that express GABA make up approximately 10-20% of rodent neocortical neurons and are incredibly diverse across species, brain regions, and layers (Tremblay, Lee, & Rudy, 2016). Cortical inhibitory interneurons project locally within and across cortical columns, target specific neuronal compartments, and receive excitatory and inhibitory synapses (Markram et al., 2004). Nearly 100% of GABAergic interneurons can be classified into three genetically distinct groups (Rudy, Fishell, Lee, & Hjerling-Leffler, 2011): cells expressing the calcium-binding protein parvalbumin (PV), cells expressing the neuropeptide somatostatin (SST), and cells expressing serotonin receptor 5HT3a. Although these markers distinguish non-overlapping groups, interneurons within these classes are diverse genetically, morphologically, and physiologically.

PV cells make up the largest population of cortical inhibitory interneurons at approximately 40% of all GABAergic neurons (Rudy et al., 2011). Many, but not all, PV interneurons are fast-spiking (B Cauli et al., 1997; Kawaguchi & Kubota, 1997; Markram et al., 2004; Petilla Interneuron Nomenclature Group et al., 2008; X. Xu & Callaway, 2009), firing action potentials at high frequencies with little spike frequency adaptation and large, fast afterhyperpolarizations. PV cells have remarkably fast signaling, from the receipt of excitation to their postsynaptic target (Pouille & Scanziani, 2001). These fast synaptic responses are attributed to low input resistance and fast membrane time constants (B Cauli et al., 1997; Connors & Gutnick, 1990; Gibson, Beierlein, & Connors, 1999; Kawaguchi & Kubota, 1997). PV

cells generally target the soma and proximal dendrites or the axon initial segment of excitatory neurons (Kawaguchi & Kubota, 1997; Petilla Interneuron Nomenclature Group et al., 2008). Collectively, these properties allow PV cells to provide reliable and precise inhibition near sites of action potential generation on pyramidal neurons. PV cells also receive excitatory input from pyramidal neurons (Avermann, Tomm, Mateo, Gerstner, & Petersen, 2012; Hofer et al., 2011; Holmgren, Harkany, Svennenfors, & Zilberter, 2003; Pala & Petersen, 2015) and strongly inhibit other PV interneurons (Pfeffer, Xue, He, Huang, & Scanziani, 2013). Thus, PV cells are in a powerful position to control spiking output and timing across populations of excitatory neurons (Cobb, Buhl, Halasy, Paulsen, & Somogyi, 1995; Miles, Tóth, Gulyás, Hájos, & Freund, 1996; Royer et al., 2012; Tamás, Buhl, & Somogyi, 1997). Both pyramidal and PV cells receive thalamocortical input, forming a disynaptic feedforward inhibitory circuit motif found throughout the cortex (Kloc & Maffei, 2014; Tremblay et al., 2016). Circuitry with PV-mediated inhibition is involved in feature selectivity (Runyan et al., 2010), gain modulation (Atallah, Bruns, Carandini, & Scanziani, 2012), and generating network oscillations (Bartos, Vida, & Jonas, 2007).

During development, PV cells arise from the medial ganglionic eminence and migrate into the cortex at approximately P13 (Butt et al., 2005; Gonchar, Wang, & Burkhalter, 2007; Q. Xu, Cobos, De La Cruz, Rubenstein, & Anderson, 2004). Physiologically, PV interneurons show mature electrical properties at the beginning of the critical period at P21 (Lazarus & Huang, 2011), similar to pyramidal neurons (McCormick & Prince, 1987). Perisomatic innervation of pyramidal neurons is apparent at eye opening, but gradually increases to mature innervation by P30 (Chattopadhyaya et al., 2004). PV interneurons target the soma and proximal dendrites of pyramidal cells and other PV interneurons at the GABA-A α1 subunit (Klausberger, Roberts, & Somogyi, 2002). Blockade of the α1 subunit prevents ocular dominance from occurring (Michela Fagiolini et al., 2004), but this receptor is also found on PV interneurons and other GABAergic interneuron populations (Bacci, Rudolph, Huguenard, & Prince, 2003; Ferando & Mody, 2014). Counterintuitively, it seems that while PV innervation is increasing, plasticity incurs with

decreased PV inhibition. After one day of monocular deprivation, pyramidal cell activity increases due to a drop in PV-mediated inhibition and a lack of excitatory drive from layer 4 (Kuhlman et al., 2013). Collectively, these findings suggest that disinhibition of pyramidal neurons invokes ocular dominance plasticity. However, it has yet to be shown if a disinhibitory circuit is engaged during normal visual experience to facilitate experience-dependent plasticity in a typically developing animal.

In contrast to somatic inhibition, the role of dendritic inhibition is unknown with respect to critical period plasticity. The bulk of plasticity occurs along the dendrites of pyramidal neurons, which are targeted by SST-expressing inhibitory interneurons (Kawaguchi & Kubota, 1997; Miles et al., 1996; Tamás et al., 1997; Y. Wang et al., 2004). While SST cells have more diverse waveforms than PV cells, the unifying characteristic of SST cells is their facilitation by incoming excitatory inputs (Beierlein, Gibson, & Connors, 2003; Kapfer, Glickfeld, Atallah, & Scanziani, 2007; Reyes et al., 1998; Silberberg & Markram, 2007; H. Xu, Jeong, Tremblay, & Rudy, 2013). SST cells also tend to have a low threshold for action potential generation and spike frequency adaptation (Gibson et al., 1999; Kawaguchi & Kubota, 1996). These properties allow SST cells to be recruited easily by excitation (Kapfer et al., 2007). Their reciprocal connectivity to pyramidal neurons drives feedback inhibition (Silberberg & Markram, 2007) via suppression of dendritic Ca^{2+} spikes in neighboring pyramidal cells (Royer et al., 2012). This circuitry is needed for surround suppression, a property which modulates the size tuning of a neuron by suppressing its response in the context of larger, widespread stimuli (Adesnik, Bruns, Taniguchi, Huang, & Scanziani, 2012). In addition to pyramidal cell dendrites, SST cells strongly inhibit all other cell types but do not inhibit each other (Pfeffer et al., 2013). Thus, SST cells are positioned favorably to selectively gate inputs within dendrites, as well as disinhibit pyramidal cell somas through the inhibition of PV cells (Cottam, Smith, & Häusser, 2013).

In addition to their morphology and physiology, SST cells show several interesting developmental changes which suggest they play a role in critical period plasticity. SST cells

migrate into the cortex from the medial ganglionic eminence and are detectable in the cortical layers at P0 (Gonchar et al., 2007). Interestingly, there is a transient increase in a subset of SST cells during the critical period, and the population decreases after critical period closure (Cavanagh & Parnavelas, 1988; Gonchar et al., 2007). Physiologically, SST cells show a gradual increase in excitability from eye opening throughout the critical period, caused by a significant increase in membrane resistance and slightly higher resting membrane potential. They also have a significant drop in decay dynamics which would increase the time of integration (Lazarus & Huang, 2011). Altogether, these properties suggest that dendritic inhibition is strongly engaged after the onset of the critical period. The role of SST-mediated inhibition during the critical period is unexplored, and it remains an outstanding question whether and how dendritic inhibition alters plasticity rules during development.

The third major class of inhibitory interneurons, 5HT3a-expressing cells, is more diverse than PV and SST-expressing groups and is poorly understood (Tremblay et al., 2016). The defining feature of this class is a fast ionotropic response to serotonin and acetylcholine (Alitto & Dan, 2012; Arroyo, Bennett, Aziz, Brown, & Hestrin, 2012; Férézou et al., 2002; SooHyun Lee, Hjerling-Leffler, Zagha, Fishell, & Rudy, 2010). 5HT3a interneurons make up the vast majority of cells in cortical layer 1 and are targets of long-range cortico-cortical inputs. 40% of 5HT3a neurons contain vasoactive intestinal peptide (VIP), a marker which is not found in any other interneuron group (Kawaguchi & Kubota, 1996; Rudy et al., 2011; X. Xu & Callaway, 2009). In contrast to the other main inhibitory groups, VIP interneurons originate from the caudal ganglionic eminence. Their unifying biophysical property is their high input resistance, which makes them very excitable (Bruno Cauli, Zhou, Tricoire, Toussay, & Staiger, 2014; SooHyun Lee et al., 2010; Prönneke et al., 2015) . VIP interneurons in layer 2/3 have the majority of their dendrites in layer 1 (Prönneke et al., 2015) and are thought to contribute to top-down processing due to their strong modulation by basal forebrain afferents (Alitto & Dan, 2012; Zhang et al., 2014). VIP interneurons also participate in disinhibitory motifs because they inhibit

most other cell types (Dávid, Schleicher, Zuschratter, & Staiger, 2007; Garcia-Junco-Clemente et al., 2017; Karnani et al., 2016; Pfeffer et al., 2013). VIP-mediated inhibition of SST cells has been shown in many sensory cortical regions (Fu et al., 2014; Soohyun Lee, Kruglikov, Huang, Fishell, & Rudy, 2013; Pi et al., 2013; Zhang et al., 2014). These interneurons have not been studied in the context of development and their role in critical period plasticity is unknown.

1.4 Neuromodulation drives cortical state and plasticity

Assuming visual experience is stable after eye-opening, what makes sensory input an especially salient feature during development? In addition to sensory input, neural responses depend on cortical state, or endogenous activity which fluctuates as a function of arousal (Ringach, 2009). Cortical state exists on a continuum, in which the extremes are synchronized or desynchronized population activity (Harris & Thiele, 2011). Here we will focus on the cholinergic system, which is heavily (although not exclusively) involved in controlling cortical state during wakefulness and other behavioral states such as arousal, attention, and plasticity (S.-H. Lee & Dan, 2012). The basal forebrain is the primary source of cortical acetylcholine and sends long-range projections to the cortex (Do et al., 2016). Cholinergic release occurs in a task-dependent manner on multiple timescales (Laplante, Morin, Quirion, & Vaucher, 2005; Parikh, Kozak, Martinez, & Sarter, 2007). Cholinergic drive acts as a salience cue: repeatedly pairing basal forebrain stimulation with a sensory input causes receptive field plasticity, in which neurons shift their response to favor the overrepresented input (Bakin & Weinberger, 1996; Froemke, Merzenich, & Schreiner, 2007; Kilgard & Merzenich, 1998). Because the basal forebrain innervates many structures, stimulation of the basal forebrain *in vivo* produces multiple effects: in the visual cortex, decorrelation occurs as a result of muscarinic receptor activation, and response reliability increases due to indirect modulation of thalamic firing (Goard & Dan, 2009; Pinto et al., 2013).

In terms of cell-specific modulation *in vivo*, acetylcholine has diffuse effects.

Interneurons in layer 1 (typically non-VIP cells) express nicotinic responses and have fast ionic responses to acetylcholine. VIP interneurons also respond robustly to acetylcholine and express both muscarinic and nicotinic receptors. All other major cell types, however, have complex responses to cholinergic release, and reports have been contradictory. For example, in acute slices, SST cells respond directly to acetylcholine, via nicotinic and muscarinic receptors (Chen, Sugihara, & Sur, 2015; Fanselow, Richardson, & Connors, 2008; Kawaguchi, 1997). But *in vivo*, SST cells have been shown to be non-responsive during basal forebrain stimulation (Alitto & Dan, 2012). Locomotion triggers basal forebrain activation (A. M. Lee et al., 2014), and there are opposing reports that SST cells increase or decrease their activity during running (Fu, Kaneko, Tang, Alvarez-Buylla, & Stryker, 2015; Polack, Friedman, & Golshani, 2013). Most likely, there are two or more groups of SST cells that differentially respond during cholinergic release, as shown by Reimer, et al (Reimer et al., 2014). PV cells, on the other hand, do not respond directly to acetylcholine (Kawaguchi, 1997; Kruglikov & Rudy, 2008), and in the visual cortex, their activity is driven by indirect effects during basal forebrain stimulation, producing PV-positive and PV-negative response groups (Alitto & Dan, 2012). PYR cells have a slow muscarinic depolarization to acetylcholine in acute slices (McCormick & Prince, 1985; but see Hedrick & Waters, 2015). *In vivo*, pyramidal responses are largely driven through an increase in glutamate, presumably from thalamocortical inputs (Alitto & Dan, 2012; Goard & Dan, 2009). Overall, the level of cholinergic release will differentially activate nicotinic and muscarinic receptors across these cell types and regions, creating a dynamic range of network modulation.

During early postnatal development, cholinergic fibers innervate the cortex steadily after birth (Dori & Parnavelas, 1989; Eckenstein & Baughman, 1984). Experience-dependent plasticity during the critical period requires basal forebrain activity, in which depletion of acetylcholine mutes the effect of monocular deprivation (Baskerville, Schweitzer, & Herron, 1997; Bear & Singer, 1986). It has also been suggested that a transmembrane nicotinic receptor inhibitor is upregulated around the closure of the critical period (Morishita, Miwa, Heintz, &

Hensch, 2010), but it is not clear which cell types are affected. The functional contribution of the cholinergic system to a critical period plasticity mechanism remains to be discovered.

1.5 Plasticity as a dendritic phenomenon, influenced by inhibition and modulation

While inhibition and neuromodulation shape cortical activity, it is unclear how these factors inform plasticity rules and contribute to a biophysical mechanism specific to the critical period. Hebbian-based thinking has dominated plasticity models, in which synaptic potentiation or depression is caused by the temporal relationship of pre- and post-synaptic spikes. Hebbian models are often employed to explain plasticity following monocular deprivation, in which the decorrelation of thalamocortical inputs from both eyes would lead to synaptic depression (Espinosa & Stryker, 2012). However, elegant experimental studies on the recovery from monocular deprivation have shown that weak inputs can still reintegrate even when decorrelated from existing inputs (Malach & Van Sluyters, 1989), and that recovery occurs in the near absence of somatic spiking (Mioche & Singer, 1989). It is additionally unclear how a Hebbian model alone could explain observations of the normally developing visual cortex, in which thalamic activity is constant and the weaker ipsilateral input is strengthened while the contralateral input is refined and maintained (Crair et al., 1998).

Recent experimental evidence emphasizes the role of postsynaptic dendritic spikes in instructing synaptic plasticity in the absence of somatic spiking (Bittner, Milstein, Grienberger, Romani, & Magee, 2017; Gambino et al., 2014; Golding, Staff, & Spruston, 2002; Kampa, Letzkus, & Stuart, 2006). Dendrites have active properties and form functionally distinct compartments from the soma (Branco & Häusser, 2010; Kerlin et al., 2018; Poirazi, Brannon, & Mel, 2003; Polsky, Mel, & Schiller, 2004; Wei et al., 2001). Dendritic spikes propagate poorly toward the soma, and somatic spikes do not necessarily backpropagate effectively into the dendritic tuft (Matthew Evan Larkum, Waters, Sakmann, & Helmchen, 2007; Sandler, Shulman, & Schiller, 2016; Schiller, Schiller, Stuart, & Sakmann, 1997; Spruston, 2008). Plasticity within

dendritic compartments could conceivably facilitate the integration of weak inputs in the developing visual cortex. Additionally, while dendritic spiking alone can drive plasticity, how well dendritic spikes and backpropagations coordinate can have profound effects on plasticity rules; for example, the interaction of dendritic spikes with somatic backpropagations within a small time window drives bursts of action potentials (M E Larkum, Zhu, & Sakmann, 1999).

What kind of dendritic activity differentiates the plasticity of the critical period from adulthood? Given that the critical period correlates with GABAergic innervation, dendritic inhibition likely contributes to a critical period plasticity mechanism. Inhibition onto dendritic compartments can alter thresholds for plasticity in at least three ways: first, by quenching synaptic activity in close proximity to the site of input; second, both distal and proximal sites of inhibition along the dendritic shaft can suppress signal propagation; and third, dendritic inhibition can decouple dendritic activity from somatic output (Bloss et al., 2016; Gidon & Segev, 2012). Dendritic inhibition can block spike generation (Larkum, Zhu, & Sakmann, 1999) but also has more nuanced effects, such as modulating the slope and threshold of dendritic activity to match behavioral context (Murayama et al., 2009). During task-specific behavior, compartmentalized Ca^{2+} currents emerge (Kerlin et al., 2018), and localized, branch-specific potentiation during learning is dependent on dendritic inhibition from SST cells (Cichon & Gan, 2015). For the critical period, an intriguing question is if compartmentalized dendritic activity emerges during simple visual experience in the juvenile but not in the adult. SST-mediated inhibition may play a role in shaping plasticity rules to invoke plasticity during the critical period.

Far less is known about the effects of neuromodulation on dendritic processing and plasticity mechanisms. In hippocampal acute slices, acetylcholine boosts back propagations into specific dendritic compartments, fostering branch-specific plasticity (Losonczy, Makara, & Magee, 2008). Cholinergic input can also drive disinhibition via inhibitory circuitry (Froemke et al., 2007; Letzkus et al., 2011). Cholinergic activity may provide the salience needed for visual input to have profound effects on circuit formation, and in combination with inhibition, these

components can determine plasticity rules. It remains an ongoing challenge to understand dendritic and somatic activity and their modulation during developmental plasticity.

1.6 Hypothesis and overview

The development of the visual system provides a well-studied foundation for understanding experience-dependent plasticity across the lifespan. We hypothesized that changes in neuromodulation and inhibition underlie the difference between juvenile and adult plasticity. Given that sensory input is constant across maturation but is the primary driver of plasticity only during the critical period, we predicted that the critical period would have distinct functional circuitry observable during normal visual experience. Here we studied the modulation of all major cortical cell types in V1, layer 2/3 during evoked activity at the peak of the critical period and following its closure. Specifically, we wondered if dendritic inhibition and modulation would converge to drive binocular matching, the primary outcome of the critical period in visual cortex.

Chapter 2 contains methods used throughout this thesis. In Chapter 3, the cholinergic modulation of inhibitory interneurons is compared across two developmental time points. In Chapter 4, we investigate the role of inhibition and neuromodulation on dendritic and somatic activity of pyramidal neurons. In Chapter 5, we test SST-mediated inhibitory drive for involvement in binocular matching. Chapter 6 is a discussion of these findings.

1.7 References

Adesnik, H., Bruns, W., Taniguchi, H., Huang, Z. J., & Scanziani, M. (2012). A neural circuit for spatial summation in visual cortex. *Nature*, *490*(7419), 226–231. doi:10.1038/nature11526

Alitto, H. J., & Dan, Y. (2012). Cell-type-specific modulation of neocortical activity by basal forebrain input. *Frontiers in Systems Neuroscience*, *6*, 79. doi:10.3389/fnsys.2012.00079

Antonini, A., Fagiolini, M., & Stryker, M. P. (1999). Anatomical correlates of functional plasticity in mouse visual cortex. *The Journal of Neuroscience*, *19*(11), 4388–4406.

Arroyo, S., Bennett, C., Aziz, D., Brown, S. P., & Hestrin, S. (2012). Prolonged disynaptic inhibition in the cortex mediated by slow, non-α7 nicotinic excitation of a specific subset of cortical interneurons. *The Journal of Neuroscience*, *32*(11), 3859–3864. doi:10.1523/JNEUROSCI.0115-12.2012

Atallah, B. V., Bruns, W., Carandini, M., & Scanziani, M. (2012). Parvalbumin-expressing interneurons linearly transform cortical responses to visual stimuli. *Neuron*, *73*(1), 159–170. doi:10.1016/j.neuron.2011.12.013

Avermann, M., Tomm, C., Mateo, C., Gerstner, W., & Petersen, C. C. H. (2012). Microcircuits of excitatory and inhibitory neurons in layer 2/3 of mouse barrel cortex. *Journal of Neurophysiology*, *107*(11), 3116–3134. doi:10.1152/jn.00917.2011

Bacci, A., Rudolph, U., Huguenard, J. R., & Prince, D. A. (2003). Major differences in inhibitory synaptic transmission onto two neocortical interneuron subclasses. *The Journal of Neuroscience*, *23*(29), 9664–9674.

Bakin, J. S., & Weinberger, N. M. (1996). Induction of a physiological memory in the cerebral cortex by stimulation of the nucleus basalis. *Proceedings of the National Academy of Sciences of the United States of America*, *93*(20), 11219–11224.

Bartos, M., Vida, I., & Jonas, P. (2007). Synaptic mechanisms of synchronized gamma oscillations in inhibitory interneuron networks. *Nature Reviews. Neuroscience*, *8*(1), 45–56. doi:10.1038/nrn2044

Baskerville, K. A., Schweitzer, J. B., & Herron, P. (1997). Effects of cholinergic depletion on experience-dependent plasticity in the cortex of the rat. *Neuroscience*, *80*(4), 1159–1169. doi:10.1016/S0306-4522(97)00064-X

Bear, M. F., & Singer, W. (1986). Modulation of visual cortical plasticity by acetylcholine and noradrenaline. *Nature*, *320*(6058), 172–176. doi:10.1038/320172a0

Beierlein, M., Gibson, J. R., & Connors, B. W. (2003). Two dynamically distinct inhibitory networks in layer 4 of the neocortex. *Journal of Neurophysiology*, *90*(5), 2987–3000. doi:10.1152/jn.00283.2003

Bittner, K. C., Milstein, A. D., Grienberger, C., Romani, S., & Magee, J. C. (2017). Behavioral time scale synaptic plasticity underlies CA1 place fields. *Science*, *357*(6355), 1033–1036. doi:10.1126/science.aan3846

Bloss, E. B., Cembrowski, M. S., Karsh, B., Colonell, J., Fetter, R. D., & Spruston, N. (2016). Structured Dendritic Inhibition Supports Branch-Selective Integration in CA1 Pyramidal Cells. *Neuron*, *89*(5), 1016–1030. doi:10.1016/j.neuron.2016.01.029

Branco, T., & Häusser, M. (2010). The single dendritic branch as a fundamental functional unit in the nervous system. *Current Opinion in Neurobiology*, *20*(4), 494–502. doi:10.1016/j.conb.2010.07.009

Butt, S. J. B., Fuccillo, M., Nery, S., Noctor, S., Kriegstein, A., Corbin, J. G., & Fishell, G. (2005). The temporal and spatial origins of cortical interneurons predict their physiological subtype. *Neuron*, *48*(4), 591–604. doi:10.1016/j.neuron.2005.09.034

Cang, J., Rentería, R. C., Kaneko, M., Liu, X., Copenhagen, D. R., & Stryker, M. P. (2005). Development of precise maps in visual cortex requires patterned spontaneous activity in the retina. *Neuron*, *48*(5), 797–809. doi:10.1016/j.neuron.2005.09.015

Cauli, B, Audinat, E., Lambolez, B., Angulo, M. C., Ropert, N., Tsuzuki, K., … Rossier, J. (1997). Molecular and physiological diversity of cortical nonpyramidal cells. *The Journal of Neuroscience*, *17*(10), 3894–3906.

Cauli, Bruno, Zhou, X., Tricoire, L., Toussay, X., & Staiger, J. F. (2014). Revisiting enigmatic cortical calretinin-expressing interneurons. *Frontiers in Neuroanatomy*, *8*, 52. doi:10.3389/fnana.2014.00052

Cavanagh, M. E., & Parnavelas, J. G. (1988). Development of somatostatin immunoreactive neurons in the rat occipital cortex: a combined immunocytochemical-autoradiographic study. *The Journal of Comparative Neurology*, *268*(1), 1–12. doi:10.1002/cne.902680102

Chattopadhyaya, B., Di Cristo, G., Higashiyama, H., Knott, G. W., Kuhlman, S. J., Welker, E., & Huang, Z. J. (2004). Experience and activity-dependent maturation of perisomatic GABAergic innervation in primary visual cortex during a postnatal critical period. *The Journal of Neuroscience*, *24*(43), 9598–9611. doi:10.1523/JNEUROSCI.1851-04.2004

Chen, N., Sugihara, H., & Sur, M. (2015). An acetylcholine-activated microcircuit drives temporal dynamics of cortical activity. *Nature Neuroscience*, *18*(6), 892–902. doi:10.1038/nn.4002

Cichon, J., & Gan, W.-B. (2015). Branch-specific dendritic Ca(2+) spikes cause persistent synaptic plasticity. *Nature*, *520*(7546), 180–185. doi:10.1038/nature14251

Cobb, S. R., Buhl, E. H., Halasy, K., Paulsen, O., & Somogyi, P. (1995). Synchronization of neuronal activity in hippocampus by individual GABAergic interneurons. *Nature*, *378*(6552), 75–78. doi:10.1038/378075a0

Connors, B. W., & Gutnick, M. J. (1990). Intrinsic firing patterns of diverse neocortical neurons. *Trends in Neurosciences*, *13*(3), 99–104. doi:10.1016/0166-2236(90)90185-D

Cottam, J. C. H., Smith, S. L., & Häusser, M. (2013). Target-specific effects of somatostatin-expressing interneurons on neocortical visual processing. *The Journal of Neuroscience*, *33*(50), 19567–19578. doi:10.1523/JNEUROSCI.2624-13.2013

Crair, M. C., Gillespie, D. C., & Stryker, M. P. (1998). The role of visual experience in the development of columns in cat visual cortex. *Science*, *279*(5350), 566–570. doi:10.1126/science.279.5350.566

Crowley, J. C., & Katz, L. C. (1999). Development of ocular dominance columns in the absence of retinal input. *Nature Neuroscience*, *2*(12), 1125–1130. doi:10.1038/16051

Dávid, C., Schleicher, A., Zuschratter, W., & Staiger, J. F. (2007). The innervation of parvalbumin-containing interneurons by VIP-immunopositive interneurons in the primary somatosensory cortex of the adult rat. *The European Journal of Neuroscience*, *25*(8), 2329–2340. doi:10.1111/j.1460-9568.2007.05496.x

Do, J. P., Xu, M., Lee, S.-H., Chang, W.-C., Zhang, S., Chung, S., … Dan, Y. (2016). Cell type-specific long-range connections of basal forebrain circuit. *eLife*, *5*. doi:10.7554/eLife.13214

Dori, I., & Parnavelas, J. G. (1989). The cholinergic innervation of the rat cerebral cortex shows two distinct phases in development. *Experimental Brain Research*, *76*(2), 417–423. doi:10.1007/BF00247899

Eckenstein, F., & Baughman, R. W. (1984). Two types of cholinergic innervation in cortex, one co-localized with vasoactive intestinal polypeptide. *Nature*, *309*(5964), 153–155.

Espinosa, J. S., & Stryker, M. P. (2012). Development and plasticity of the primary visual cortex. *Neuron*, *75*(2), 230–249. doi:10.1016/j.neuron.2012.06.009

Fagiolini, M, & Hensch, T. K. (2000). Inhibitory threshold for critical-period activation in primary visual cortex. *Nature*, *404*(6774), 183–186. doi:10.1038/35004582

Fagiolini, Michela, Fritschy, J.-M., Löw, K., Möhler, H., Rudolph, U., & Hensch, T. K. (2004). Specific GABAA circuits for visual cortical plasticity. *Science*, *303*(5664), 1681–1683. doi:10.1126/science.1091032

Faguet, J., Maranhao, B., Smith, S. L., & Trachtenberg, J. T. (2009). Ipsilateral eye cortical maps are uniquely sensitive to binocular plasticity. *Journal of Neurophysiology*, *101*(2), 855–861. doi:10.1152/jn.90893.2008

Fanselow, E. E., Richardson, K. A., & Connors, B. W. (2008). Selective, state-dependent activation of somatostatin-expressing inhibitory interneurons in mouse neocortex. *Journal of Neurophysiology*, *100*(5), 2640–2652. doi:10.1152/jn.90691.2008

Ferando, I., & Mody, I. (2014). Interneuronal GABAA receptors inside and outside of synapses. *Current Opinion in Neurobiology*, *26*, 57–63. doi:10.1016/j.conb.2013.12.001

Férézou, I., Cauli, B., Hill, E. L., Rossier, J., Hamel, E., & Lambolez, B. (2002). 5-HT3 receptors mediate serotonergic fast synaptic excitation of neocortical vasoactive intestinal peptide/cholecystokinin interneurons. *The Journal of Neuroscience*, *22*(17), 7389–7397.

Froemke, R. C., Merzenich, M. M., & Schreiner, C. E. (2007). A synaptic memory trace for cortical receptive field plasticity. *Nature*, *450*(7168), 425–429. doi:10.1038/nature06289

Fu, Y., Kaneko, M., Tang, Y., Alvarez-Buylla, A., & Stryker, M. P. (2015). A cortical disinhibitory circuit for enhancing adult plasticity. *eLife*, *4*, e05558. doi:10.7554/eLife.05558

Fu, Y., Tucciarone, J. M., Espinosa, J. S., Sheng, N., Darcy, D. P., Nicoll, R. A., … Stryker, M. P. (2014). A cortical circuit for gain control by behavioral state. *Cell*, *156*(6), 1139–1152. doi:10.1016/j.cell.2014.01.050

Gambino, F., Pagès, S., Kehayas, V., Baptista, D., Tatti, R., Carleton, A., & Holtmaat, A. (2014). Sensory-evoked LTP driven by dendritic plateau potentials in vivo. *Nature*, *515*(7525), 116–119. doi:10.1038/nature13664

Garcia-Junco-Clemente, P., Ikrar, T., Tring, E., Xu, X., Ringach, D. L., & Trachtenberg, J. T. (2017). An inhibitory pull-push circuit in frontal cortex. *Nature Neuroscience*, *20*(3), 389–392. doi:10.1038/nn.4483

Gibson, J. R., Beierlein, M., & Connors, B. W. (1999). Two networks of electrically coupled inhibitory neurons in neocortex. *Nature*, *402*(6757), 75–79. doi:10.1038/47035

Gidon, A., & Segev, I. (2012). Principles governing the operation of synaptic inhibition in dendrites. *Neuron*, *75*(2), 330–341. doi:10.1016/j.neuron.2012.05.015

Goard, M., & Dan, Y. (2009). Basal forebrain activation enhances cortical coding of natural scenes. *Nature Neuroscience*, *12*(11), 1444–1449. doi:10.1038/nn.2402

Godement, P., Salaün, J., & Imbert, M. (1984). Prenatal and postnatal development of retinogeniculate and retinocollicular projections in the mouse. *The Journal of Comparative Neurology*, *230*(4), 552–575. doi:10.1002/cne.902300406

Golding, N. L., Staff, N. P., & Spruston, N. (2002). Dendritic spikes as a mechanism for cooperative long-term potentiation. *Nature*, *418*(6895), 326–331. doi:10.1038/nature00854

Gonchar, Y., Wang, Q., & Burkhalter, A. (2007). Multiple distinct subtypes of GABAergic neurons in mouse visual cortex identified by triple immunostaining. *Frontiers in Neuroanatomy*, *1*, 3. doi:10.3389/neuro.05.003.2007

Gordon, J. A., & Stryker, M. P. (1996). Experience-dependent plasticity of binocular responses in the primary visual cortex of the mouse. *The Journal of Neuroscience*, *16*(10), 3274–3286.

Hanover, J. L., Huang, Z. J., Tonegawa, S., & Stryker, M. P. (1999). Brain-derived neurotrophic factor overexpression induces precocious critical period in mouse visual cortex. *The Journal of Neuroscience*, *19*(22), RC40.

Harris, K. D., & Thiele, A. (2011). Cortical state and attention. *Nature Reviews. Neuroscience*, *12*(9), 509–523. doi:10.1038/nrn3084

Hedrick, T., & Waters, J. (2015). Acetylcholine excites neocortical pyramidal neurons via nicotinic receptors. *Journal of Neurophysiology*, *113*(7), 2195–2209. doi:10.1152/jn.00716.2014

Hensch, T. K., Fagiolini, M., Mataga, N., Stryker, M. P., Baekkeskov, S., & Kash, S. F. (1998). Local GABA circuit control of experience-dependent plasticity in developing visual cortex. *Science*, *282*(5393), 1504–1508.

Hofer, S. B., Ko, H., Pichler, B., Vogelstein, J., Ros, H., Zeng, H., … Mrsic-Flogel, T. D. (2011). Differential connectivity and response dynamics of excitatory and inhibitory neurons in visual cortex. *Nature Neuroscience*, *14*(8), 1045–1052. doi:10.1038/nn.2876

Holmgren, C., Harkany, T., Svennenfors, B., & Zilberter, Y. (2003). Pyramidal cell communication within local networks in layer 2/3 of rat neocortex. *The Journal of Physiology*, *551*(Pt 1), 139–153. doi:10.1113/jphysiol.2003.044784

Huang, Z J, Kirkwood, A., Pizzorusso, T., Porciatti, V., Morales, B., Bear, M. F., … Tonegawa, S. (1999). BDNF regulates the maturation of inhibition and the critical period of plasticity in mouse visual cortex. *Cell*, *98*(6), 739–755. doi:10.1016/S0092-8674(00)81509-3

Huang, Z Josh. (2009). Activity-dependent development of inhibitory synapses and innervation pattern: role of GABA signalling and beyond. *The Journal of Physiology*, *587*(Pt 9), 1881–1888. doi:10.1113/jphysiol.2008.168211

Hubel, D. H., & Wiesel, T. N. (1970). The period of susceptibility to the physiological effects of unilateral eye closure in kittens. *The Journal of Physiology*, *206*(2), 419–436. doi:10.1113/jphysiol.1970.sp009022

Kampa, B. M., Letzkus, J. J., & Stuart, G. J. (2006). Requirement of dendritic calcium spikes for induction of spike-timing-dependent synaptic plasticity. *The Journal of Physiology*, *574*(Pt 1), 283–290. doi:10.1113/jphysiol.2006.111062

Kapfer, C., Glickfeld, L. L., Atallah, B. V., & Scanziani, M. (2007). Supralinear increase of recurrent inhibition during sparse activity in the somatosensory cortex. *Nature Neuroscience*, *10*(6), 743–753. doi:10.1038/nn1909

Karnani, M. M., Jackson, J., Ayzenshtat, I., Hamzehei Sichani, A., Manoocheri, K., Kim, S., & Yuste, R. (2016). Opening holes in the blanket of inhibition: localized lateral disinhibition by VIP interneurons. *The Journal of Neuroscience*, *36*(12), 3471–3480. doi:10.1523/JNEUROSCI.3646-15.2016

Kasamatsu, T., & Pettigrew, J. D. (1976). Depletion of brain catecholamines: failure of ocular dominance shift after monocular occlusion in kittens. *Science*, *194*(4261), 206–209.

Kawaguchi, Y. (1997). Selective cholinergic modulation of cortical GABAergic cell subtypes. *Journal of Neurophysiology*, *78*(3), 1743–1747. doi:10.1152/jn.1997.78.3.1743

Kawaguchi, Y., & Kubota, Y. (1996). Physiological and morphological identification of somatostatin- or vasoactive intestinal polypeptide-containing cells among GABAergic cell subtypes in rat frontal cortex. *The Journal of Neuroscience*, *16*(8), 2701–2715.

Kawaguchi, Y., & Kubota, Y. (1997). GABAergic cell subtypes and their synaptic connections in rat frontal cortex. *Cerebral Cortex*, *7*(6), 476–486. doi:10.1093/cercor/7.6.476

Kerlin, A., Mohar, B., Flickinger, D., MacLennan, B. J., Davis, C., Spruston, N., & Svoboda, K. (2018). Functional clustering of dendritic activity during decision-making. *BioRxiv*. doi:10.1101/440396

Kilgard, M. P., & Merzenich, M. M. (1998). Cortical map reorganization enabled by nucleus basalis activity. *Science*, *279*(5357), 1714–1718. doi:10.1126/science.279.5357.1714

Klausberger, T., Roberts, J. D. B., & Somogyi, P. (2002). Cell type- and input-specific differences in the number and subtypes of synaptic GABA(A) receptors in the hippocampus. *The Journal of Neuroscience*, *22*(7), 2513–2521. doi:20026228

Kloc, M., & Maffei, A. (2014). Target-specific properties of thalamocortical synapses onto layer 4 of mouse primary visual cortex. *The Journal of Neuroscience*, *34*(46), 15455–15465. doi:10.1523/JNEUROSCI.2595-14.2014

Kruglikov, I., & Rudy, B. (2008). Perisomatic GABA release and thalamocortical integration onto neocortical excitatory cells are regulated by neuromodulators. *Neuron*, *58*(6), 911–924. doi:10.1016/j.neuron.2008.04.024

Kuhlman, S. J., Olivas, N. D., Tring, E., Ikrar, T., Xu, X., & Trachtenberg, J. T. (2013). A disinhibitory microcircuit initiates critical-period plasticity in the visual cortex. *Nature*, *501*(7468), 543–546. doi:10.1038/nature12485

Kuppermann, B. D., & Kasamatsu, T. (1984). Enhanced binocular interaction in the visual cortex of normal kittens subjected to intracortical norepinephrine perfusion. *Brain Research*, *302*(1), 91–99. doi:10.1016/0006-8993(84)91288-5

Laplante, F., Morin, Y., Quirion, R., & Vaucher, E. (2005). Acetylcholine release is elicited in the visual cortex, but not in the prefrontal cortex, by patterned visual stimulation: a dual in vivo microdialysis study with functional correlates in the rat brain. *Neuroscience*, *132*(2), 501–510. doi:10.1016/j.neuroscience.2004.11.059

Larkum, M E, Zhu, J. J., & Sakmann, B. (1999). A new cellular mechanism for coupling inputs arriving at different cortical layers. *Nature*, *398*(6725), 338–341. doi:10.1038/18686

Larkum, Matthew Evan, Waters, J., Sakmann, B., & Helmchen, F. (2007). Dendritic spikes in apical dendrites of neocortical layer 2/3 pyramidal neurons. *The Journal of Neuroscience*, *27*(34), 8999–9008. doi:10.1523/JNEUROSCI.1717-07.2007

Lazarus, M. S., & Huang, Z. J. (2011). Distinct maturation profiles of perisomatic and dendritic targeting GABAergic interneurons in the mouse primary visual cortex during the critical period of ocular dominance plasticity. *Journal of Neurophysiology*, *106*(2), 775–787. doi:10.1152/jn.00729.2010

Lee, A. M., Hoy, J. L., Bonci, A., Wilbrecht, L., Stryker, M. P., & Niell, C. M. (2014). Identification of a brainstem circuit regulating visual cortical state in parallel with locomotion. *Neuron*, *83*(2), 455–466. doi:10.1016/j.neuron.2014.06.031

Lee, S.-H., & Dan, Y. (2012). Neuromodulation of brain states. *Neuron*, *76*(1), 209–222. doi:10.1016/j.neuron.2012.09.012

Lee, SooHyun, Hjerling-Leffler, J., Zagha, E., Fishell, G., & Rudy, B. (2010). The largest group of superficial neocortical GABAergic interneurons expresses ionotropic serotonin receptors. *The Journal of Neuroscience*, *30*(50), 16796–16808. doi:10.1523/JNEUROSCI.1869-10.2010

Lee, Soohyun, Kruglikov, I., Huang, Z. J., Fishell, G., & Rudy, B. (2013). A disinhibitory circuit mediates motor integration in the somatosensory cortex. *Nature Neuroscience*, *16*(11), 1662–1670. doi:10.1038/nn.3544

Lehmann, K., & Löwel, S. (2008). Age-dependent ocular dominance plasticity in adult mice. *Plos One*, *3*(9), e3120. doi:10.1371/journal.pone.0003120

Letzkus, J. J., Wolff, S. B. E., Meyer, E. M. M., Tovote, P., Courtin, J., Herry, C., & Lüthi, A. (2011). A disinhibitory microcircuit for associative fear learning in the auditory cortex. N*ature, 480(*7377), 331–335. doi:10.1038/nature10674

Losonczy, A., Makara, J. K., & Magee, J. C. (2008). Compartmentalized dendritic plasticity and input feature storage in neurons. *Nature*, *452*(7186), 436–441. doi:10.1038/nature06725

Malach, R., & Van Sluyters, R. C. (1989). Strabismus does not prevent recovery from monocular deprivation: A challenge for simple Hebbian models of synaptic modification. *Visual Neuroscience*, *3*(03), 267–273. doi:10.1017/S0952523800010014

Markram, H., Toledo-Rodriguez, M., Wang, Y., Gupta, A., Silberberg, G., & Wu, C. (2004). Interneurons of the neocortical inhibitory system. N*ature Reviews. Neuroscience,* 5*(*10), 793–807. doi:10.1038/nrn1519

McCormick, D. A., & Prince, D. A. (1985). Two types of muscarinic response to acetylcholine in mammalian cortical neurons. *Proceedings of the National Academy of Sciences of the United States of America*, *82*(18), 6344–6348. doi:10.1073/pnas.82.18.6344

McCormick, D. A., & Prince, D. A. (1987). Post-natal development of electrophysiological properties of rat cerebral cortical pyramidal neurones. *The Journal of Physiology*, *393*, 743–762.

Miles, R., Tóth, K., Gulyás, A. I., Hájos, N., & Freund, T. F. (1996). Differences between somatic and dendritic inhibition in the hippocampus. *Neuron*, 1*6(*4), 815–823. doi:10.1016/S0896-6273(00)80101-4

Mioche, L., & Singer, W. (1989). Chronic recordings from single sites of kitten striate cortex during experience-dependent modifications of receptive-field properties. *Journal of Neurophysiology*, *62*(1), 185–197. doi:10.1152/jn.1989.62.1.185

Morishita, H., Miwa, J. M., Heintz, N., & Hensch, T. K. (2010). Lynx1, a cholinergic brake, limits plasticity in adult visual cortex. *Science*, *330*(6008), 1238–1240. doi:10.1126/science.1195320

Murayama, M., Pérez-Garci, E., Nevian, T., Bock, T., Senn, W., & Larkum, M. E. (2009). Dendritic encoding of sensory stimuli controlled by deep cortical interneurons. *Nature*, *457*(7233), 1137–1141. doi:10.1038/nature07663

Pala, A., & Petersen, C. C. H. (2015). In vivo measurement of cell-type-specific synaptic connectivity and synaptic transmission in layer 2/3 mouse barrel cortex. *Neuron*, *85*(1), 68–75. doi:10.1016/j.neuron.2014.11.025

Parikh, V., Kozak, R., Martinez, V., & Sarter, M. (2007). Prefrontal acetylcholine release controls cue detection on multiple timescales. N*euron,* 5*6(*1), 141–154. doi:10.1016/j.neuron.2007.08.025

Petilla Interneuron Nomenclature Group, Ascoli, G. A., Alonso-Nanclares, L., Anderson, S. A., Barrionuevo, G., Benavides-Piccione, R., … Yuste, R. (2008). Petilla terminology: nomenclature of features of GABAergic interneurons of the cerebral cortex. *Nature Reviews. Neuroscience*, *9*(7), 557–568. doi:10.1038/nrn2402

Pfeffer, C. K., Xue, M., He, M., Huang, Z. J., & Scanziani, M. (2013). Inhibition of inhibition in visual cortex: the logic of connections between molecularly distinct interneurons. N*ature Neuroscience,* 1*6(*8), 1068–1076. doi:10.1038/nn.3446

Pi, H.-J., Hangya, B., Kvitsiani, D., Sanders, J. I., Huang, Z. J., & Kepecs, A. (2013). Cortical interneurons that specialize in disinhibitory control. *Nature*, *503*(7477), 521–524. doi:10.1038/nature12676

Pinto, L., Goard, M. J., Estandian, D., Xu, M., Kwan, A. C., Lee, S.-H., … Dan, Y. (2013). Fast modulation of visual perception by basal forebrain cholinergic neurons. *Nature Neuroscience*, *16*(12), 1857–1863. doi:10.1038/nn.3552

Poirazi, P., Brannon, T., & Mel, B. W. (2003). Pyramidal neuron as two-layer neural network. *Neuron*, *37*(6), 989–999. doi:10.1016/S0896-6273(03)00149-1

Polack, P.-O., Friedman, J., & Golshani, P. (2013). Cellular mechanisms of brain state-dependent gain modulation in visual cortex. *Nature Neuroscience*, *16*(9), 1331–1339. doi:10.1038/nn.3464

Polsky, A., Mel, B. W., & Schiller, J. (2004). Computational subunits in thin dendrites of pyramidal cells. *Nature Neuroscience*, *7*(6), 621–627. doi:10.1038/nn1253

Pouille, F., & Scanziani, M. (2001). Enforcement of temporal fidelity in pyramidal cells by somatic feed-forward inhibition. *Science*, *293*(5532), 1159–1163. doi:10.1126/science.1060342

Prönneke, A., Scheuer, B., Wagener, R. J., Möck, M., Witte, M., & Staiger, J. F. (2015). Characterizing VIP Neurons in the Barrel Cortex of VIPcre/tdTomato Mice Reveals Layer-Specific Differences. *Cerebral Cortex*, *25*(12), 4854–4868. doi:10.1093/cercor/bhv202

Reimer, J., Froudarakis, E., Cadwell, C. R., Yatsenko, D., Denfield, G. H., & Tolias, A. S. (2014). Pupil fluctuations track fast switching of cortical states during quiet wakefulness. *Neuron*, *84*(2), 355–362. doi:10.1016/j.neuron.2014.09.033

Reyes, A., Lujan, R., Rozov, A., Burnashev, N., Somogyi, P., & Sakmann, B. (1998). Target-cell-specific facilitation and depression in neocortical circuits. *Nature Neuroscience*, *1*(4), 279–285. doi:10.1038/1092

Ringach, D. L. (2009). Spontaneous and driven cortical activity: implications for computation. *Current Opinion in Neurobiology*, *19*(4), 439–444. doi:10.1016/j.conb.2009.07.005

Royer, S., Zemelman, B. V., Losonczy, A., Kim, J., Chance, F., Magee, J. C., & Buzsáki, G. (2012). Control of timing, rate and bursts of hippocampal place cells by dendritic and somatic inhibition. *Nature Neuroscience*, *15*(5), 769–775. doi:10.1038/nn.3077

Rudy, B., Fishell, G., Lee, S., & Hjerling-Leffler, J. (2011). Three groups of interneurons account for nearly 100% of neocortical GABAergic neurons. *Developmental Neurobiology*, *71*(1), 45–61. doi:10.1002/dneu.20853

Runyan, C. A., Schummers, J., Van Wart, A., Kuhlman, S. J., Wilson, N. R., Huang, Z. J., & Sur, M. (2010). Response features of parvalbumin-expressing interneurons suggest precise roles for subtypes of inhibition in visual cortex. *Neuron*, *67*(5), 847–857. doi:10.1016/j.neuron.2010.08.006

Sandler, M., Shulman, Y., & Schiller, J. (2016). A novel form of local plasticity in tuft dendrites of neocortical somatosensory layer 5 pyramidal neurons. *Neuron*, *90*(5), 1028–1042. doi:10.1016/j.neuron.2016.04.032

Schiller, J., Schiller, Y., Stuart, G., & Sakmann, B. (1997). Calcium action potentials restricted to distal apical dendrites of rat neocortical pyramidal neurons. *The Journal of Physiology*, *505 (Pt 3)*, 605–616. doi:10.1111/j.1469-7793.1997.605ba.x

Silberberg, G., & Markram, H. (2007). Disynaptic inhibition between neocortical pyramidal cells mediated by Martinotti cells. *Neuron*, *53*(5), 735–746. doi:10.1016/j.neuron.2007.02.012

Smith, S. L., & Trachtenberg, J. T. (2007). Experience-dependent binocular competition in the visual cortex begins at eye opening. *Nature Neuroscience*, *10*(3), 370–375. doi:10.1038/nn1844

Spruston, N. (2008). Pyramidal neurons: dendritic structure and synaptic integration. *Nature Reviews. Neuroscience*, *9*(3), 206–221. doi:10.1038/nrn2286

Tamás, G., Buhl, E. H., & Somogyi, P. (1997). Fast IPSPs elicited via multiple synaptic release sites by different types of GABAergic neurone in the cat visual cortex. *The Journal of Physiology*, *500 (Pt 3)*, 715–738.

Tremblay, R., Lee, S., & Rudy, B. (2016). Gabaergic interneurons in the neocortex: from cellular properties to circuits. *Neuron*, *91*(2), 260–292. doi:10.1016/j.neuron.2016.06.033

Wang, B.-S., Sarnaik, R., & Cang, J. (2010). Critical period plasticity matches binocular orientation preference in the visual cortex. *Neuron*, *65*(2), 246–256. doi:10.1016/j.neuron.2010.01.002

Wang, Y., Toledo-Rodriguez, M., Gupta, A., Wu, C., Silberberg, G., Luo, J., & Markram, H. (2004). Anatomical, physiological and molecular properties of Martinotti cells in the somatosensory cortex of the juvenile rat. *The Journal of Physiology*, *561*(Pt 1), 65–90. doi:10.1113/jphysiol.2004.073353

Wei, D. S., Mei, Y. A., Bagal, A., Kao, J. P., Thompson, S. M., & Tang, C. M. (2001). Compartmentalized and binary behavior of terminal dendrites in hippocampal pyramidal neurons. *Science*, *293*(5538), 2272–2275. doi:10.1126/science.1061198

Wiesel, T. N., & Hubel, D. H. (1963). SINGLE-CELL RESPONSES IN STRIATE CORTEX OF KITTENS DEPRIVED OF VISION IN ONE EYE. *Journal of Neurophysiology*, *26*, 1003–1017. doi:10.1152/jn.1963.26.6.1003

Xu, H., Jeong, H.-Y., Tremblay, R., & Rudy, B. (2013). Neocortical somatostatin-expressing GABAergic interneurons disinhibit the thalamorecipient layer 4. *Neuron*, *77*(1), 155–167. doi:10.1016/j.neuron.2012.11.004

Xu, Q., Cobos, I., De La Cruz, E., Rubenstein, J. L., & Anderson, S. A. (2004). Origins of cortical interneuron subtypes. *The Journal of Neuroscience*, *24*(11), 2612–2622. doi:10.1523/JNEUROSCI.5667-03.2004

Xu, X., & Callaway, E. M. (2009). Laminar specificity of functional input to distinct types of inhibitory cortical neurons. *The Journal of Neuroscience*, *29*(1), 70–85. doi:10.1523/JNEUROSCI.4104-08.2009

Zhang, S., Xu, M., Kamigaki, T., Hoang Do, J. P., Chang, W.-C., Jenvay, S., … Dan, Y. (2014). Selective attention. Long-range and local circuits for top-down modulation of visual cortex processing. *Science*, *345*(6197), 660–665. doi:10.1126/science.1254126

Chapter 2: Methods

2.1 Animals

All procedures were done in compliance with the Office of Animal Research Oversight, the Institutional Animal Care and Use Committee, at the University of California, Los Angeles. The following mouse lines were used from Jackson Laboratories: SST-IRES-Cre (stock no. 018973), PV-Cre (stock no. 08069), VIP-IRES-Cre (stock no. 010908), and ChAT-Cre (stock no. 006410). For optical identification of interneurons, mice were crossed with Ai9-expressing mice (stock no. 007905). All mice were heterozygous for their respective transgenes, and both male and female mice were used. Mice were group housed under a normal 12/12 light-dark cycle.

2.2 Cranial window surgeries

All two-photon imaging was carried out through a cranial window. For all ages, surgical preparation included administration of anti-inflammatory Carprofen, the affixation of an aluminum headbar to the skull, the removal of bone over the primary visual cortex, injection of viral vectors, and the placement of a glass coverslip over the exposed region. Body temperature was maintained at 37°C. Under isoflurane anesthesia, the scalp was retracted and Vetbond was used to coat the skull surface and the edges of the exposed area, followed by a layer of black dental acrylic. An aluminum headbar was affixed with dental acrylic to this surface, caudal to the area of interest over V1. A 3mm-diameter area over V1 (centered at 1.5mm from bregma and 3mm from the midline) was removed using a high speed drill. Following virus injection, the craniotomy was sealed with coverglass using Vetbond to create an imaging window. All remaining exposed regions of skull and surgery margins were sealed with Vetbond and acrylic. Animals were given a one-week period or more for recovery before imaging. For adult mice, injections and surgeries were performed altogether, 2 weeks prior to imaging at P56. For

imaging at P28, mice were injected via a small burrhole over V1 at P14, and the headbar and craniotomy surgeries were performed at P21.

2.3 Virus injections

For calcium imaging, either CaMKII-GCaMP6 or flex-GCaMP6s (UPenn Vector Core: AAV1.CamKII.GCaMP6f.WPRE.SV40, number AV-1-PV3435, and AAV1.Syn.Flex.GCaMP6s.WPRE.SV40, number AV-1-PV2821) were expressed in cortical neurons (titer: 10^{13} genomes/ml). For all age groups, virus was injected 2 weeks prior to imaging. Virus injection was done using a glass micropipette and a PicoSprizer III (Parker) (15 p.s.i., 10 ms pulses, 3 s between pulses). For imaging Cre-dependent interneuron classes, virus containing flex-GCaMP6s was used, injected at a beginning depth of 350 μm and moving up every 50 μm, with the last injection depth being 100 μm below the pial surface, for a total of approximately 1.5 μL of injected virus across cortical layer 2/3. For imaging pyramidal cell dendrites, a viral vector containing CaMKII-GCaMP6f was used, and approximately 50 nL of undiluted virus was injected at a depth of 300 μm from the cortical surface in the center of V1. The low volume for these experiments was beneficial to achieving optimal sparsity for observing pyramidal cell processes. For optogenetic experiments, flex-ChR2 (AAV1.CAGGS.Flex.ChR2-tdTomato.WPRE.SV40, number AV-1-18917P, titer: 10^{13} genomes/ml) was used in multiple Cre-dependent lines. For stimulating SST cells in V1, flex-ChR2 and GCaMP6s were expressed in SST neurons expressing Cre. Injections were done as for interneuron populations, but with a 1:1 ratio of each virus (approximately 0.75 μL of each). For pyramidal cell imaging with SST cell activation, flex-ChR2 and CaMKII-GCaMP were injected in a 50nL injection as stated above, with viruses mixed in a 1:1 ratio. For optogenetic manipulation of the nucleus basalis, flex-ChR2 was injected at coordinates of 1.8 mm lateral and 0.5 mm posterior to bregma, at a depth of 4.3mm, at a volume of approximately 0.5 μL. For experiments using inhibitory DREADDs, a Cre-dependent virus was used (AAV2.hSyn.DIO.hM4D(Gi).mCherry, number 44362-AAV2,

Addgene, titer $7x10^{12}$genomes/ml) and was mixed with flex-GCaMP6s at a 2:1 ratio to account for the lower titer of the DREADD-containing virus. Approximately 1-2 µL were injected into V1. For binocular matching experiments, CaMKII-GCaMP6f and flex-DREADD were co-injected at this ratio and volume at P10, and craniotomies were performed as usual at P21.

2.4 Two-photon calcium imaging and visual stimulation

Calcium responses of specific cell types and processes were acquired using a resonant-scanning two-photon microscope (Neurolabware) controlled by Scanbox acquisition software. A Coherent Chameleon Ultra II laser (Coherent Inc.) was used for GCaMP excitation, fixed at a wavelength of 920 nm. The objective used was a 16x water-immersion lens (Nikon, 0.8NA, 3 mm working distance). Image sequences were captured at 15.5 Hz at a depth of 100-300 microns below the pia. A dichroic mirror (Semrock) was used to separate red and green fluorescence: for red fluorescence detection, the laser wavelength was adjusted to 1000 nm. All testing was done with awake, head-fixed mice that were free to move on a spherical treadmill. Prior to testing, mice had at least two days of training to acclimate to the treadmill and head-fixation. Treadmill movement was captured by a Dalsa Genie M1280 camera (Teledyne Dalsa), which was synchronized to microscope scanning. Visual stimuli were presented on a large LCD monitor directly in front of the animal, 18 cm from the eye. Visual stimuli, created with Psychtoolbox in MATLAB, consisted of nonrepeating natural movies with intermittent gray screens (9s on, 14s off). Spontaneous response data was collected with a blank gray screen. For measuring receptive field properties, the binocular zone was identified using a sparse noise visual stimulus which revealed the amount of neuronal activity at the center of the visual field. Following localization, ipsilateral and contralateral inputs to binocular neurons were recorded with an opaque patch placed immediately in front of the eye to temporarily occlude visual input. Evoked responses were then recorded using a random sinusoidal grating, varying in orientation (0-170 degrees) and spatial frequency (0-0.15 cycles/degree), presented at 4Hz for a total of 15

minutes.

2.5 Analysis of two-photon imaging data

Collected data was processed using the pipeline provided by Scanbox software. Recorded frames were aligned with a recursive Lucas-Kanade algorithm. Regions of interest were created in a semi-automated manner, in which correlation coefficients among pixels could be thresholded and used to determine areas of significant correlated activity. Neuropil-subtracted signals were extracted from these regions of interest. These signals were z-scored, or for amplitude comparison, ΔF/F was calculated. For pyramidal cells, signals were deconvolved using the Vanilla algorithm, which is a linear filter with a static nonlinearity. The parameters of the temporal filter and static nonlinearity were determined by maximizing the correlation of the deconvolved signal with neuronal spiking from a community-contributed database (Berens et al., 2017). We used this method for both somatic and dendritic Ca^{2+} signals. While deconvolution has not been validated physiologically for dendritic Ca^{2+} transients, other findings indicate that there is a strongly correlative relationship among dendritic Ca^{2+} transients, spiking, and membrane potential (Smith, Smith, Branco, & Häusser, 2013). To avoid assumptions on the physiological basis of these Ca^{2+} transients, we use the term “event probability” to denote transients of significant size and slope.

For all correlation analyses, Spearman’s correlation coefficient was used. For comparisons of amplitude, the median response in ΔF/F was determined across evoked epochs and/or periods of movement or quiescence. In some cases, comparisons were normalized to give a percentage. For calculating fold change in dendritic Ca^{2+} events, we took the ratio of event probabilities between sister branches, performed a log-transformation, and took the absolute value.

For receptive field analyses, a spatiotemporal kernel was computed for each cell based on the average responses to the randomized grating and smoothed with a Gaussian filter.

Signal to noise for each kernel was determined by taking the maximum response divided by the mean (SNR). Binocular neurons were classified by SNRs greater than 1.5 for both ipsilateral and contralateral-driven responses. Orientation preference (θ) was determined by calculating the circular variance, and the difference between preferred orientations of ipsilateral and contralateral inputs is given by $\Delta\theta$, in degrees.

2.6 *In vivo* optogenetic manipulations of SST cells or nucleus basalis

For full-field stimulation of SST cells in V1, a high power LED (ThorLabs) with a blue-light filter (470 nm, Semrock) was added to the two-photon pathway. LED intensity was a maximum of 10 mW mm^{-1} at the center of the cranial window surface, which was measured by a power meter (Thorlabs). LED triggering was synced to laser scanning through Scanbox, and activation of the LED silenced a gated photomultiplier (Hamamatsu) prior to LED light delivery, so that light from the LED was not collected and the integrity of the PMT was preserved. Blue light was delivered in 10ms pulses, repeated 25 times at 15Hz. Stimulation was done during both periods of stillness and movement, and when done within the same imaging session, at least 30 seconds was left between stimulation periods.

To selectively stimulate the nucleus basalis, mice were generated to express Cre in SST cells and also in neurons expressing choline acetyltransferase (ChAT), an enzyme responsible for the synthesis of acetylcholine. In each mouse, within the same hemisphere, a local injection of a flexed channelrhodopsin (ChR2) was made into the nucleus basalis and, separately, flexed-GCaMP6s was injected into visual cortex. While neurons expressing ChAT or SST are present in both areas, SST neurons of the basal forebrain do not project to cortex (Do et al., 2016), and cortical ChAT-positive neurons make up less than 1% of all cortical interneurons (Gonchar, Wang, & Burkhalter, 2007). A fiber-optic cannula (Prizmatix) was implanted over the injected region of the nucleus basalis one to two weeks prior to imaging, following virus injections.

Cannulas were 4.3mm long and were inserted at a 30-degree angle, 2 mm rostral of the injection site. This allowed space for the objective while keeping the end of the optical fiber approximately 0.5 mm away from the nucleus basalis. Similar to full-field stimulation experiments in V1, blue light (~460nm) was administered in 10ms pulses, 25 times at 15Hz at 5-6mW. To minimize any natural activation of the basal forebrain during these experiments, mice were trained to be still and observed a gray screen throughout recordings.

2.7 DREADD manipulation of SST cells during development

To suppress SST cell activity over a prolonged period during development, we used a Cre-dependent inhibitory DREADD (hM4Di) in SST-Cre mice. To validate DREADD-mediated suppression of SST interneurons, flexed GCaMP6s and DREADDs were co-expressed in SST cells. Following the craniotomy and a period of recovery, evoked activity of SST cells was recorded using natural movie scenes. CNO (C0832, Sigma Aldrich) was dissolved in saline to make a 0.5 mg per ml solution, containing 0.5% DMSO to prevent separation. After baseline recordings, CNO was administered via intraperitoneal injection at a dose of 0.10 ml per 20 g body weight, or 2.5 mg/kg. 2 hours after the CNO injection, we re-imaged the same SST cells and recorded evoked activity with natural movie scenes. We also imaged at 4 and 8 hours to determine how long the effect lasted. In a separate group, we administered CNO to mice without DREADD expression under the same procedure to determine any unexpected effects of CNO or its metabolite, clozapine, on SST cells.

To assess the role of SST cell activity on the process of binocular matching in excitatory cells, we expressed hM4Di DREADDs in SST cells and GCaMP6f in pyramidal neurons. This was accomplished by injecting a flexed DREADD viral vector along with CaMKII-GCaMP6f in the binocular zone of primary visual cortex in SST-Cre mice at postnatal day 10. 2 weeks of recovery was given for adequate expression. Craniotomies were performed on P21 and CNO injections began at P24. In these experiments, mice received CNO (2.5 mg/kg) every 8-12

hours from P24-P27. 12 or more hours from the last dose of CNO, the ipsilateral and contralateral inputs to binocular neurons were tested. Control groups, either expressing DREADD and receiving saline, or not expressing DREADD and receiving CNO, underwent the same procedure.

2.8 Acute slice preparation

Whole cell recordings were done in acute slices from P28 and P56 mice. TdTomato-expressing mouse lines (SST-Cre/Ai9 mice; PV-Cre/Ai9; VIP-Cre/Ai9) were used for targeting specific interneuron subtypes. Animals were anesthetized with isoflurane and perfused with ice-cold sucrose-ACSF. 300 μM-thick coronal slices from the visual cortex were cut on a vibratome in ice-cold sucrose-ACSF solution. Slices were incubated in regular ACSF for 30 minutes at 25 degrees Celsius prior to recording at room temperature. Sucrose-ACSF was perfused with carbogen and contained (in mM): sucrose, 222; glucose, 11; NaHCO3, 26; NaH2PO4, 1; KCl, 3; MgCl, 7; and CaCl, 0.5. Regular ACSF contained (in mM): sucrose, 4; MgCl, 2; CaCl, 2.5; and NaCl, 124. A low-chloride K-gluconate intracellular solution was used to record cells in current clamp mode, containing (in mM): K-gluconate, 126; KCl, 4; HEPES, 10; ATP-Mg, 4; GTP-Na, 0.3; and Na-phosphocreatine, 10; pH 7.4, 300 mOsm. A high-chloride internal solution was used to record IPSCs in voltage clamp mode, containing (in mM): KCl, 120; HEPES, 10; Mg-ATP, 4; GTP-Na, 0.3; and Na-phosphocreatine, 10; pH 7.4, 295 mOsm. Cholinergic responses were tested through local application of cholinergic agonist carbachol (CCh, 2 mM), in which CCh was added in small amounts to the bath (0.3-0.5 μL). Excitatory and inhibitory synaptic activities were blocked using bath-applied CNQX (10 μM) and GABAzine (10 μM), respectively.

2.9 Intracellular recording and analysis

Cells in V1, layer 2/3 were visualized with an Olympus BX61WI microscope coupled with a 40x water immersion lens (Olympus), infrared-DIC optics, and CCD camera (Qimaging).

Slices were screened for cell bodies containing tdTomato using a custom fluorescence filter. Glass pipettes (4 −7 MΩ) were pulled with a Sutter Instruments P1000 puller. Data was collected and acquired with a MultiClamp 700B amplifier and a Digidata 1440A system (Molecular Devices), with WinWCP software (Strathclyde). For all cells, response to current steps, input resistance, and access resistance was measured before drug application and after washout (>30 min) to verify the health of each cell. Only cells without significant changes in current-step responses were used for further analysis. Firing rate and changes in membrane potential were analyzed using Clampfit software and custom-written MATLAB code.

2.10 Statistics

All statistical analyses were done using non-parametric procedures in MATLAB. Significance levels were set to $\alpha<0.05$ for all two-group comparisons. Mann-Whitney U tests were employed for testing differences between independent groups, while groups with repeated measures were compared with the Wilcoxon signed-rank test. In comparisons involving more than two groups, custom-written MATLAB code was used to tailor an ANOVA to non-normally distributed data with unequal variances, for independent and non-independent groupings: F-statistics were computed as the ratio between sum of squares among groups and sum of squares within groups. P-values were calculated by comparing the F-statistic derived from the data and the average F-statistic generated from resampling the shuffled data 10,000 times. Our data required 2 types of ANOVAs: 2-way ANOVA with repeated measures and one-way ANOVA with repeated measures (Kruskal-Wallis test). ANOVAs were followed by post-hoc comparisons with either the Wilcoxon signed-rank test or the Mann-Whitney U test when justified. The Bonferroni method was used to correct α for multiple comparisons.

2.11 References

Berens, P., Freeman, J., Deneux, T., Chenkov, N., McColgan, T., Speiser, A., … Bethge, M. (2017). Community-based benchmarking improves spike inference from two-photon calcium imaging data. *BioRxiv*. doi:10.1101/177956

Do, J. P., Xu, M., Lee, S.-H., Chang, W.-C., Zhang, S., Chung, S., … Dan, Y. (2016). Cell type-specific long-range connections of basal forebrain circuit. *eLife*, *5*. doi:10.7554/eLife.13214

Gonchar, Y., Wang, Q., & Burkhalter, A. (2007). Multiple distinct subtypes of GABAergic neurons in mouse visual cortex identified by triple immunostaining. *Frontiers in Neuroanatomy*, *1*, 3. doi:10.3389/neuro.05.003.2007

Smith, S. L., Smith, I. T., Branco, T., & Häusser, M. (2013). Dendritic spikes enhance stimulus selectivity in cortical neurons in vivo. *Nature*, *503*(7474), 115–120. doi:10.1038/nature12600

Chapter 3: Investigation of major inhibitory classes across development

3.1 Introduction

In the visual cortex, the critical period opens when GABAergic interneurons begin to innervate pyramidal neurons (Chattopadhyaya et al., 2004; Huang et al., 1999), and both excitatory and inhibitory cells start to show mature physiological properties (Lazarus & Huang, 2011). It has remained unknown how inhibition facilitates a plasticity mechanism specific to development. Inhibition is highly organized and targets specific domains of pyramidal neurons. In layer 2/3, PV cells target pyramidal cell somas and proximal dendrites while SST cells target apical dendrites (Kawaguchi & Kubota, 1997; Markram et al., 2004). Both inhibitory cell types possess the capability to shape synaptic input and somatic output, but how inhibition functionally contributes to critical period plasticity is not understood.

Prior work concerning inhibition during the critical period has focused exclusively on PV-specific changes during monocular deprivation. GABA-A receptors with the α1 subunit express on pyramidal cell somas and must be active for the critical period to occur (Fagiolini et al., 2004). However, GABA-A α1 subunits are also expressed on inhibitory interneurons (Bacci, Rudolph, Huguenard, & Prince, 2003; Ferando & Mody, 2014); thus, the loss of plasticity as a result of the inactivation of GABA-A α1 only confirms the necessity of the inhibitory network to the critical period. As somatic innervation increases throughout the critical period, it would seem that increased somatic inhibitory drive would be integral to plasticity. Instead, it seems that PV cells functionally contribute to critical period plasticity via disinhibition. Immediately following monocular deprivation, PV cells lose excitatory drive from layer 4, causing a disinhibition of pyramidal neurons, and the suppression of PV interneurons facilitates ocular dominance plasticity (Kuhlman et al., 2013).

However, monocular deprivation can only reveal so much about critical period plasticity; sensory deprivation constitutes an extreme form of plasticity and does not necessarily reflect the

plasticity mechanisms of normal development. Monocular deprivation involves the loss of excitation from the deprived eye, whereas typical critical period plasticity selectively strengthens weaker inputs despite constant feedforward excitation from both eyes. The activity of PV neurons and other inhibitory classes during normal visual experience have not been investigated during the critical period. Furthermore, once the eye opens, visual experience is stable across the lifespan. Sensory input and cortical state drive cortical responses (Ringach, 2009); if sensory input is constant, it seems likely that drivers of cortical state, namely neuromodulatory pathways, are causing differences in cortical processing and plasticity across maturation. How neuromodulation and inhibitory circuits converge to sculpt plasticity during the critical period is unknown.

To gauge cell type-specific changes in neuromodulation across development, we examined spontaneous and visually-evoked responses of layer 2/3 inhibitory interneurons *in vivo*. We used the Cre-lox system to selectively express GCaMP6s in each of the main inhibitory interneuron classes (Rudy, Fishell, Lee, & Hjerling-Leffler, 2011). Using resonant-scanning 2-photon microscopy, we recorded fluorescent changes in alert, head-fixed mice running or resting on a spherical treadmill. Because the basal forebrain is engaged during locomotion, running provided an indirect measure of cholinergic release (A. M. Lee et al., 2014). We made observations at P28, the peak of the critical period of V1, or at P56, a time-point well beyond critical period closure (Gordon & Stryker, 1996) and a commonly used age of study for adult mice.

3.2 SST interneurons show an age-dependent shift in cholinergic modulation

At P28, the spontaneous activities (recorded with a blank gray screen) of approximately 80% of SST cells were positively correlated with locomotion; by P56, the distribution of coefficients was significantly left-shifted closer to 0 (**Fig. 1a-b**), indicating that behavioral state had less impact on the SST cell population as a whole after critical period closure. While some

cells remained correlated to movement, these correlations were weaker than at P28, and more SST cells had a negative correlation to movement (approximately 40%). Visually evoked responses (recorded with non-repeating natural movies) of SST cells showed a similar trend, in which the median change in visually evoked GCaMP6s fluorescence was larger at P28 during periods of locomotion than during periods of still. By P56, however, state-dependent differences in visually evoked responses were absent (**Fig. 1c-d, Supplementary Fig. 1**).

Because the majority of SST cells are positively correlated with running at P28 but not at P56, we examined whether SST cells are differentially responsive to acetylcholine during the critical period. To do so, we measured acetylcholine-mediated responses of V1, layer 2/3 SST cells in acute brain slices using whole-cell patch-clamp recordings. SST cells were targeted by their co-expression of the red-fluorescent protein tdTomato. In agreement with earlier findings in which recordings were done in developing cortex (Chen, Sugihara, & Sur, 2015; Fanselow, Richardson, & Connors, 2008; Kawaguchi, 1997), SST cells recorded from P28 slices responded robustly to carbachol (2mM, bath application), a non-selective cholinergic agonist. This response was due to the direct actions of carbachol on SST cells, as carbachol provoked SST cell activity even when synaptic signaling of local excitatory and inhibitory neurons was blocked. At P56, by contrast, SST cells responded weakly, if at all to carbachol, despite healthy responses to current injections (**Fig. 1e-f**) indicating that SST cells are directly responsive to acetylcholine prior to critical period closure, but not thereafter. Resting membrane potential was unchanged (**Supplementary Fig. 2**), as most intrinsic electrophysiological changes during development happen prior to P28 (Lazarus & Huang, 2011; McCormick & Prince, 1987). To test the responsiveness of SST neurons to basal forebrain stimulation across age, we used mice bred to express Cre in both ChAT-positive and SST-positive neurons and injected Cre-dependent ChR2 into the basal forebrain and Cre-dependent GCaMP6s into V1 (**Fig. 1g-h, Supplementary Fig. 3**). While both cell subtypes are present in both areas, SST neurons of the basal forebrain do not project to the visual cortex (Do et al., 2016), and cortical ChAT+ neurons

make up less than 1% of all cortical interneurons (Gonchar, Wang, & Burkhalter, 2007). The basal forebrain was stimulated using an optical fiber, placed at an angle 0.5 mm above the nucleus basalis. We found that blue-light (~460nm) stimulation, administered in 10ms pulses, 25 times at 15Hz, had a differential effect on SST neurons across age groups: at P28, almost all recorded SST neurons increased their activity in response to basal forebrain stimulation. In contrast, at P56, SST cells showed on average no response, with some cells responding very weakly and some showing minimal suppression (**Fig. 1i-j**), as previously reported in adult mice (Alitto & Dan, 2012). Overall, there is an age-dependent component to SST cell activation by acetylcholine for a large proportion of the SST cell population, which may explain conflicting reports in the literature (Alitto & Dan, 2012; Chen et al., 2015; Fu et al., 2014; Polack, Friedman, & Golshani, 2013).

3.3 VIP interneurons consistently respond to acetylcholine across age

Because SST cells primarily receive inhibition from VIP cells (Soohyun Lee, Kruglikov, Huang, Fishell, & Rudy, 2013; Pfeffer, Xue, He, Huang, & Scanziani, 2013; Pi et al., 2013), we also measured VIP interneuron activity at both developmental time points. Behavioral state had a consistent impact on VIP activity across ages. *In vivo*, GCaMP6s responses in VIP cells were strongly enhanced during periods of locomotion at P28 and at P56 (**Fig. 2a-b**), and in acute slices, VIP cells fired robustly during carbachol application at both ages (**Fig. 2c-d**). These measures extend earlier findings, from either developing or mature cortex, that VIP cells respond strongly to acetylcholine (Chen et al., 2015; Fu et al., 2014; Kawaguchi, 1997). Given that VIP cells are reliably responsive to acetylcholine and strongly inhibit SST cells, we tested whether carbachol would evoke varied inhibitory currents in SST cells (presumably via VIP-mediated inhibition) at both P28 and P56. Under voltage-clamp with a high chloride internal solution, IPSCs were clearly evident in SST cells at both ages following the application of

carbachol (**Fig. 3**), indicating that cholinergic activation of VIP cells invariably inhibit SST cells and their other targets across maturation.

3.4 PV interneurons are differentially inhibited during cholinergic modulation across age

SST cells send inhibitory input to all other cell types, including fast-spiking PV cells, which in turn target the perisomatic region of pyramidal cells (Markram et al., 2004; Pfeffer et al., 2013). Therefore, a second possible outcome of SST-mediated inhibitory drive is suppression of PV cells and the subsequent disinhibition of pyramidal cell somas (Chen et al., 2015; Cottam, Smith, & Häusser, 2013). With this in mind, we examined GCaMP6s responses of PV cells in alert, head-fixed mice, during periods of locomotion and rest, at P28 and P56. At P28, spontaneous responses of PV cells were poorly correlated with running, displaying a distribution of coefficients centered at 0. By P56, their responses were largely positively correlated with running (**Fig. 4a-b**). Similar shifts were observed during visual stimulation with natural movies (**Fig. 4c-d**), with PV cell amplitudes strongly facilitated during running at P56, but not at P28. Whole-cell recordings from PV cells in acute cortical slices showed no direct responses to carbachol at either P28 or P56 (**Fig. 4e-f**), suggesting that the modulation of their responses *in vivo* during running is indirect, consistent with other findings (Alitto & Dan, 2012). In acute slices, carbachol induced large GABA-mediated inhibitory currents in PV cells at P28 **(Fig. 4g-h)**. At P56, this inhibitory drive was significantly weakened, corresponding with the loss of cholinergic responsivity of SST cells. Thus, during locomotion and cholinergic release, PV cell activity is somewhat suppressed during the critical period and enhanced in adulthood – a developmental shift opposite to what we found in SST cells.

3.5 Summary and discussion

These data describe age and state-dependent changes in inhibitory activity across maturation. We find that a large proportion of SST cells respond to locomotion and basal

forebrain stimulation during the critical period but not thereafter. This shift can explain contrary findings across experimental preparations: electrophysiological recordings often use tissue from pups postnatal day P21 or younger (Chen et al., 2015; Kawaguchi, 1997), and *in vivo* studies more often use adults (Alitto & Dan, 2012; Fu et al., 2014). It is worth noting that even in adult mice, some SST cells respond to locomotion; this corroborates findings that there are SST cells that are either inhibited or activated in adult V1 during movement (Polack et al., 2013; Reimer et al., 2014). We find that during basal forebrain stimulation, some SST neurons weakly activate during cholinergic release in adult mice. The age-dependent difference in amplitude could reflect changes in cholinergic receptors: perhaps the underlying root of these differences lies in the loss of nicotinic receptor modulation on SST cells. Another group has reported the upregulation of a transmembrane protein that inhibits nicotinic receptor activity, specifically at critical period closure (Morishita, Miwa, Heintz, & Hensch, 2010) but has yet to be linked to SST cells. Additionally, prior studies on SST populations suggest there is cell death that occurs within the SST population that coincides with critical period closure (Cavanagh & Parnavelas, 1988; Forloni, Hohmann, & Coyle, 1990). More studies focusing on age-specific changes within the heterogeneous population of SST cells are needed to explain the root cause of critical period closure, and functional groups of SST cells have yet to be characterized.

It appears that SST cells receive reliable inhibition during cholinergic release across maturation. This inhibition is most likely originating from VIP interneurons, which strongly inhibit SST cells (Pfeffer et al., 2013) and also respond to acetylcholine (Alitto & Dan, 2012; Arroyo, Bennett, Aziz, Brown, & Hestrin, 2012; SooHyun Lee, Hjerling-Leffler, Zagha, Fishell, & Rudy, 2010). In developing cortex, SST cells represent the crossroads of top-down and bottom-up cortical processing, receiving both local excitatory drive (Adesnik, Bruns, Taniguchi, Huang, & Scanziani, 2012; Silberberg & Markram, 2007) and fast nicotinic neuromodulatory input (Chen et al., 2015; Kawaguchi, 1997). It should be noted that we have described the function of inhibitory circuitry during high levels of arousal, during periods of running. Cortical state

fluctuates on a continuum, on a moment-to-moment basis even during quiet wakefulness (Harris & Thiele, 2011; Reimer et al., 2014). The diffuse expression of nicotinic and muscarinic receptors provides wide dynamic range based on the amount of cholinergic release (Alitto & Dan, 2012). Functional groups across various levels of arousal should be delineated across specific cells, cortical layers, brain regions, and age.

Furthermore, interactions among inhibitory interneurons and their contributions to cortical processing are not fully understood. The functional relevance of VIP to SST cells is particularly nebulous: the elevated response of VIP cells (and not SST) to acetylcholine in adult mice suggests that VIP suppresses SST during elevated arousal, and that this contributes to the desynchronized responses of pyramidal neurons during cholinergic release and associated behaviors, namely attention. However, the direct activation of SST cells is also capable of desynchronizing the cortex (Chen et al., 2015). This leaves the function of the VIP-to-SST pathway unclear in terms of cortical state across development. Computational work has shown that pathway-specific gating improves when SST and VIP cells receive concurrent inputs (Yang, Murray, & Wang, 2016). Our work suggests that VIP-mediated inhibition is still intact during development, but the relevance of this connection remains vague.

Our data also outlines a pathway to disinhibition via PV cells. Although not directly tested here, SST cells strongly inhibit PV cells in layer 2/3 of V1 (Cottam et al., 2013; Pfeffer et al., 2013), and SST cells and PV cells have mirrored shits in their correlation to movement while VIP cells remain stable. It remains unclear under what circumstances SST inhibitory drive occurs on PV cells in adulthood, and perhaps the dissolution of this pathway contributes to moderate adult plasticity. In adult mice that have learned a visual task, ensembles of PV and pyramidal neurons become more selective while SST cells are decorrelated, suggesting that the SST-PV pathway is not utilized in adulthood (Khan et al., 2018). These circuit motifs remain open for investigation in different behavioral states and across learning regimes.

The distinct modulation of SST cells in developing cortex has broad implications for

cortical processing, and our data suggests that pyramidal cell activity will also be impacted by altered inhibitory drive during periods of cholinergic release. The following chapters will focus on how these inhibitory changes affect somatic and dendritic activity in pyramidal neurons and the significance of elevated SST activity to the normal course of binocular development.

3.6 Figures

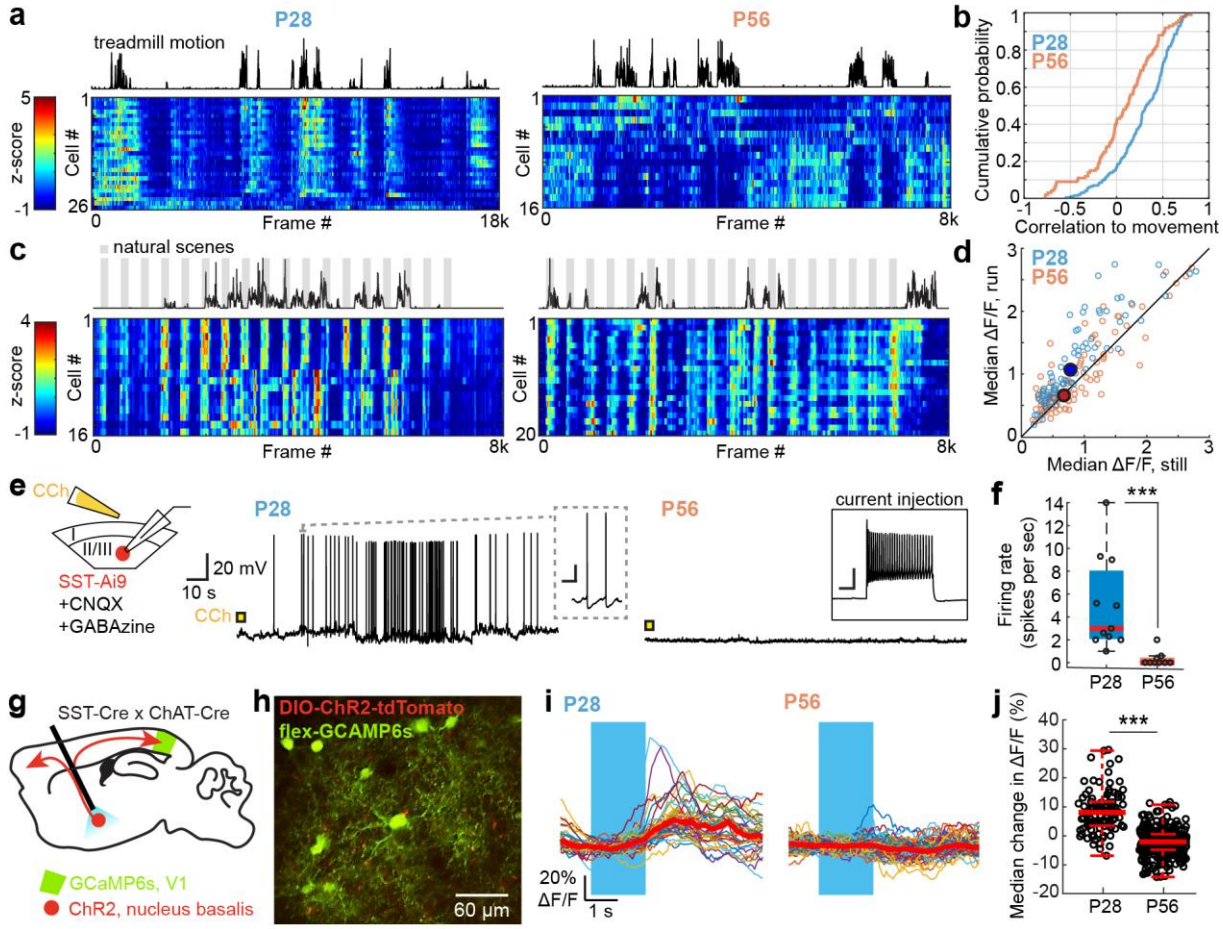

Figure 1. SST cells lose cholinergic sensitivity after critical period closure.

a, Heat map time series of z-scored GCaMP6s spontaneous responses of SST cells recorded in a P28 (left) and a P56 (right) mouse. Z-scores from individual cells plotted per frame (15.5 fps), with warmer colors indicating increases in fluorescence.

b, Cumulative distribution of correlation coefficients to running for all SST cells recorded in all mice at P28 (blue) and P56 (orange) (P28: n = 200; P56: n = 100; P = 5.73E-07, Mann-Whitney U test).

c, As in **a**, but for visually-evoked SST responses to non-repeating natural movie scenes.

d, Plot of each cell's visually-evoked median ΔF/F as a function of behavioral state, for all recorded cells (P28: n = 94, P56: n = 102; P28 run to P56 run, P = 4.63E-06, Mann-Whitney U test).

e, Left, schematic of experimental approach to whole-cell current clamp recordings of SST cell responses to bath application of carbachol (CCh) in the presence of synaptic blockers. Middle, example of responses recorded from a cell in a slice taken from a P28 mouse; inset shows evoked SST waveform, scale bar = 0.5 s and 10 mV. Right, example from a P56 mouse; inset shows a healthy response to current injection despite lack of response to CCh. In both plots, time of CCh application is denoted by the colored square.

f, Boxplot of SST cell firing rates evoked by CCh as a function of age (P28: n = 11; P56: n = 9; P = 2.90E-04, Mann-Whitney U test). For these plots, the red central mark denotes the median and the outer edges correspond to the upper and lower percentiles, with whiskers extending to 2σ.

g, Schematic of *in vivo* optical activation of the nucleus basalis with concurrent imaging in V1.

h, V1 SST cells labeled with GCaMP6s and visible ChR2+ butons from the nucleus basalis.

i, Representative SST cell activity after nucleus basalis stimulation (blue) in a P28 and a P56 mouse. The median response is shown in red (P28: n = 40; P56: n = 67).

j, Boxplot of median percent change in ΔF/F for SST cells after nucleus basalis stimulation as a function of age (P28: n = 101, P56: n = 345; P = 2.89E-33, Mann-Whitney U test). Boxplot parameters as described in **f**.

***P<0.001.

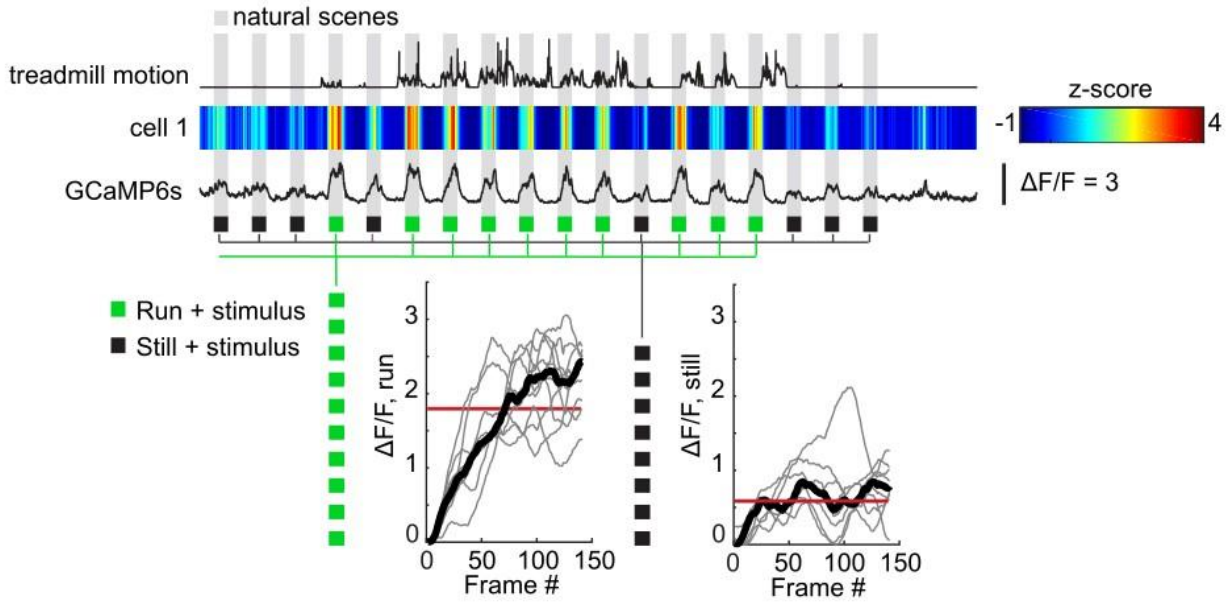

Supplementary Figure 1. Analysis of ΔF/F during still or run events.

Example P28 SST cell GCaMP6s responses during natural scenes with variable running activity. Treadmill motion and corresponding GCaMP6s signal is shown (15.5 fps), with grey bars denoting periods of visual stimulation. Z-score of GCaMP signal is denoted by the color map, and the trace denotes ΔF/F. Each presentation of the visual stimulus is classified as either a run (green) or still (black) trial. ΔF/F of GCaMP6s from all run (left) or still (right) trials are plotted. The median (red) of the median (black) ΔF/F response is taken to give an average value for still or run trials.

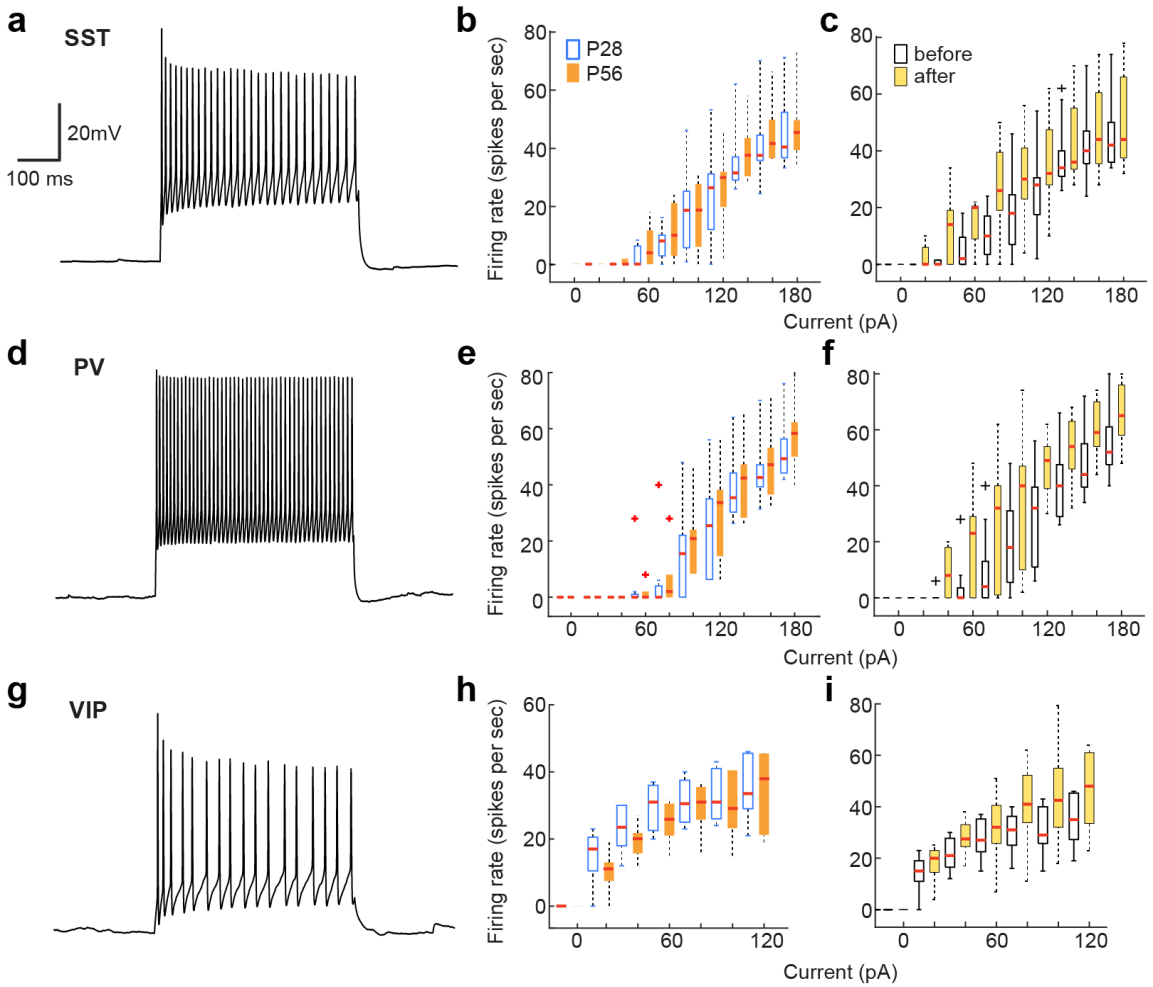

Supplementary Figure 2. Current injection responses for SST, PV, and VIP cells across age and condition.

a, Example current injection responses showing distinct waveform from a SST cell.

b, Change in voltage with 20 pA current steps for each cell type at P28 or P56. No significant change in excitability was found between age groups (P28, n = 11; P56, n = 9; two-way repeated measures ANOVA followed by Mann-Whitney U, all p values > 0.00625, Bonferroni corrected alpha).

c, Evoked spiking for all cells before carbachol application (open boxes) and following washout (yellow boxes), for respective cell types. No significant change in response to current injection was found after carbachol application (n = 19; repeated measures ANOVA followed by Wilcoxon signed-rank test, all p values >0.0055, Bonferroni corrected alpha).

d, Example PV cell waveform.

e, As in **b**, but for PV cells. No significant change in excitability was found between age groups (P28, n = 8; P56, n = 9; two-way repeated measures ANOVA followed by Mann-Whitney U, all p values > 0.0071, Bonferroni corrected alpha).

f, As in **c**, but for PV cell responses before and following carbachol washout. No significant change was found (n = 17; repeated measures ANOVA followed by Wilcoxon signed-rank test, all p values > 0.0062, Bonferroni corrected alpha).

g, Example VIP cell waveform.

h, As in **b**, but for VIP cells. No significant change in excitability was found between age groups (P28, n = 10; P56, n = 8; two-way repeated measures ANOVA followed by Mann-Whitney U, all p values > 0.0083, Bonferroni corrected alpha).

i, As in **c**, but for VIP cell responses before and following carbachol washout. No significant change was found (n = 18; repeated measures ANOVA followed by Wilcoxon signed-rank test, all p values > 0.0083, Bonferroni corrected alpha).

Boxplot parameters as in Fig. 1.

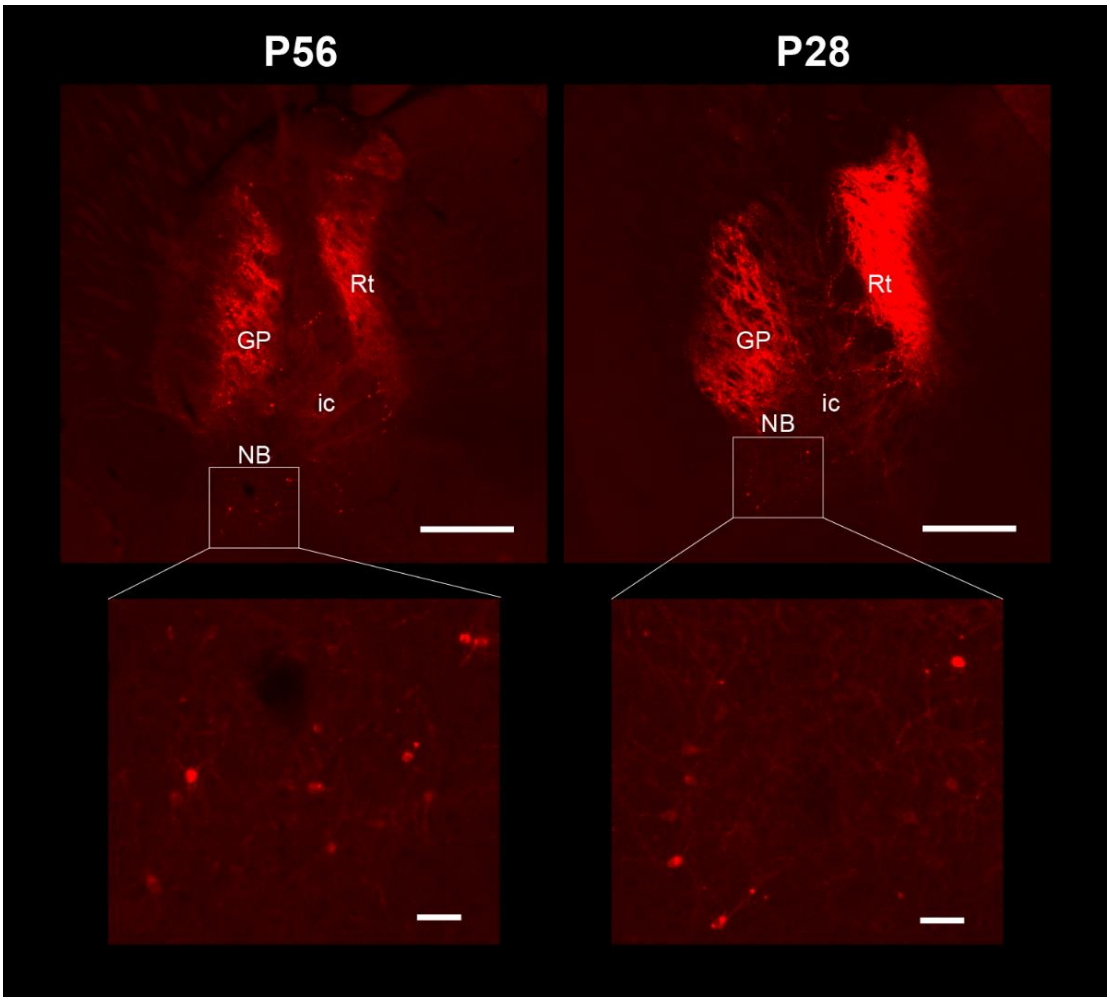

Supplementary Figure 3. Verification of basal forebrain injection sites in representative juvenile and adult mice.

ChAT-positive neurons in the nucleus basalis (NB), the dorsal region of the basal forebrain, expressing tdTomato-tagged ChR2. Cell bodies and their ascending projections to visual cortex are visible in a P56 (left) and P28 (right) mouse. The same injection coordinates were used for both ages, detailed in the methods section. Scale bars are 0.5 mm (top) and 60 µm (bottom). Abbreviations: internal capsule (ic), globus pallidus (GP), and thalamic reticular nucleus (Rt).

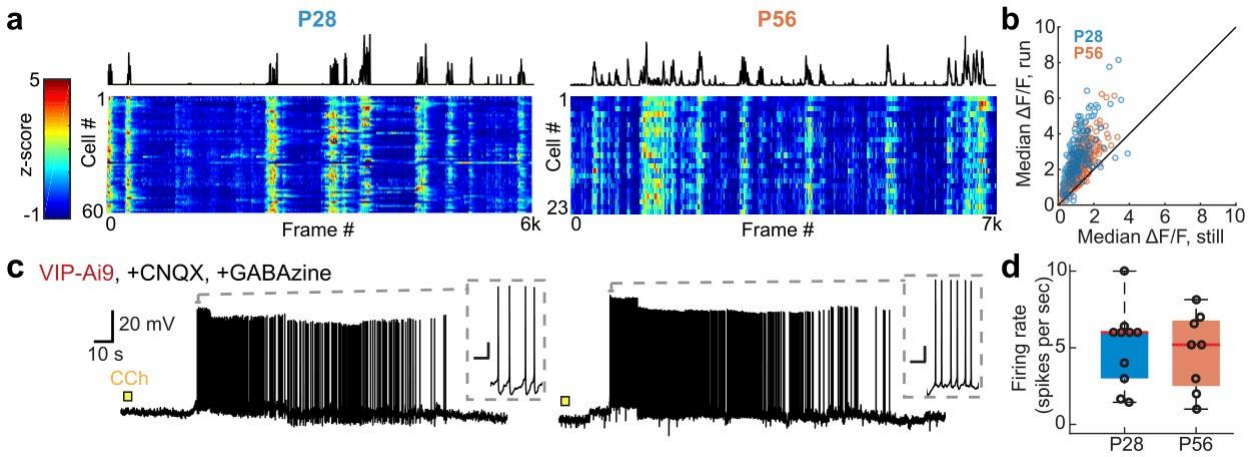

Figure 2. VIP cells show no age-dependent changes in cholinergic modulation.

a, As in Figure 1, example VIP cell populations from P28 and P56.

b, Plot of each cell's visually-evoked median ΔF/F as a function of behavioral state, for all recorded cells (P28, n = 220, still to run, P = 1.63E-64; P56, n = 305, P = 1.75E-60, Wilcoxon signed-rank test).

c, Example traces of VIP cell response to CCh application at P28 (left) and P56 (right). Recordings were made under current clamp and in the presence of synaptic blockers. Colored box denotes time of CCh application. Insets show evoked VIP cell waveform, scale bars = .25 s,10mV.

d, Boxplot of VIP cell firing rates evoked by CCh as a function of age (P28, n = 10, P56, n = 8, P = 0.9804, Mann-Whitney U test).

Boxplot parameters as in Fig. 1.

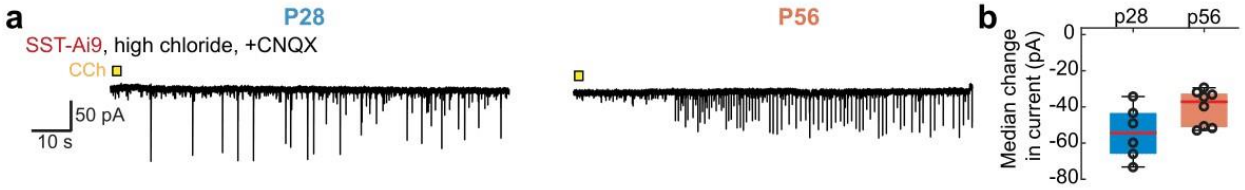

Figure 3. CCh-induced IPSCs on SST cells are present across development.

a, Example whole-cell recordings of SST cell responses to CCh in voltage-clamp mode at P28 (left) or P56 (right).

b, Median IPSC amplitudes evoked by CCh application for all recorded SST cells at P28 and P56 (P28, n = 6, P56, n=8, P = 0.4136, Mann-Whitney U test).

Boxplot parameters as in Fig. 1.

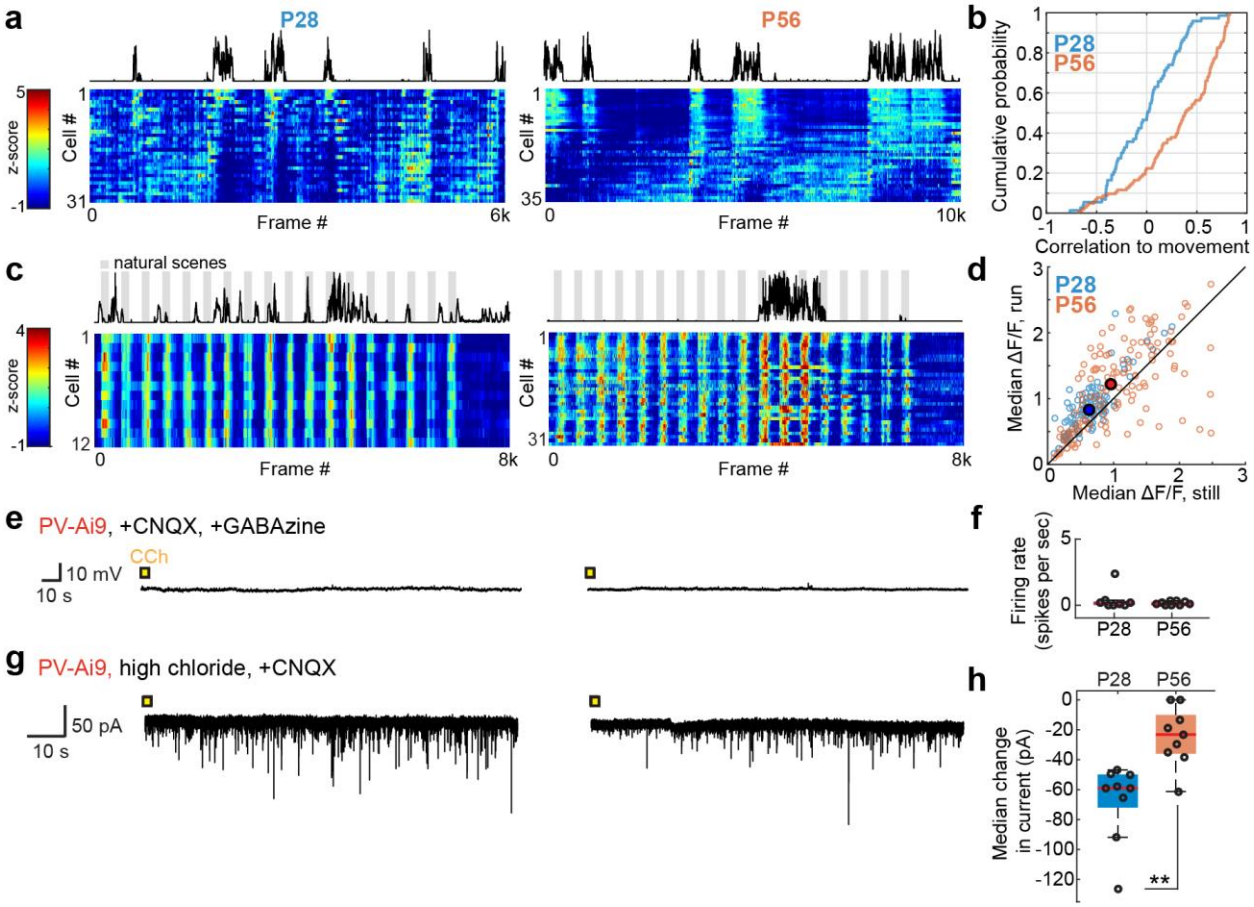

Figure 4. Inhibitory drive onto PV cells weakens after critical period closure.

a, Representative time series heat maps of spontaneous PV cell responses from P28 (left) and P56 (right) mice.

b, Cumulative distribution of coefficients to running for all recorded PV cells (P28: n = 73; P56: n = 103; P = 3.91E-08, Mann-Whitney U test).

c, As in **a,** but showing PV cell responses to non-repeating natural movie scenes.

d, Plot of each cell's visually-evoked median ΔF/F as a function of behavioral state, for all recorded cells (P28: n = 101; P56: n = 162; P28 run to P56 run, P = 8.82E-05, Mann-Whitney U test).

e, Example traces of PV cell response to CCh application at P28 (left) and P56 (right). Recordings were made under current clamp and in the presence of synaptic blockers. Colored box denotes time of CCh application.

f, Plot of CCh-evoked responses for all PV cells recorded in slices taken from P28 and P56 mice (P28: n=8; P56: n=9; P = 0.8346, Mann-Whitney U test).

g, Examples of voltage-clamped whole cell recordings of PV cell responses to bath application of CCh at P28 (left) or P56 (right).

h, Plot of median IPSC amplitude evoked by CCh application for all recorded PV cells at P28 and P56 (P28: n = 9; P56: n = 9; P = 0.0012, Mann-Whitney U test).

**P<0.01. Boxplot and heat map parameters as in Fig. 1.

3.7 References

Adesnik, H., Bruns, W., Taniguchi, H., Huang, Z. J., & Scanziani, M. (2012). A neural circuit for spatial summation in visual cortex. *Nature*, *490*(7419), 226–231. doi:10.1038/nature11526

Alitto, H. J., & Dan, Y. (2012). Cell-type-specific modulation of neocortical activity by basal forebrain input. *Frontiers in Systems Neuroscience*, *6*, 79. doi:10.3389/fnsys.2012.00079

Arroyo, S., Bennett, C., Aziz, D., Brown, S. P., & Hestrin, S. (2012). Prolonged disynaptic inhibition in the cortex mediated by slow, non-α7 nicotinic excitation of a specific subset of cortical interneurons. *The Journal of Neuroscience*, *32*(11), 3859–3864. doi:10.1523/JNEUROSCI.0115-12.2012

Bacci, A., Rudolph, U., Huguenard, J. R., & Prince, D. A. (2003). Major differences in inhibitory synaptic transmission onto two neocortical interneuron subclasses. *The Journal of Neuroscience*, *23*(29), 9664–9674.

Cavanagh, M. E., & Parnavelas, J. G. (1988). Development of somatostatin immunoreactive neurons in the rat occipital cortex: a combined immunocytochemical-autoradiographic study. *The Journal of Comparative Neurology*, *268*(1), 1–12. doi:10.1002/cne.902680102

Chattopadhyaya, B., Di Cristo, G., Higashiyama, H., Knott, G. W., Kuhlman, S. J., Welker, E., & Huang, Z. J. (2004). Experience and activity-dependent maturation of perisomatic GABAergic innervation in primary visual cortex during a postnatal critical period. *The Journal of Neuroscience*, *24*(43), 9598–9611. doi:10.1523/JNEUROSCI.1851-04.2004

Chen, N., Sugihara, H., & Sur, M. (2015). An acetylcholine-activated microcircuit drives temporal dynamics of cortical activity. *Nature Neuroscience*, *18*(6), 892–902. doi:10.1038/nn.4002

Cottam, J. C. H., Smith, S. L., & Häusser, M. (2013). Target-specific effects of somatostatin-expressing interneurons on neocortical visual processing. *The Journal of Neuroscience*, *33*(50), 19567–19578. doi:10.1523/JNEUROSCI.2624-13.2013

Do, J. P., Xu, M., Lee, S.-H., Chang, W.-C., Zhang, S., Chung, S., … Dan, Y. (2016). Cell type-specific long-range connections of basal forebrain circuit. *eLife*, *5*. doi:10.7554/eLife.13214

Fagiolini, M., Fritschy, J.-M., Löw, K., Möhler, H., Rudolph, U., & Hensch, T. K. (2004). Specific GABAA circuits for visual cortical plasticity. *Science*, *303*(5664), 1681–1683. doi:10.1126/science.1091032

Fanselow, E. E., Richardson, K. A., & Connors, B. W. (2008). Selective, state-dependent activation of somatostatin-expressing inhibitory interneurons in mouse neocortex. *Journal of Neurophysiology*, *100*(5), 2640–2652. doi:10.1152/jn.90691.2008

Ferando, I., & Mody, I. (2014). Interneuronal GABAA receptors inside and outside of synapses. *Current Opinion in Neurobiology*, *26*, 57–63. doi:10.1016/j.conb.2013.12.001

Forloni, G., Hohmann, C., & Coyle, J. T. (1990). Developmental expression of somatostatin in mouse brain. I. Immunocytochemical studies. *Brain Research. Developmental Brain Research*, *53*(1), 6–25. doi:10.1016/0165-3806(90)90120-N

Fu, Y., Tucciarone, J. M., Espinosa, J. S., Sheng, N., Darcy, D. P., Nicoll, R. A., … Stryker, M. P. (2014). A cortical circuit for gain control by behavioral state. *Cell*, *156*(6), 1139–1152. doi:10.1016/j.cell.2014.01.050

Gonchar, Y., Wang, Q., & Burkhalter, A. (2007). Multiple distinct subtypes of GABAergic neurons in mouse visual cortex identified by triple immunostaining. *Frontiers in Neuroanatomy*, *1*, 3. doi:10.3389/neuro.05.003.2007

Gordon, J. A., & Stryker, M. P. (1996). Experience-dependent plasticity of binocular responses in the primary visual cortex of the mouse. *The Journal of Neuroscience*, *16*(10), 3274–3286.

Harris, K. D., & Thiele, A. (2011). Cortical state and attention. *Nature Reviews. Neuroscience*, *12*(9), 509–523. doi:10.1038/nrn3084

Huang, Z. J., Kirkwood, A., Pizzorusso, T., Porciatti, V., Morales, B., Bear, M. F., … Tonegawa, S. (1999). BDNF regulates the maturation of inhibition and the critical period of plasticity in mouse visual cortex. *Cell*, *98*(6), 739–755. doi:10.1016/S0092-8674(00)81509-3

Kawaguchi, Y. (1997). Selective cholinergic modulation of cortical GABAergic cell subtypes. *Journal of Neurophysiology*, *78*(3), 1743–1747. doi:10.1152/jn.1997.78.3.1743

Kawaguchi, Y., & Kubota, Y. (1997). GABAergic cell subtypes and their synaptic connections in rat frontal cortex. *Cerebral Cortex*, *7*(6), 476–486. doi:10.1093/cercor/7.6.476

Khan, A. G., Poort, J., Chadwick, A., Blot, A., Sahani, M., Mrsic-Flogel, T. D., & Hofer, S. B. (2018). Distinct learning-induced changes in stimulus selectivity and interactions of GABAergic interneuron classes in visual cortex. *Nature Neuroscience*, *21*(6), 851–859. doi:10.1038/s41593-018-0143-z

Kuhlman, S. J., Olivas, N. D., Tring, E., Ikrar, T., Xu, X., & Trachtenberg, J. T. (2013). A disinhibitory microcircuit initiates critical-period plasticity in the visual cortex. *Nature*, *501*(7468), 543–546. doi:10.1038/nature12485

Lazarus, M. S., & Huang, Z. J. (2011). Distinct maturation profiles of perisomatic and dendritic targeting GABAergic interneurons in the mouse primary visual cortex during the critical period of ocular dominance plasticity. *Journal of Neurophysiology*, *106*(2), 775–787. doi:10.1152/jn.00729.2010

Lee, A. M., Hoy, J. L., Bonci, A., Wilbrecht, L., Stryker, M. P., & Niell, C. M. (2014). Identification of a brainstem circuit regulating visual cortical state in parallel with locomotion. *Neuron*, *83*(2), 455–466. doi:10.1016/j.neuron.2014.06.031

Lee, SooHyun, Hjerling-Leffler, J., Zagha, E., Fishell, G., & Rudy, B. (2010). The largest group of superficial neocortical GABAergic interneurons expresses ionotropic serotonin receptors. *The Journal of Neuroscience*, *30*(50), 16796–16808. doi:10.1523/JNEUROSCI.1869-10.2010

Lee, Soohyun, Kruglikov, I., Huang, Z. J., Fishell, G., & Rudy, B. (2013). A disinhibitory circuit mediates motor integration in the somatosensory cortex. *Nature Neuroscience*, *16*(11), 1662–1670. doi:10.1038/nn.3544

Markram, H., Toledo-Rodriguez, M., Wang, Y., Gupta, A., Silberberg, G., & Wu, C. (2004). Interneurons of the neocortical inhibitory system. *Nature Reviews. Neuroscience*, *5*(10), 793–807. doi:10.1038/nrn1519

McCormick, D. A., & Prince, D. A. (1987). Post-natal development of electrophysiological properties of rat cerebral cortical pyramidal neurones. *The Journal of Physiology*, *393*, 743–762.

Morishita, H., Miwa, J. M., Heintz, N., & Hensch, T. K. (2010). Lynx1, a cholinergic brake, limits plasticity in adult visual cortex. *Science*, *330*(6008), 1238–1240. doi:10.1126/science.1195320

Pfeffer, C. K., Xue, M., He, M., Huang, Z. J., & Scanziani, M. (2013). Inhibition of inhibition in visual cortex: the logic of connections between molecularly distinct interneurons. *Nature Neuroscience*, *16*(8), 1068–1076. doi:10.1038/nn.3446

Pi, H.-J., Hangya, B., Kvitsiani, D., Sanders, J. I., Huang, Z. J., & Kepecs, A. (2013). Cortical interneurons that specialize in disinhibitory control. *Nature*, *503*(7477), 521–524. doi:10.1038/nature12676

Polack, P.-O., Friedman, J., & Golshani, P. (2013). Cellular mechanisms of brain state-dependent gain modulation in visual cortex. *Nature Neuroscience*, *16*(9), 1331–1339. doi:10.1038/nn.3464

Reimer, J., Froudarakis, E., Cadwell, C. R., Yatsenko, D., Denfield, G. H., & Tolias, A. S. (2014). Pupil fluctuations track fast switching of cortical states during quiet wakefulness. *Neuron*, *84*(2), 355–362. doi:10.1016/j.neuron.2014.09.033

Ringach, D. L. (2009). Spontaneous and driven cortical activity: implications for computation. *Current Opinion in Neurobiology*, *19*(4), 439–444. doi:10.1016/j.conb.2009.07.005

Rudy, B., Fishell, G., Lee, S., & Hjerling-Leffler, J. (2011). Three groups of interneurons account for nearly 100% of neocortical GABAergic neurons. *Developmental Neurobiology*, *71*(1), 45–61. doi:10.1002/dneu.20853

Silberberg, G., & Markram, H. (2007). Disynaptic inhibition between neocortical pyramidal cells mediated by Martinotti cells. *Neuron*, *53*(5), 735–746. doi:10.1016/j.neuron.2007.02.012

Yang, G. R., Murray, J. D., & Wang, X.-J. (2016). A dendritic disinhibitory circuit mechanism for pathway-specific gating. *Nature Communications*, *7*, 12815. doi:10.1038/ncomms12815

Chapter 4: Pyramidal cells are differentially engaged across development

4.1 Introduction

Synaptic plasticity is a dendritic phenomenon, in which the activation of inputs and the resulting postsynaptic dendritic activity determines synaptic strength (Bittner, Milstein, Grienberger, Romani, & Magee, 2017; Golding, Staff, & Spruston, 2002; Kampa, Letzkus, & Stuart, 2006; Sjöström, Rancz, Roth, & Häusser, 2008). Somatic spikes and backpropagations contribute to but are not necessary for plasticity (Bittner et al., 2017; Golding et al., 2002; Hardie & Spruston, 2009; Kampa et al., 2006; Lisman & Spruston, 2005). Both global and local Ca^{2+} transients within the dendritic arbor reflect changes in synaptic potentiation (Cichon & Gan, 2015; Kitamura & Häusser, 2011; Sheffield & Dombeck, 2015). During learning in adult cortex, dendritic Ca^{2+} transients occur in a branch-specific manner, resulting in highly localized synaptic potentiation (Cichon & Gan, 2015; Kerlin et al., 2018). Plasticity rules within developing cortex are not known, nor how dendritic activity of the critical period might diverge from the adult.

It is clear that visual experience profoundly sculpts cortical circuitry during the postnatal critical period (Espinosa & Stryker, 2012; Levelt & Hübener, 2012), but thereafter, synaptic plasticity is gated by attention and reinforcement (de Villers-Sidani & Merzenich, 2011). Because visual input remains constant after eye-opening, changes in modulation likely contribute to the developmental switch in plasticity. Given that plasticity rules are dictated in part by dendritic and somatic activity, compartment-specific modulation of pyramidal neurons likely differs across critical period closure. Whole-cell measurements indicate that pyramidal neurons gain mature physiology by P21 (McCormick & Prince, 1987) and have adult-like firing rates during the critical period (Kuhlman et al., 2013). In acute slices, pyramidal neurons show a small, muscarinic depolarization in response to bath-applied acetylcholine (McCormick & Prince, 1985; but see Hedrick & Waters, 2015). During basal forebrain stimulation *in vivo*, pyramidal cells show muscarinic-dependent responses but primarily respond to amplified glutamatergic

thalamocortical inputs (Alitto & Dan, 2012; Goard & Dan, 2009). In the previous chapter, we have shown that SST cells have a developmental switch in cholinergic drive, subsequently affecting PV cells. Because these inhibitory interneurons target specific domains within excitatory cells (Markram et al., 2004), changes in inhibition has significant consequences for excitatory processing. Here, we examine dendritic and somatic activity of pyramidal neurons *in vivo* with respect to age and behavioral state.

4.2 Elevated behavioral state decorrelates dendritic branches at P28

To detect changes in dendritic inhibition, we measured visually-evoked dendritic Ca^{2+} responses (CaMKII-GCaMP6f) in the apical dendrites of V1, layer 2/3 pyramidal neurons from P28 and P56 age groups. Measurements of Ca^{2+} influx within dendritic branches reflect the level of synaptic activity (Kerlin et al., 2018; Kitamura & Häusser, 2011; Smith, Smith, Branco, & Häusser, 2013). Dendritic activity was evoked using non-repeating natural movie scenes. We recorded from sister dendrites, or bifurcations, within the imaging plane. Ca^{2+} signals were extracted from these branches and temporally deconvolved with the Vanilla algorithm (Berens et al., 2017), which detects significant increases in signal slope using a linear filter with a static nonlinearity. Deconvolution produces a probability measure of Ca^{2+} events, deemed 'event probability' (**Fig.5a-b**). Comparisons of deconvolved signals reflect what is found with ΔF/F (**Supplementary Fig. 4**).

At both ages, all dendritic branches had increased Ca^{2+} activity during running (**Fig. 5c**). This is consistent with other recordings of pyramidal dendrites (Murayama & Larkum, 2009) as well as pyramidal cell somas (Mineault, Tring, Trachtenberg, & Ringach, 2016; Niell & Stryker, 2010). Age-dependent differences did emerge when comparing either event probabilities or ΔF/F between sister branches. During periods of rest, the activity between sister dendrites were well synchronized; however, during the critical period, dendritic Ca^{2+} events became discordant during periods of movement. This was due to an increase in activity in one branch relative to its

sister, measured as a log-transformed fold change. This activity also resulted in a decrease in the correlation between sister branches (**Fig. 5d-e, Supplementary Fig. 5**). In contrast, behavioral state did not impact these measures in adult mice. Similar patterns of activity occurred in the absence of visual stimulation but were not statistically significant (**Supplementary Fig. 6a-c**). Evoked dendritic responses, therefore, appear to be uniquely modulated during the critical period, when branch-specific signals emerge as a function of behavioral state during visual experience.

4.3 P28 somatic responses in pyramidal neurons show increased firing during locomotion

To assess changes in somatic activity during movement across age, we measured GCaMP6f responses from pyramidal cell bodies at P28 and P56. In pyramidal cell somas, running increases activity, primarily due to an increase in excitatory drive (Alitto & Dan, 2012). Our results were consistent with this, as running increased pyramidal cell amplitudes during visually-evoked recordings at both P28 and P56 (**Fig. 5f**). In the absence of visual stimulation, there were no age-specific changes in pyramidal cell amplitudes during movement or the correlation to movement (**Supplementary Fig. 6d-e**). This indicates that there is no significant change of cholinergic input to pyramidal cells. However, at P28, visually-evoked somatic responses to natural movies were more positively correlated with locomotive state than were responses at P56 (**Fig. 5g**). When Ca^{2+} signals were deconvolved to yield inferred spike rate, we found a larger increase in event probability during running at P28 than at P56 (**Fig. 5h**). Therefore, there is a change in the indirect pathways that facilitate pyramidal cell excitation during the critical period. Based on our earlier findings, this could be a result of SST-mediated PV suppression and subsequent somatic disinhibition on pyramidal neurons.

4.4 SST-mediated inhibition produces branch-specific decoupling and somatic disinhibition

To directly test the hypothesis that SST cell activity drives both the emergence of branch-specific dendritic activity and disinhibition in pyramidal cells, we manipulated the activity of SST cells in adult visual cortex while simultaneously measuring visually-evoked dendritic or somatic activity. We first verified that the activity of SST cells expressing ChR2 could be controlled *in vivo* by light pulses via light-emitting diode (LED; 470nm). A viral vector containing Cre-dependent ChR2 (flex-ChR2-tdTomato) was injected into V1, layer 2/3 of SST-Cre mice, resulting in a restricted expression of ChR2 in SST cells. We found that trains of LED pulses of 10ms duration (15 Hz, 10 mW per mm^2) caused significant activation of SST neurons, measured via GCaMP6s fluorescent changes (**Supplementary Fig. 7**). In separate experiments, we co-expressed flex-ChR2-tdTomato and CaMKII-GCaMP6f: this enabled us to optically control SST cell activity while simultaneously monitoring GCaMP6f responses in pyramidal cell dendrites at P56 (**Fig. 6a**). Evoked activities of sister dendrites were recorded across periods of movement and rest to obtain a baseline level of dendritic activity and covariance. Under baseline conditions, sister dendrites had a pattern of activity typical for P56, as reported in Figure 5: overall Ca^{2+} activity increased during periods of movement, and no branch-specific changes occurred respective of behavioral state (fold change or correlation). This changed during and immediately after optogenetic stimulation SST cells. SST cell stimulation had little impact on overall dendritic Ca^{2+} activity in either locomotive or resting state (**Fig. 6b**), but effectively promoted the emergence of branch-specific dendritic activity when mice were running; the ratio of Ca^{2+} event probability between sister dendrites increased (**Fig. 6c)** and their correlation coefficients decreased (**Fig. 6d**). Responses of pyramidal cell somas were also elevated over baseline measurements during SST stimulation (**Fig. 6e-g**). Interestingly, these patterns of activity were only present when stimulation of SST cells occurred during locomotion. Therefore, with concurrent SST stimulation and neuromodulation in adult

cortex, a pattern of pyramidal cell activity similar to that of the juvenile critical period can be restored.

4.5. Summary and discussion

These data show the age-specific effects of inhibition and cholinergic modulation on pyramidal cell activity. During periods of high arousal, SST cells promote branch-specific dendritic activity and somatic disinhibition within pyramidal cells. Our findings corroborate the idea that SST-mediated inhibition produces nuanced effects on the dendritic tree during learning behavior (Bloss et al., 2016; Gidon & Segev, 2012): a recent report shows that SST interneurons contribute to branch-specific synaptic potentiation during motor learning (Cichon & Gan, 2015). The level of precision of SST-mediated inhibition *in vivo* is still unclear: a single point of inhibition can act precisely to quench activity at the synapse, effectively disrupting excitation along the branch, and it can also depress synapses from distal positions on the dendrite (Gidon & Segev, 2012).

Interestingly, inhibition from SST cells was not sufficient to reinstate dendritic decorrelation or somatic spiking in adult mice: movement was also required. Modulatory components involved in plasticity --such as muscarinic cholinergic receptors or norepinephrine-- could contribute to these effects. We did not directly investigate differences in pyramidal cell cholinergic modulation across development, but our recordings of state changes in the absence of visual stimulation indicate that there is no age-specific difference in cholinergic modulation of pyramidal cells. Visual input is needed for age-specific effects to occur within specific pyramidal cell compartments. This is consistent with the observations that cholinergic modulation of pyramidal cell responses are largely indirect, resulting from the modulation of other intracortical and distributed circuits (Alitto & Dan, 2012). Furthermore, while little is known about the impacts of inhibition at the level of the dendrite, even less is known about neuromodulation. *In vivo*, the diffuse effects of acetylcholine make determining circuit activity difficult, and different levels of

cholinergic release will drive differential activity within neural circuitry (Alitto & Dan, 2012). Additionally, there are other cholinergic circuits involved: L1 interneurons inhibit PV cells (Letzkus et al., 2011) and pyramidal cell dendrites (Abs et al., 2018). It is possible that these cholinergic circuits not investigated here contribute to our findings.

We also observe an increase in somatic firing during running at P28 relative to P56, concurrent with the inhibition of PV cells. Our data is consistent with a model in which disinhibition is a common circuit motif utilized during experience-dependent plasticity. Disinhibition driven by cholinergic mechanisms has been shown to be involved in plasticity during learning behaviors in adult mice (Abs et al., 2018; Froemke, Merzenich, & Schreiner, 2007; Letzkus et al., 2011). The disinhibition of pyramidal cells through the suppression of PV cells also occurs during experience-dependent plasticity driven by monocular deprivation during the critical period. PV interneurons lose excitatory drive and their pyramidal cell targets show increased firing rates, which drives the strengthening of the open eye (Kuhlman et al., 2013). Deprivation studies therefore reflect changes in bottom-up sensory processing, in which plasticity is incurred by eliminating the competitive input's activity. Our findings suggest that disinhibition is still utilized during competitive plasticity of normal development, but is engaged through cholinergic-mediated intracortical inhibition of PV cells. The timing of dendritic and somatic activity with cholinergic modulation has profound implications for plasticity rules, such as branch-specific potentiation (Losonczy, Makara, & Magee, 2008) and the aligning of dendritic and somatic spikes (Li, Morita, Robinson, & Small, 2013). Our findings provide a contextual framework for further investigations of *in vivo* cortical plasticity mechanisms.

4.6 Figures

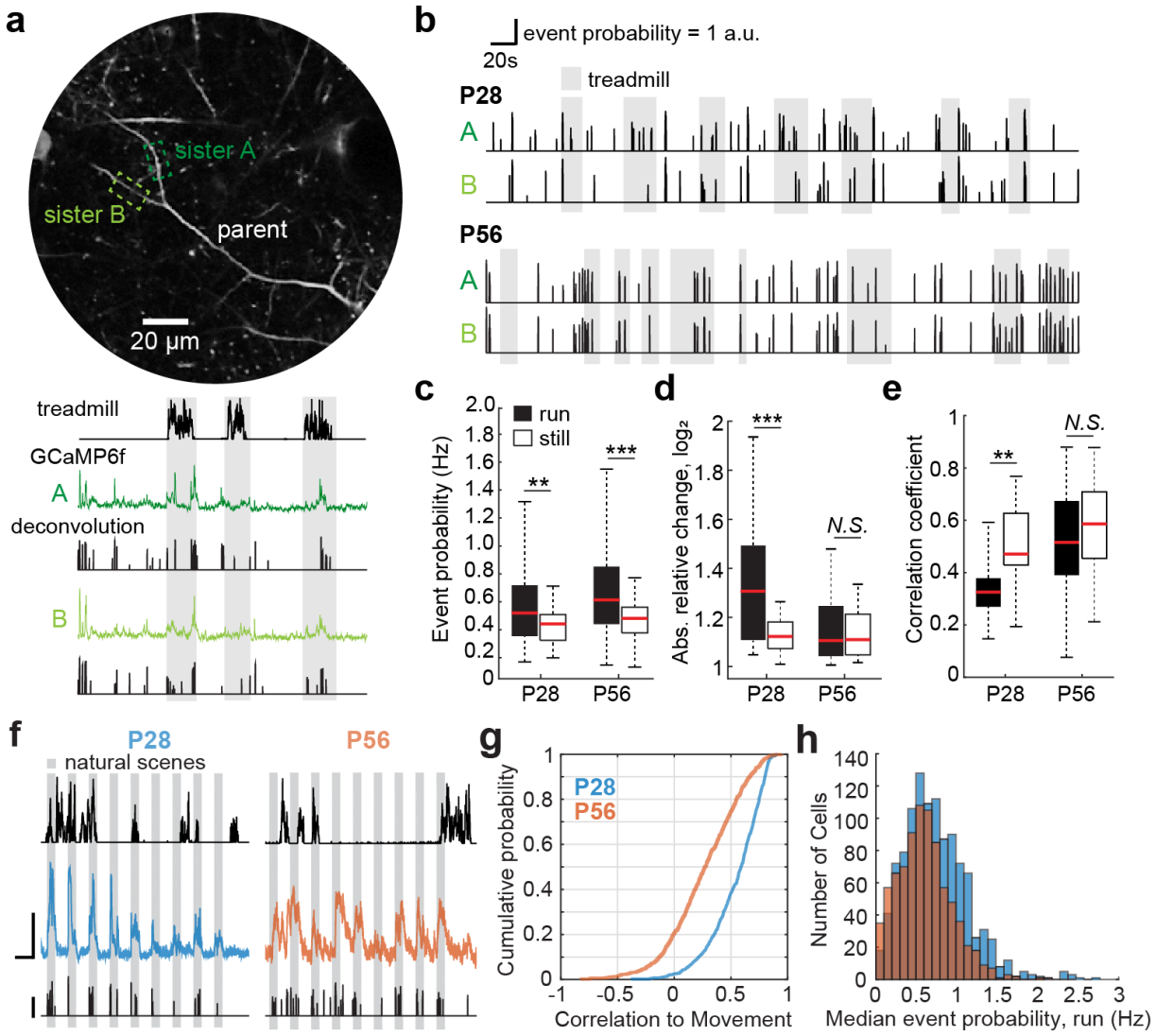

Figure 5. Movement evokes branch-specific Ca^{2+} spikes in apical L2/3 dendrites and increased somatic firing during the critical period.

a, Representative sister dendrites from a P56 mouse expressing GCaMP6f with corresponding time-series of Ca^{2+} signals, deconvolution, and treadmill motion (below). Deconvolution gives a probability of significant Ca^{2+} events. Gray bars mark periods of locomotion across traces.

b, Examples of temporally deconvolved GCaMP6f traces showing event probability in sister dendrites from a P28 and P56 mouse.

c, Boxplot of event probability by state and age (P28, n = 36 branches, P = 0.0128; P56, n = 96 branches, P = 4.19E-05, Wilcoxon signed-rank test).

d, Boxplots of absolute value of the log-transformed change in event probabilities between sister branches by age and state (P28, n = 18 branch pairs, P= 0.007; p56, n = 48 branch pairs, P=0.79, Wilcoxon signed-rank test).

e, Boxplots of correlation coefficients between event probability time series in sister branches (P28, n = 18 branch pairs , P = 0.0104; P56, n = 48 branch pairs , P = 0.05, Wilcoxon signed-rank test).

f, Example GCaMP6f responses to visual stimulation from a pyramidal cell soma at P28 (top) and P56 (bottom). 3 time series plots are shown: locomotion plotted at the top, z-scored GCaMP6f response in the middle, and the temporally deconvolved spike probability at the bottom. Scale bars are 20s and 2 S.D. Event probability scale bar = 1 a.u.

g, Plot of cumulative distributions of the correlation coefficients of GCaMP6s signals to running for all recorded pyramidal neurons (P28: n = 1187; P56: n = 821 cells; P = 5.03E-82, Mann-Whitney U test).

h, Histogram of median spike probability per second measured during running in P28 (blue) and P56 (orange) mice (P28: n = 1187; P56: n = 821; P = 0.0114, Mann-Whitney U test).

**P<0.01, ***P<0.001, *N.S.* = Not significant. Boxplot parameters as in Fig 1.

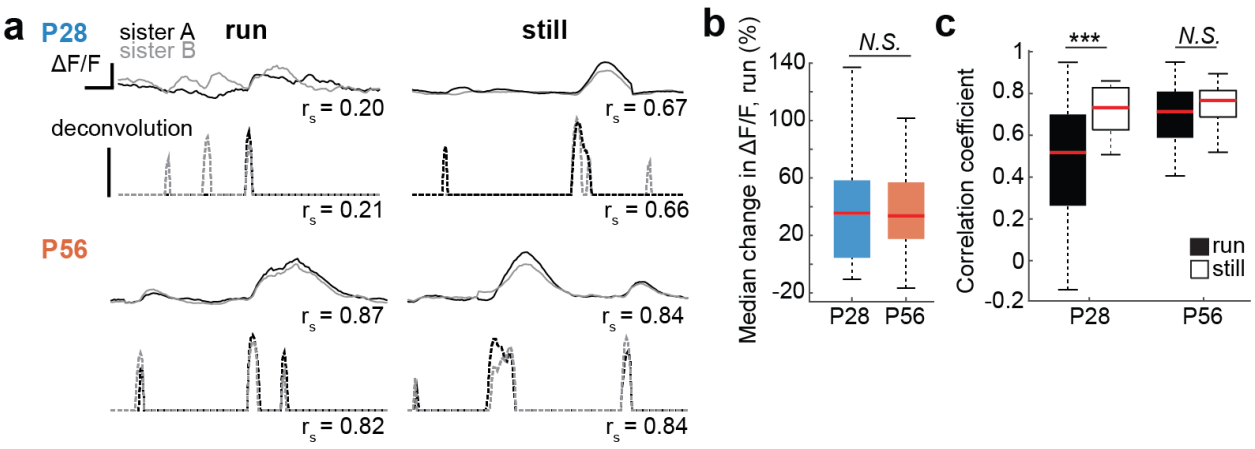

Supplementary Figure 4. Deconvolution and ΔF/F comparisons produce analogous findings in sister dendrites.

a, (Top) A time series showing ΔF/F and concurrent deconvolution for still and run epochs in a sister dendrite from a P28 mouse. Note the deconvolution is based in significant changes in slope. Spearman's correlation coefficients (r_s) are shown. ΔF/F has been filtered for clarity. (Bottom) same as top for sister dendrites from a P56 mouse. Scale bars are ΔF/F = 1, event probability = 1, a.u., over 1 sec.

b, Median percent change in ΔF/F from still to run, for all P28 and P56 branches (P28, n = 36 branches, P56, n = 96 branches, P = 0.6608, Mann-Whitney U test).

c, Correlation of ΔF/F between sister dendrites to movement at P28 or P56. (P28, n = 18 branch pairs, still to run, P = 5.36E-04; P56, n = 48 branch pairs**,** still to run, P = 0.043, Wilcoxon signed-rank test).

***P<0.001, *N.S.* = Not significant. Boxplot parameters as in Fig. 1.

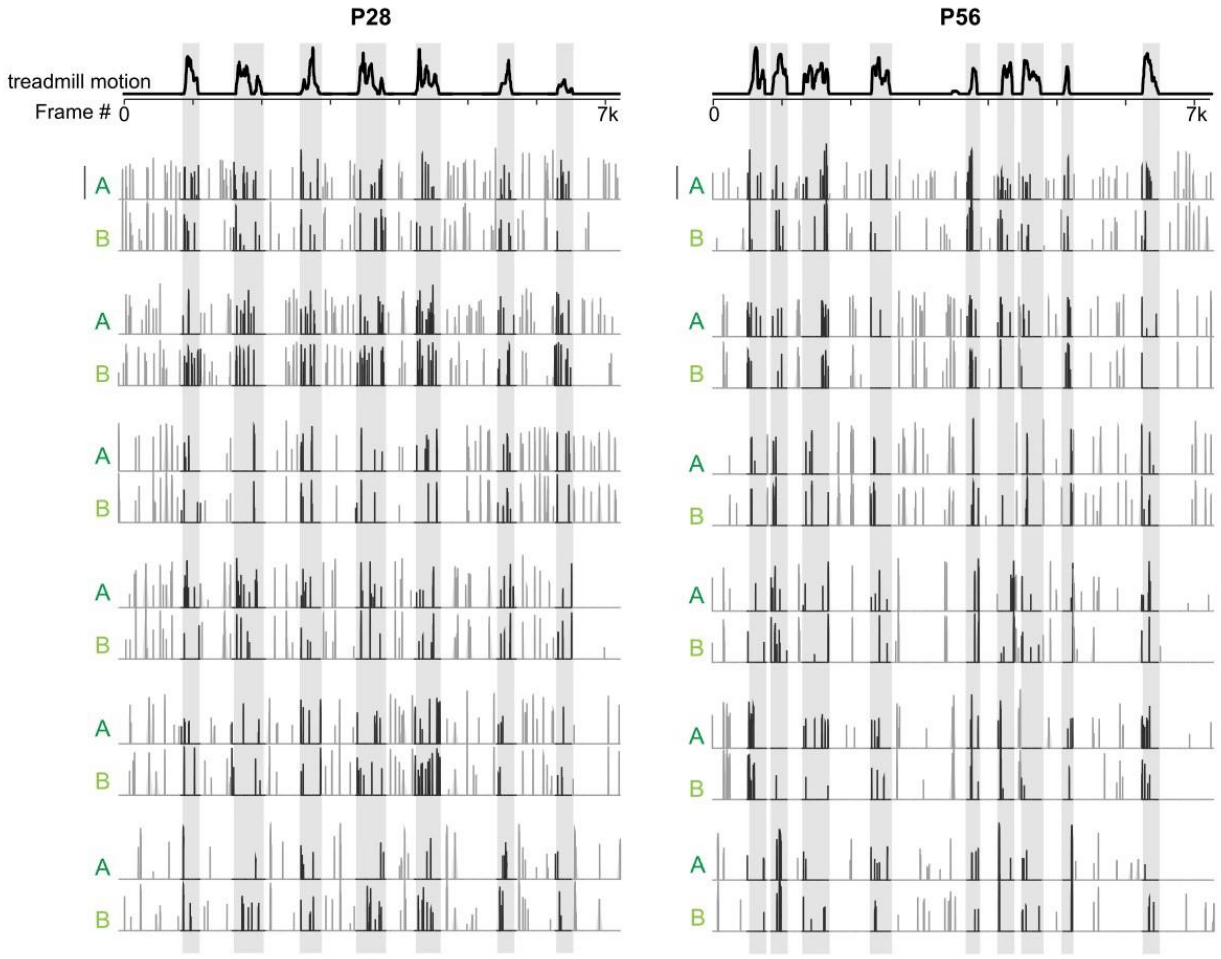

Supplementary Figure 5. Example visually-evoked P28 and P56 sister dendrite activity.

Examples of temporally deconvolved GCaMP6f traces showing event probability in sister dendrites from a P28 and P56 mouse. Gray bars mark periods of locomotion across traces. (Left) P28 sister dendrites show decorrelated activity during movement. (Right) P56 sister dendrites maintain synchronized activity across run and still epochs. Scale bar indicates event probability = 1 a.u.

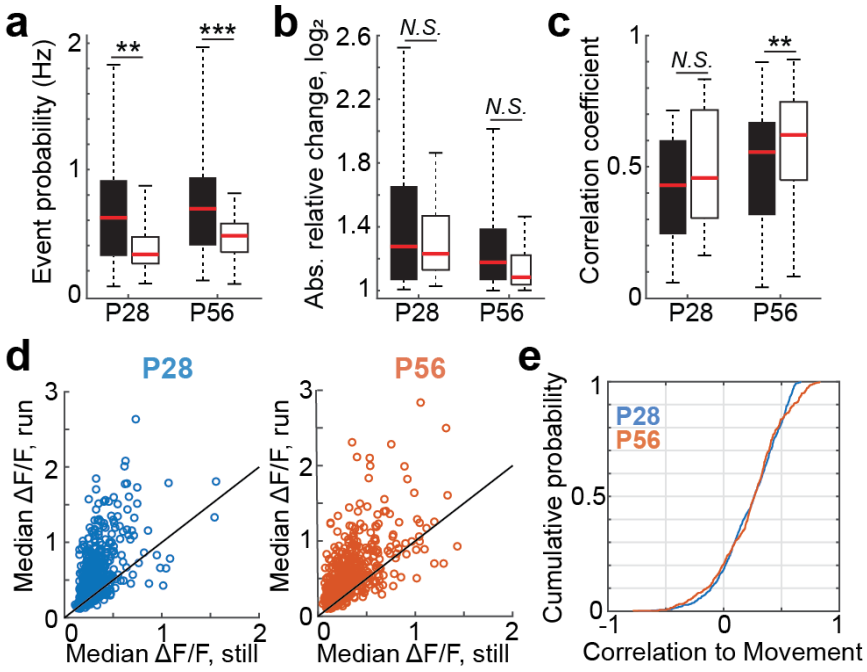

Supplementary Figure 6. P28 and P56 modulation of PYR cell somas and dendrites during spontaneous activity.

a, Boxplots of temporally deconvolved event probabilities of dendrites during gray screen viewing at P28 and P58 during in running and still conditions. (P28, n = 36 branches; still to run, P = 0.0044; P56, n = 96 branches, still to run, P = 4.36E-06, Wilcoxon sign rank test).

b, Boxplots of the fold change between sister branches as a function of age and behavioral state (P28, n = 18 branch pairs, P = 0.987; P56, n = 56 branch pairs, still to run, P = 0.02, Wilcoxon sign rank test).

c, Boxplots of the correlation coefficients between event probability time series of sister branches as a function of age and behavioral state (P28, n = 18 branch pairs, P = 0.2914; P56, n = 56 branch pairs, still to run, P = 0.0042, Wilcoxon sign rank test).

d, Plot of each cell's visually-evoked median ΔF/F as a function of behavioral state, for all recorded cells, at P28 and P56, in the absence of visual stimulation (P28, n = 563 cells, still to run, P = 4.31E-60; P56, n = 723 cells, P = 1.94E-89, Wilcoxon sign rank test).

e, Plot of cumulative distributions of the correlation coefficients of GCaMP6f signals to running for all recorded pyramidal neurons while viewing a gray screen. (P28: n = 860 cells; P56: n = 513 cells; P = 0.993, Mann-Whitney U test).

**P<0.01, ***P<0.001, *N.S.* = Not significant. Boxplot parameters as in Fig. 1.

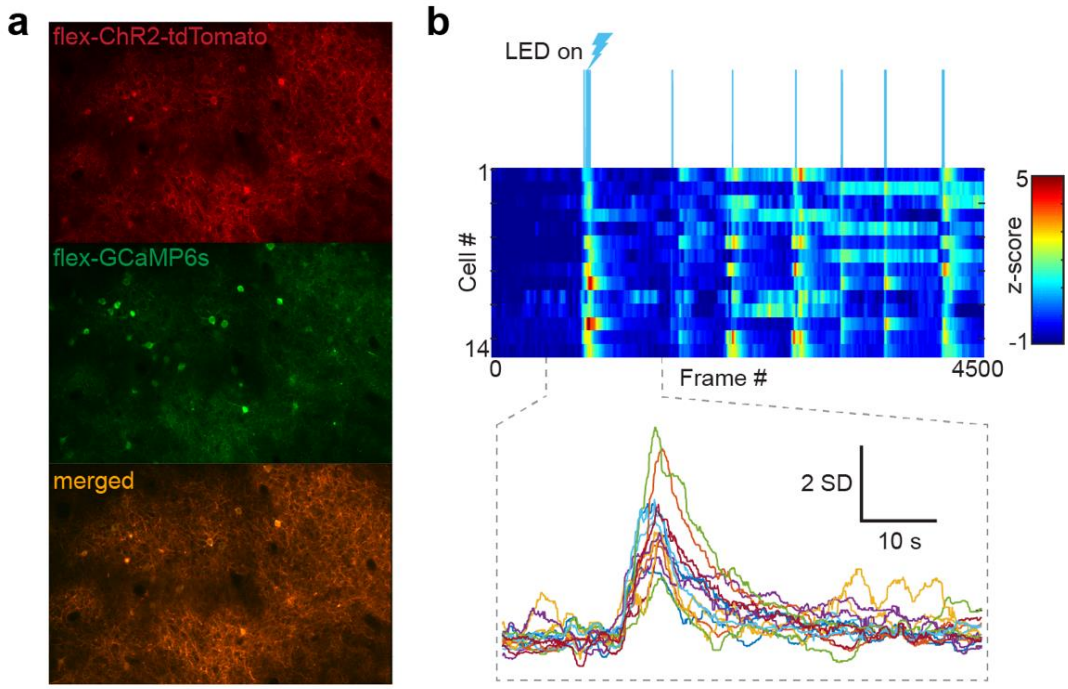

Supplementary Figure 7. Verification of ChR2-driven SST cell activity *in vivo*.

a, SST cells expressing both ChR2-tdTomato and GCaMP6s.

b, Representative time series heat map of SST cell GCaMP6s responses to optogenetic stimulation. Z-scores from individual cells plotted per frame (15.5 fps); color scale is -1 to 5 z-scores. (Top) Blue bars denote LED light pulses. (Bottom) Inset showing z-scored traces and significant increase in GCaMP6 signal for 14 cells.

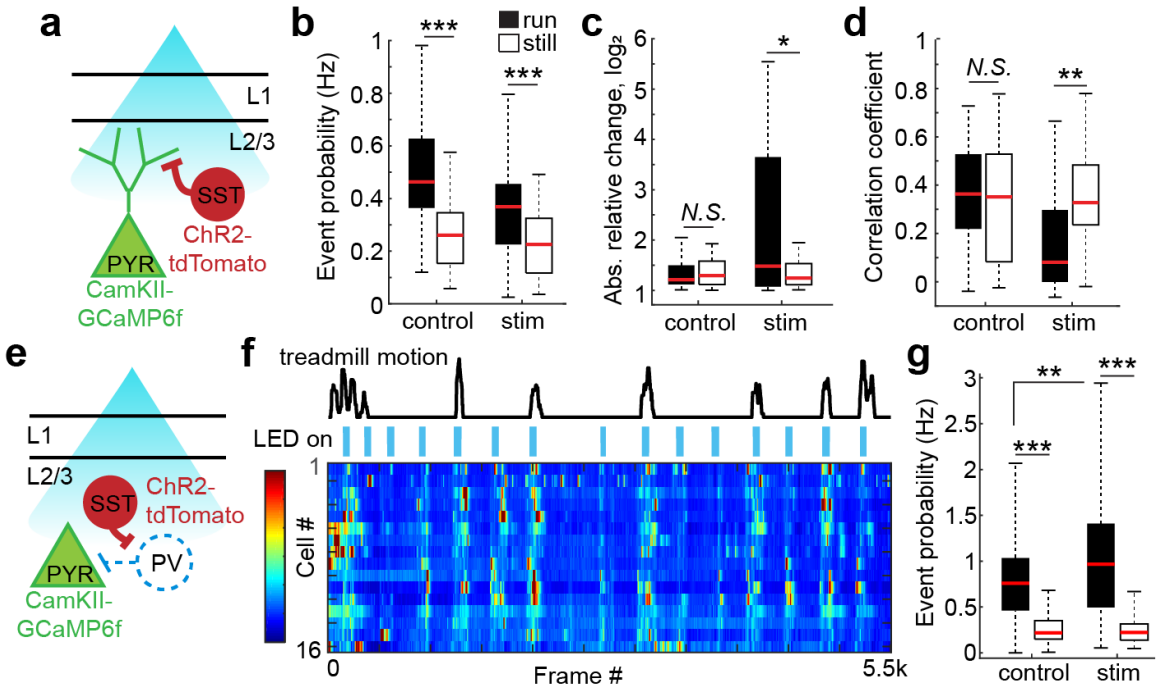

Figure 6. Optogenetic stimulation of SST cells increases compartmentalized dendritic responses and somatic firing in P56 mice.

a, Schematic of optogenetic setup, in which blue light drives L2/3 SST cells expressing ChR2-tdTomato, and time series responses of pyramidal cell dendrites expressing CaMKII-GCaMP6f are recorded in P56 mice.

b, Boxplots of temporally deconvolved event probabilities of dendrites in P56 mice recorded during before (control) and during (stim) blue light stimulation trials in running and still conditions (n = 82 branches; control still to run, P = 4.16E-05; stim still to run, P = 4.96E-10, Wilcoxon signed-rank test).

c, Boxplots of the absolute value of the log-transformed change between sister branches as a function of SST optogenetic stimulation and behavioral state (n = 41 branch pairs; control still to run, P = 0.2735; stim still to run, P = 0.0232, Wilcoxon signed-rank test).

d, Boxplots of the correlation coefficients between event probability time series of sister branches in P56 mice as a function of SST optogenetic stimulation and behavioral state (n = 41 branch pairs; control still to run, P = 0.9535; stim still to run, P = 0.0044, Wilcoxon signed-rank test).

e, As in **a**, with the exception that pyramidal cell somas are recorded.

f, Representative time series heat map of pyramidal cell responses in a P56 mouse with optogenetic stimulation of SST cells. Z-scores from individual cells plotted per frame (15.5 fps); color scale is -1 to 5 z-scores. Top, black trace denotes locomotion; blue bars denote optogenetic stimulation.

g, Boxplots of GCaMP6f spike probabilities as a function of behavioral state recorded from pyramidal cell somas in P56 mice before (control) or during (stim) optogenetic SST cell stimulation (n = 79; control still to run, P = 1.14E-11, stim still to run, P = 1.10E-11, stim run to control run, P = 6.00E-03, Wilcoxon signed-rank test with post-hoc Bonferroni correction).

*P<0.05, **P<0.01, ***P<0.001, *N.S.* = Not significant. Boxplot parameters as in Fig 1.

4.7 References

Abs, E., Poorthuis, R. B., Apelblat, D., Muhammad, K., Pardi, M. B., Enke, L., … Letzkus, J. J. (2018). Learning-Related Plasticity in Dendrite-Targeting Layer 1 Interneurons. *Neuron*. doi:10.1016/j.neuron.2018.09.001

Alitto, H. J., & Dan, Y. (2012). Cell-type-specific modulation of neocortical activity by basal forebrain input. *Frontiers in Systems Neuroscience*, *6*, 79. doi:10.3389/fnsys.2012.00079

Berens, P., Freeman, J., Deneux, T., Chenkov, N., McColgan, T., Speiser, A., … Bethge, M. (2017). Community-based benchmarking improves spike inference from two-photon calcium imaging data. *BioRxiv*. doi:10.1101/177956

Bittner, K. C., Milstein, A. D., Grienberger, C., Romani, S., & Magee, J. C. (2017). Behavioral time scale synaptic plasticity underlies CA1 place fields. *Science*, *357*(6355), 1033–1036. doi:10.1126/science.aan3846

Bloss, E. B., Cembrowski, M. S., Karsh, B., Colonell, J., Fetter, R. D., & Spruston, N. (2016). Structured Dendritic Inhibition Supports Branch-Selective Integration in CA1 Pyramidal Cells. *Neuron*, *89*(5), 1016–1030. doi:10.1016/j.neuron.2016.01.029

Cichon, J., & Gan, W.-B. (2015). Branch-specific dendritic Ca(2+) spikes cause persistent synaptic plasticity. *Nature*, *520*(7546), 180–185. doi:10.1038/nature14251

de Villers-Sidani, E., & Merzenich, M. M. (2011). Lifelong plasticity in the rat auditory cortex: basic mechanisms and role of sensory experience. *Progress in Brain Research*, *191*, 119–131. doi:10.1016/B978-0-444-53752-2.00009-6

Espinosa, J. S., & Stryker, M. P. (2012). Development and plasticity of the primary visual cortex. *Neuron*, *75*(2), 230–249. doi:10.1016/j.neuron.2012.06.009

Froemke, R. C., Merzenich, M. M., & Schreiner, C. E. (2007). A synaptic memory trace for cortical receptive field plasticity. *Nature*, *450*(7168), 425–429. doi:10.1038/nature06289

Gidon, A., & Segev, I. (2012). Principles governing the operation of synaptic inhibition in dendrites. *Neuron*, *75*(2), 330–341. doi:10.1016/j.neuron.2012.05.015

Goard, M., & Dan, Y. (2009). Basal forebrain activation enhances cortical coding of natural scenes. *Nature Neuroscience*, *12*(11), 1444–1449. doi:10.1038/nn.2402

Golding, N. L., Staff, N. P., & Spruston, N. (2002). Dendritic spikes as a mechanism for cooperative long-term potentiation. *Nature*, *418*(6895), 326–331. doi:10.1038/nature00854

Hardie, J., & Spruston, N. (2009). Synaptic depolarization is more effective than back-propagating action potentials during induction of associative long-term potentiation in hippocampal pyramidal neurons. *The Journal of Neuroscience*, *29*(10), 3233–3241. doi:10.1523/JNEUROSCI.6000-08.2009

Hedrick, T., & Waters, J. (2015). Acetylcholine excites neocortical pyramidal neurons via nicotinic receptors. *Journal of Neurophysiology*, *113*(7), 2195–2209. doi:10.1152/jn.00716.2014

Kampa, B. M., Letzkus, J. J., & Stuart, G. J. (2006). Requirement of dendritic calcium spikes for induction of spike-timing-dependent synaptic plasticity. *The Journal of Physiology*, *574*(Pt 1), 283–290. doi:10.1113/jphysiol.2006.111062

Kerlin, A., Mohar, B., Flickinger, D., MacLennan, B. J., Davis, C., Spruston, N., & Svoboda, K. (2018). Functional clustering of dendritic activity during decision-making. *BioRxiv*. doi:10.1101/440396

Kitamura, K., & Häusser, M. (2011). Dendritic calcium signaling triggered by spontaneous and sensory-evoked climbing fiber input to cerebellar Purkinje cells in vivo. *The Journal of Neuroscience*, *31*(30), 10847–10858. doi:10.1523/JNEUROSCI.2525-10.2011

Kuhlman, S. J., Olivas, N. D., Tring, E., Ikrar, T., Xu, X., & Trachtenberg, J. T. (2013). A disinhibitory microcircuit initiates critical-period plasticity in the visual cortex. *Nature*, *501*(7468), 543–546. doi:10.1038/nature12485

Letzkus, J. J., Wolff, S. B. E., Meyer, E. M. M., Tovote, P., Courtin, J., Herry, C., & Lüthi, A. (2011). A disinhibitory microcircuit for associative fear learning in the auditory cortex. *Nature*, *480*(7377), 331–335. doi:10.1038/nature10674

Levelt, C. N., & Hübener, M. (2012). Critical-period plasticity in the visual cortex. *Annual Review of Neuroscience*, *35*, 309–330. doi:10.1146/annurev-neuro-061010-113813

Li, X., Morita, K., Robinson, H. P. C., & Small, M. (2013). Control of layer 5 pyramidal cell spiking by oscillatory inhibition in the distal apical dendrites: a computational modeling study. *Journal of Neurophysiology*, *109*(11), 2739–2756. doi:10.1152/jn.00397.2012

Lisman, J., & Spruston, N. (2005). Postsynaptic depolarization requirements for LTP and LTD: a critique of spike timing-dependent plasticity. *Nature Neuroscience*, *8*(7), 839–841. doi:10.1038/nn0705-839

Losonczy, A., Makara, J. K., & Magee, J. C. (2008). Compartmentalized dendritic plasticity and input feature storage in neurons. *Nature*, *452*(7186), 436–441. doi:10.1038/nature06725

Markram, H., Toledo-Rodriguez, M., Wang, Y., Gupta, A., Silberberg, G., & Wu, C. (2004). Interneurons of the neocortical inhibitory system. *Nature Reviews. Neuroscience*, *5*(10), 793–807. doi:10.1038/nrn1519

McCormick, D. A., & Prince, D. A. (1985). Two types of muscarinic response to acetylcholine in mammalian cortical neurons. *Proceedings of the National Academy of Sciences of the United States of America*, *82*(18), 6344–6348. doi:10.1073/pnas.82.18.6344

McCormick, D. A., & Prince, D. A. (1987). Post-natal development of electrophysiological properties of rat cerebral cortical pyramidal neurones. *The Journal of Physiology*, *393*, 743–762.

Mineault, P. J., Tring, E., Trachtenberg, J. T., & Ringach, D. L. (2016). Enhanced spatial resolution during locomotion and heightened attention in mouse primary visual cortex. *The Journal of Neuroscience*, *36*(24), 6382–6392. doi:10.1523/JNEUROSCI.0430-16.2016

Murayama, M., & Larkum, M. E. (2009). Enhanced dendritic activity in awake rats. *Proceedings of the National Academy of Sciences of the United States of America*, *106*(48), 20482–20486. doi:10.1073/pnas.0910379106

Niell, C. M., & Stryker, M. P. (2010). Modulation of visual responses by behavioral state in mouse visual cortex. *Neuron*, *65*(4), 472–479. doi:10.1016/j.neuron.2010.01.033

Sheffield, M. E. J., & Dombeck, D. A. (2015). Calcium transient prevalence across the dendritic arbour predicts place field properties. *Nature*, *517*(7533), 200–204. doi:10.1038/nature13871

Sjöström, P. J., Rancz, E. A., Roth, A., & Häusser, M. (2008). Dendritic excitability and synaptic plasticity. *Physiological Reviews*, *88*(2), 769–840. doi:10.1152/physrev.00016.2007

Smith, S. L., Smith, I. T., Branco, T., & Häusser, M. (2013). Dendritic spikes enhance stimulus selectivity in cortical neurons in vivo. *Nature*, *503*(7474), 115–120. doi:10.1038/nature12600

Chapter 5: SST-mediated inhibition is necessary for binocular matching

5.1 Introduction

Thus far, we have characterized functional circuitry during normal experience across maturation. One outstanding question arises from our dataset: how does cholinergic drive on SST interneurons impact experience-dependent plasticity? Most investigations of the critical period have utilized monocular deprivation to infer molecular and cellular contributions to plasticity, but this paradigm does not reflect experience-dependent plasticity of the typically developing visual cortex. In normal development, thalamic drive is intact from both eyes, and visual experience is needed to strengthen the ipsilateral input while maintaining the contralateral input (Crair, Gillespie, & Stryker, 1998; Faguet, Maranhao, Smith, & Trachtenberg, 2009). By the end of the critical period, binocular neurons must be preferentially driven by ipsilateral and contralateral inputs that have similar orientation preferences. Early in the critical period, ipsilateral inputs often drive divergent orientation preferences relative to contralateral inputs within the same neuron, but by P31, these inputs are largely matched (Wang, Sarnaik, & Cang, 2010). Thus, visual experience drives binocular matching during the critical period. Here, we tested the effect of SST-mediated inhibition on the development of the binocular zone. We hypothesized that the inhibition from SST neurons and the resulting changes in pyramidal cell excitation are requirements for the experience-dependent refinement of binocular receptive fields.

5.2 Validation of chemogenetic suppression of SST cells

To understand the contribution of SST-mediated inhibition to the development of the visual cortex, we suppressed SST cell activity in layer 2/3 of V1 for a prolonged period during development using inhibitory designer receptors exclusively activated by designer drugs (DREADDs). These receptors can be selectively expressed in SST cells and activated with an

intraperitoneal injection of clozapine-N-oxide, or CNO (Cichon & Gan, 2015). Because strong suppression of inhibitory cells can induce seizures, we used a dose of CNO which does not induce seizures but still has measurable effects of cell activity for several hours (Alexander et al., 2009). *In vivo*, CNO is metabolized into clozapine, which crosses the blood-brain barrier and binds to both DREADDs and other endogenous targets, including serotonin and dopamine receptors (Gomez et al., 2017). We included control groups to probe for any residual effects of CNO or DREADD expression.

To test the efficacy of DREADDs on SST cells, we selectively expressed Cre-dependent hM4Di-DREADD receptors in SST cells along with flex-GCaMP6s in adult mice. After two weeks of recovery and sufficient viral expression, we recorded SST cell activity before and after CNO administration. Baseline activity was collected by recording SST cell responses to natural movie scenes (**Supplementary Fig. 8a, top**). CNO was then administered systemically via intraperitoneal injection (2.5mg/kg), and evoked responses from the same cells were recorded at time points of 2, 4, and 8 hours later. We find that following CNO administration, SST cells have significantly lower evoked amplitudes (**Supplementary Fig. 8a-b**). In separate experiments without viral expression of DREADDs, SST cells did not show significant changes in amplitude after the same dose of CNO at any time point (**Supplementary Fig. 8b**), indicating that without the expression of DREADDs, any indirect effects of clozapine do not impact evoked activity of SST cells. In contrast, SST cells which co-expressed the hM4Di receptor showed significant decreases in evoked amplitudes following CNO administration, with an average reduction of 25% ΔF/F at 2 hours and 35% ΔF/F at 4 hours. After 8 hours, SST cells showed partial recovery from CNO-induced suppression, and some cells had average evoked amplitudes indistinguishable from baseline measurements.

5.3 Reduction of SST cell activity during the critical period preferentially affects inputs from the ipsilateral eye

During the normal progression of binocular development, the ipsilateral input is most sensitive to experience (Crair et al., 1998; Faguet et al., 2009). In order to specifically suppress SST cell activity and measure activity driven by ipsilateral and contralateral inputs in binocular neurons, we expressed hM4Di-DREADDs in SST cells and CaMKII-GCaMP6f in excitatory cells. Two additional groups acted as controls, in which mice did not receive either the DREADD viral vector or CNO. Virus injections occurred at P10, and craniotomies were performed at P21. Following 3 days of recovery, P24 mice were given intraperitoneal injections of CNO (2.5mg/kg) every 8-12 hours but continued to live in normal light conditions. Based on our validation experiments, SST cells are moderately suppressed throughout this period. On P28, after 12 or more hours from the last dose of CNO, the binocular zone in layer 2/3 was imaged. Ipsilateral and contralateral activity was selectively evoked by temporarily occluding the opposite eye, using a visual stimulus consisting of a static grating with randomized orientation and spatial frequency. The tuning of each neuron as well as its inferred (deconvolved) firing rate was assessed for each eye. Binocular neurons were classified post hoc as cells with significant ipsilateral and contralateral tuning, determined by a signal to noise ratio of 1.5 or greater.

We find that ipsilateral and contralateral afferents effectively drove binocular neurons in both control and experimental groups (**Figure 7a and d**). No differences across control groups were found, and these data were pooled for comparisons to experimental groups. Tuning of contralateral inputs, evaluated by the signal to noise ratio, was unaffected by SST suppression, but inferred spike rates increased moderately (**Figure 7a-c**). By contrast, responses evoked by ipsilateral eye stimulation were somewhat degraded: tuning had a lower signal to noise ratio and inferred firing rates were lower than in controls (**Figure 7d-f**). Therefore, SST cells appear to be involved in the selective strengthening of the ipsilateral input during the critical period; with reduced SST cell-mediated inhibition, the ipsilateral input worsens despite normal visual input.

5.4 Suppression of SST cells during the critical period prevents binocular matching

The most salient outcome of critical period plasticity in the visual cortex is the emergence of binocular matching, in which either ipsilateral or contralateral inputs drive similar tuning preferences within any given binocular neuron. At P20, most binocular cells have poorly matched orientation preferences between the two eyes, but with adequate visual experience by P31, the majority of the binocular population has ipsilateral and contralateral tuning preferences that differ by 10 degrees or less, which is comparable to adults at P60 (Wang et al., 2010). We hypothesized that suppression of SST cells during P24-P27 would interfere with experience-dependent refinement of the binocular zone.

From the same dataset described above, we assessed discrepancies in orientation preference between the two eyes at P28. Both experimental and control groups had binocular neurons with matched or unmatched orientation preference between ipsilateral and contralateral inputs (**Figure 7g**). Consistent with the findings from Wang et al. (2010), the majority of neurons in both control groups had minimal deviations in orientation tuning (**Figure 7h, top**). Thus, neither the presence of the hM4Di receptor nor the metabolism of CNO affected the development of binocular matching. In contrast, mice with DREADD-mediated suppression of SST cells had highly divergent tuning between the two eyes (**Figure 7h, bottom**). While monocular responses were largely intact, the suppression of SST cells resulted in the absence of matching between contralateral and ipsilateral inputs. Collectively, these findings indicate that SST cells mediate the maturation of ipsilateral eye inputs and binocular matching during normal development.

5.5 Summary and discussion

Here we show suppression of SST cells alters the strength of the ipsilateral input and degrades binocular matching. Throughout these experiments, mice retained normal visual experience; therefore, inhibitory drive from SST cells is necessary for the process in which

visual input sculpts cortical circuitry. Our findings are consistent with Wang et al. (2010), in which at P28, the majority of binocular neurons have similar orientation preferences between the two eyes. Additionally, Wang et al. (2010) report that after dark-rearing, which deters the development of the GABAergic system (Morales, Choi, & Kirkwood, 2002), binocular matching does not develop. Here, we demonstrate that without strong SST cell inhibitory drive, binocular matching cannot occur.

Given the close connectivity between SST and PV cells (Cottam, Smith, & Häusser, 2013; Pfeffer, Xue, He, Huang, & Scanziani, 2013), it is expected that DREADD-mediated suppression of SST cells will permit elevated PV cell activity, which likely contributes to the profound differences in binocular matching observed in this study. To date, studies of critical period plasticity and circuitry have largely focused on PV cells. What might be the outcome of these experiments if PV cells were selectively suppressed instead of SST cells? When PV cell activity is reduced, an ocular dominance shift can be invoked after critical period closure (Kuhlman et al., 2013). Our observations indicate that this suppression occurs during normal development via the SST-mediated disinhibitory circuit. If PV cells were suppressed during the critical period more so than usual, it is unclear if this would accelerate or degrade the integration of ipsilateral input. In isolation, a somatic action potential can broadly lower thresholds for excitation in the dendrite via backpropagation, but a general increase in somatic firing may not be sufficient to strengthen the weak ipsilateral input while the contralateral input is maintained. Emergent from our findings is a model in which arousal and visual experience drive patterns of both dendritic and somatic activity that facilitates binocular matching. Understanding the overall plasticity mechanism will elucidate how locally and/or globally-generated dendritic activity contributes to the rapid formation and elimination of synapses characteristic of the critical period.

Notably, while circuitry at P21 is more stable than at eye-opening (Anastasiades et al., 2016), inhibitory circuits are still developing throughout the critical period. PV cells show adult

physiological properties by P21 (Lazarus & Huang, 2011), but continue to innervate pyramidal neurons up to P28 (Chattopadhyaya et al., 2004). Interestingly, SST cells themselves show changes in decay time over this same period (Lazarus & Huang, 2011), indicating that their integration window becomes elongated during the critical period. Thus, our work is effectively a snapshot in a dynamically changing system. The morphology, physiology, and genetic expression of cortical neurons and interneurons will need to be detailed to understand plasticity mechanisms across maturation.

5.6 Figures

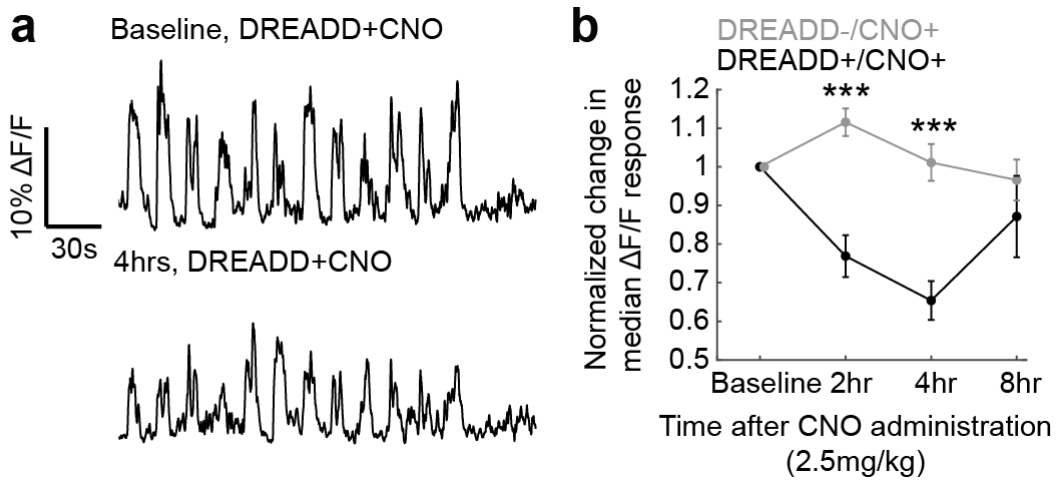

Supplementary Figure 8. Verification of chemogenetic control of SST cells using DREADDs.

a, (Top) Example evoked responses of a SST cell expressing DREADD receptors. (Bottom) Evoked responses from the same SST cell 4 hours after intraperitoneal administration of CNO (2.5mg/kg).

b, Measurement of change in median evoked ΔF/F in SST cells after CNO administration over an 8 hour period, in animals with or without DREADD expression (DREADD-/CNO+: n = 25 cells, DREADD+/CNO+: n = 21 cells. 2hr, DREADD- to DREADD+: P = 1.41E-04. 4hr, DREADD- to DREADD+: P = 7.98E-05. Wilcoxon signed-rank test). Error bars are S.E.M.

***P<0.001.

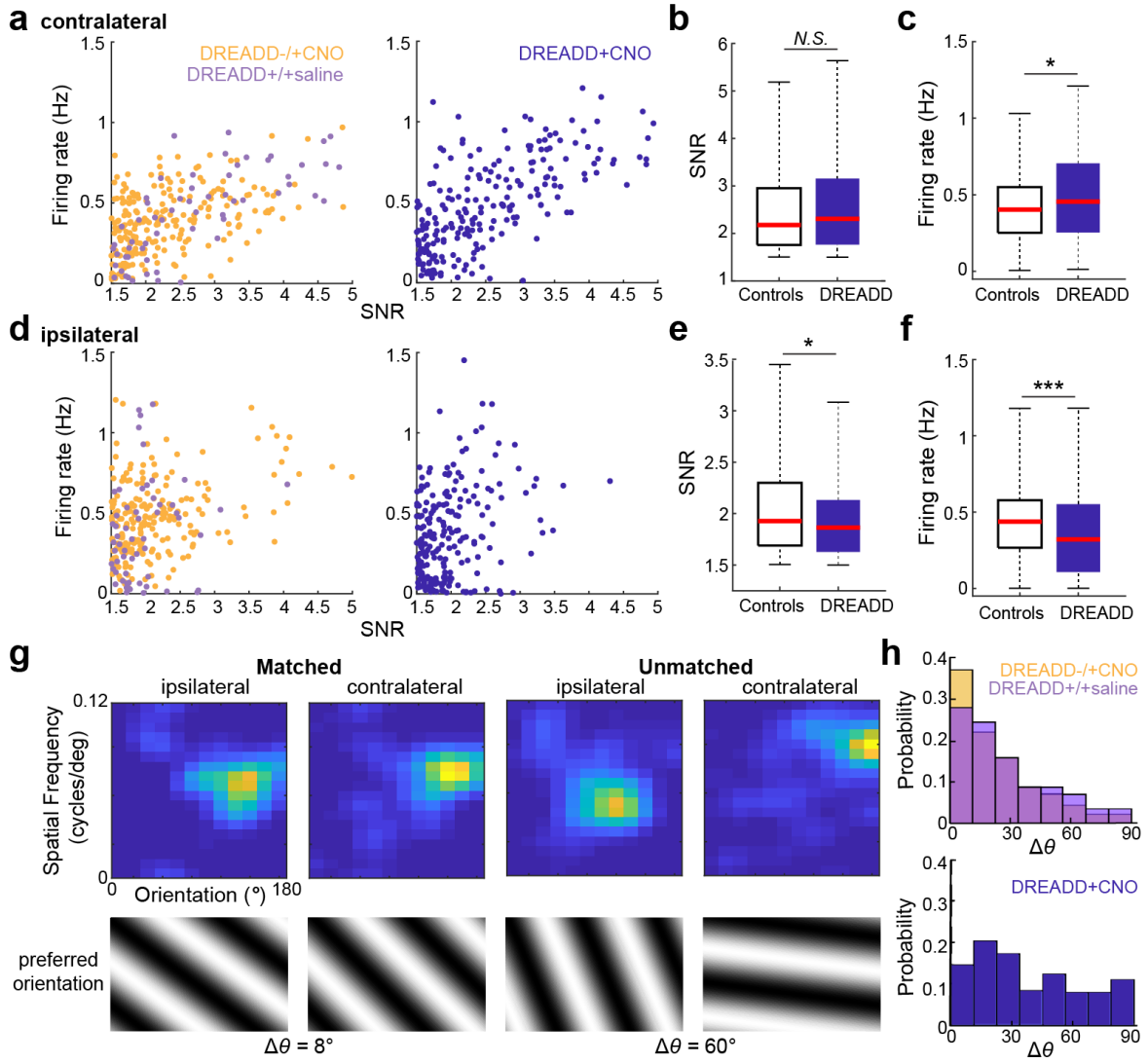

Figure 7. Suppression of SST cells during the critical period prevents binocular matching.
a, Contralateral response properties of all recorded binocular neurons in P28 mice, from control groups (left) or mice with DREADD-mediated SST cell suppression prior to recording (right). Controls include data from mice that expressed DREADD receptors but received saline and mice that did not have DREADD receptors that received CNO. Each cell's activity is plotted by deconvolved firing rate and the signal-to-noise ratio of the contralateral receptive field (DREADD-/+CNO, n = 223 cells; DREADD+/+saline, n = 60 cells; DREADD+CNO, n = 226 cells).

b, Boxplots of the signal-to-noise ratios of contralateral receptive fields for either pooled controls or the experimental group (Controls, n = 283 cells, DREADD, n = 226 cells, P = 0.3520, Mann-Whitney U test).

c, Boxplots of the inferred firing rate of contralateral responses in control or experimental groups (Controls, n = 283 cells, DREADD, n = 226 cells, P = 0.0145, Mann-Whitney U test).

d, As in **a**, but for ipsilateral responses.

e, Boxplots of signal-to-noise ratios of ipsilateral receptive fields for either control or experimental groups (Controls, n = 283 cells, DREADD, n = 226 cells, P = 0.0234, Mann-Whitney U test).

f, Boxplots of the inferred firing rate of ipsilateral responses in control or experimental groups (Controls, n = 283 cells, DREADD, n = 226 cells, P = 1.1637E-4, Mann-Whitney U test).

g, Example binocular neurons showing matched (left) or unmatched (right) ipsilateral and contralateral receptive fields. Plots are individually normalized to show the maximum response in the spatial frequency and orientation domains. Below, the preferred orientation is shown for each input, and the discrepancy in preferred orientation ($\Delta\theta$) is noted.

h, Histograms showing the probability distribution of $\Delta\theta$ in binocular neurons in either control (top) or experimental (bottom) groups. (Controls, n = 283 cells, DREADD+CNO, n = 226 cells, P = 2.67E-10, Mann-Whitney U test).

*P<0.05, ***P<0.001, *N.S.* = Not significant. Boxplot parameters as in Fig. 1.

5.7 References

Alexander, G. M., Rogan, S. C., Abbas, A. I., Armbruster, B. N., Pei, Y., Allen, J. A., … Roth, B. L. (2009). Remote control of neuronal activity in transgenic mice expressing evolved G protein-coupled receptors. *Neuron*, *63*(1), 27–39. doi:10.1016/j.neuron.2009.06.014

Anastasiades, P. G., Marques-Smith, A., Lyngholm, D., Lickiss, T., Raffiq, S., Kätzel, D., … Butt, S. J. B. (2016). GABAergic interneurons form transient layer-specific circuits in early postnatal neocortex. *Nature Communications*, *7*, 10584. doi:10.1038/ncomms10584

Chattopadhyaya, B., Di Cristo, G., Higashiyama, H., Knott, G. W., Kuhlman, S. J., Welker, E., & Huang, Z. J. (2004). Experience and activity-dependent maturation of perisomatic GABAergic innervation in primary visual cortex during a postnatal critical period. *The Journal of Neuroscience*, *24*(43), 9598–9611. doi:10.1523/JNEUROSCI.1851-04.2004

Cichon, J., & Gan, W.-B. (2015). Branch-specific dendritic Ca(2+) spikes cause persistent synaptic plasticity. *Nature*, *520*(7546), 180–185. doi:10.1038/nature14251

Cottam, J. C. H., Smith, S. L., & Häusser, M. (2013). Target-specific effects of somatostatin-expressing interneurons on neocortical visual processing. *The Journal of Neuroscience*, *33*(50), 19567–19578. doi:10.1523/JNEUROSCI.2624-13.2013

Crair, M. C., Gillespie, D. C., & Stryker, M. P. (1998). The role of visual experience in the development of columns in cat visual cortex. *Science*, *279*(5350), 566–570. doi:10.1126/science.279.5350.566

Faguet, J., Maranhao, B., Smith, S. L., & Trachtenberg, J. T. (2009). Ipsilateral eye cortical maps are uniquely sensitive to binocular plasticity. *Journal of Neurophysiology*, *101*(2), 855–861. doi:10.1152/jn.90893.2008

Gomez, J. L., Bonaventura, J., Lesniak, W., Mathews, W. B., Sysa-Shah, P., Rodriguez, L. A., … Michaelides, M. (2017). Chemogenetics revealed: DREADD occupancy and activation via converted clozapine. *Science*, *357*(6350), 503–507. doi:10.1126/science.aan2475

Kuhlman, S. J., Olivas, N. D., Tring, E., Ikrar, T., Xu, X., & Trachtenberg, J. T. (2013). A disinhibitory microcircuit initiates critical-period plasticity in the visual cortex. *Nature*, *501*(7468), 543–546. doi:10.1038/nature12485

Lazarus, M. S., & Huang, Z. J. (2011). Distinct maturation profiles of perisomatic and dendritic targeting GABAergic interneurons in the mouse primary visual cortex during the critical period of ocular dominance plasticity. *Journal of Neurophysiology*, *106*(2), 775–787. doi:10.1152/jn.00729.2010

Morales, B., Choi, S.-Y., & Kirkwood, A. (2002). Dark rearing alters the development of GABAergic transmission in visual cortex. *The Journal of Neuroscience*, *22*(18), 8084–8090.

Pfeffer, C. K., Xue, M., He, M., Huang, Z. J., & Scanziani, M. (2013). Inhibition of inhibition in visual cortex: the logic of connections between molecularly distinct interneurons. *Nature Neuroscience*, *16*(8), 1068–1076. doi:10.1038/nn.3446

Wang, B.-S., Sarnaik, R., & Cang, J. (2010). Critical period plasticity matches binocular orientation preference in the visual cortex. *Neuron*, *65*(2), 246–256. doi:10.1016/j.neuron.2010.01.002

Chapter 6: Discussion

6.1 Overview of findings

Our data define a functional neural circuit specific to the critical period, in which acetylcholine directly activates SST cells, and the resulting inhibitory drive enhances branch-specific dendritic responses and somatic spiking. After critical period closure, SST cells lose cholinergic input, and these pyramidal cell responses are no longer observable during simple sensory experience. It has long been accepted that inhibition and acetylcholine are needed for critical period plasticity (Bear & Singer, 1986; Levelt & Hübener, 2012; Rasmusson, 2000; Trachtenberg, 2015). The mechanism through which these components act, however, has not been clear. Our data identify SST cells and their control of dendritic and somatic spiking as the conduit. SST cells provide inhibition directly at synaptic inputs, and the gating of input is likely involved in a cortical plasticity mechanism. With less SST-mediated inhibition, binocular matching did not develop; conceivably, inhibition at particular dendritic synapses may be needed to facilitate matching and competition between strong (contralateral) and weak (ipsilateral) inputs. While it is not known how dendritic inhibition and somatic disinhibition interact to promote or discourage plasticity, or how similar critical period and adult cortical plasticity mechanisms are, the shift in cholinergic innervation of SST cells will have significant effects on cortical processing. The developmental switch at SST neurons likely underlies the transition from plasticity driven by passive sensory experiences to plasticity driven by rewarded or attended experiences.

6.2 Neuromodulation drives unique cortical processing during the critical period

We have described the differential activity of SST cells across development and the implications for dendritic and somatic activity in excitatory neurons. While SST cell activity is necessary for the emergence of branch-specific dendritic responses and somatic disinhibition, it

is not sufficient: concurrent SST cell activation and elevated behavioral state was needed to restore branch-specific responses and somatic spiking in adult cortex. The simplest explanation for this result is that coincident activity of SST inhibition and cholinergic depolarization must occur on pyramidal cells to foster this pattern of activity. Additionally, the release of norepinephrine could also contribute to this outcome; norepinephrine is released into the cortex during heightened arousal and is needed in addition to acetylcholine for critical period plasticity (Bear & Singer, 1986). Like acetylcholine, norepinephrine has diverse effects on GABAergic cell types, including the depolarization of SST cells (Kawaguchi & Shindou, 1998). Whether and how norepinephrine interacts with cortical circuitry specifically during the critical period is not known. Other neurotransmitters that may be released during changes in cortical state, such as serotonin, have yet to be studied in the context of critical period plasticity or the circuitry detailed here.

It should also be noted that because locomotion strongly engages the basal forebrain (A. M. Lee et al., 2014), the circuitry we have described is possibly unique to high levels of arousal. Muscarinic and nicotinic receptors are differentially expressed across excitatory and inhibitory populations, and different levels of cholinergic release will have differential outcomes in cortical processing (Alitto & Dan, 2012). In juvenile cortex, SST cells strongly respond to acetylcholine in micromolar amounts (Chen, Sugihara, & Sur, 2015), and our data indicate that adult SST cells are less susceptible to fluctuations in cortical state. Additionally, many studies have focused on the muscarinic activation of SST cells (Beierlein, Gibson, & Connors, 2000; Kawaguchi, 1997; Muñoz, Tremblay, Levenstein, & Rudy, 2017), but SST cells also show fast nicotinic responses (Chen et al., 2015; Urban-Ciecko, Jouhanneau, Myal, Poulet, & Barth, 2018). Given the strong age-dependent activation of SST cells by acetylcholine, it is likely that there is a change in nicotinic receptor expression on SST cells, although muscarinic receptors could also be downregulated after critical period closure. It is also possible that cholinergic receptors are inhibited by a transmembrane protein which is upregulated during critical period

closure (Morishita, Miwa, Heintz, & Hensch, 2010), but it is not known if this protein is found on SST cells. The age-dependent cholinergic activation of SST cells can explain some discrepancies in the literature: studies involving acute slices from juvenile cortex report robust SST spiking with cholinergic application (Chen et al., 2015; Fanselow, Richardson, & Connors, 2008; Kawaguchi, 1997), and *in vivo* studies done in adult mice show no SST response to basal forebrain stimulation (Alitto & Dan, 2012) or locomotion (Fu et al., 2014).

SST cells are a heterogeneous population, and functional groups must exist within SST cells given their morphological, physiological, and genetic diversity. A recent study shows that in adult mice, there are two classes of SST cells which are either depolarized or inhibited during locomotion (Reimer et al., 2014). Our data suggest that the majority of SST cells respond to acetylcholine during the critical period, but thereafter the response weakens significantly and may give rise to two distinct functional groups. There is also a decrease in the SST cell population across critical period closure (Cavanagh & Parnavelas, 1988; Gonchar, Wang, & Burkhalter, 2007); an interesting possibility is that SST cells with a robust response to acetylcholine undergo cell death following the critical period. Additionally, it is not known if the somatostatin hormone itself influences signaling or structural plasticity during development. Functional groups of SST cells and their engagement across development and the continuum of cortical state remain to be fully understood.

6.3 A switch in SST cell activation has broad implications for cortical circuits

Because SST cells inhibit all other classes of cortical neurons (Pfeffer, Xue, He, Huang, & Scanziani, 2013), their age-dependent switch in cholinergic excitability has consequences for many other circuits. SST cells strongly inhibit PV cells in visual cortex (Cottam, Smith, & Häusser, 2013; Pfeffer et al., 2013), and PV cells also form a feedforward inhibitory motif with pyramidal cells, as both pyramidal cells and PV cells receive thalamocortical input (Tremblay, Lee, & Rudy, 2016). During the critical period, PV cells are more inhibited during periods of

locomotion or with carbachol application. Basal forebrain activation decreases PV cell activity, increases glutamatergic activity through nicotinic receptors, and switches thalamic activity to a tonic firing mode (Goard & Dan, 2009; Kruglikov & Rudy, 2008), all of which facilitate the excitation of pyramidal cells. After the critical period closes, we find a decrease in IPSCs on PV cells during carbachol application, and thalamic feedforward inhibition appears to tighten during periods of locomotion. While we did not directly probe the connection between PV and SST cells, the change in cholinergic drive is only seen on SST cells and not VIP cells; thus, the maintenance and use of the SST-to-PV connection is unclear in adults. Our *in vivo* observations suggest that after the critical period, there are at least two functional groups of PV cells with differential responses to basal forebrain activity, consistent with other *in vivo* findings in adult mice (Alitto & Dan, 2012). It is possible that a partial or total loss of cholinergic activation of SST cells contributes to the formation of specific functional groups of both SST and PV cells.

We did not investigate changes in visual processing that may result from a developmental switch in SST cell activity. PV and SST cells contribute to visual processing via gain control and surround suppression, respectively (Adesnik et al., 2012; Atallah, Bruns, Carandini, & Scanziani, 2012). PV cells appear to have a divisive effect on evoked pyramidal cell responses, while SST cells sharpen selectivity (N. R. Wilson, Runyan, Wang, & Sur, 2012), although these assignments remain contentious. Interestingly, pyramidal-to-SST connections are strengthened via nicotinic activity (Urban-Ciecko et al., 2018), and the presence of strong nicotinic excitation in SST cells could facilitate the formation of disynaptic inhibitory circuits during development. This is consistent with the experience-dependent development of surround modulation (Pecka, Han, Sader, & Mrsic-Flogel, 2014). Visual acuity also develops during this time, and spatial acuity is known to increase during locomotion, due to the increase in gain in neurons tuned to high spatial frequencies (Niell & Stryker, 2010; Mineault, Tring, Trachtenberg, & Ringach, 2016). While the functional circuits needed to perform these operations are most likely in place at eye-opening, the cholinergic excitability of SST cells may contribute their

experience-dependent tuning, with the end result being mature visual acuity and stereopsis.

Our data show that VIP-positive cells in layer 2/3 do not change their cholinergic response as a function of age. Canonical circuits often show a pathway in which VIP cells can disinhibit pyramidal neurons through the suppression of SST cells and some PV cells (Pfeffer et al., 2013; Pi et al., 2013). The activation of both SST cells and VIP cells during development makes the role of VIP cells uncertain. However, computational modeling shows that synaptic gating on pyramidal dendrites is improved when SST cells and VIP cells are simultaneously active (Yang, Murray, & Wang, 2016). VIP cells likely contribute more to altering cortical state in adults, when they form the majority interneurons directly activated by cholinergic input. Our findings suggest SST cells are the site of convergence for top-down and bottom-up sensory processing during the critical period.

Several other cortical circuits not studied here could be also be involved in a critical period plasticity mechanism. Layer 1 (L1) inhibitory interneurons are strongly driven by acetylcholine (Alitto & Dan, 2012; Christophe et al., 2002; S. Lee, Hjerling-Leffler, Zagha, Fishell, & Rudy, 2010), and like SST cells in layer 2/3, L1 interneurons can also form a disinhibitory circuit by targeting PV cells in visual and auditory cortex (Letzkus et al., 2011). Furthermore, in auditory cortex, a specific subgroup of L1 interneurons expressing neuron-derived neurotrophic factor also receive inhibition primarily from SST interneurons and inhibit apical tuft dendrites of pyramidal neurons (Abs et al., 2018), forming a second possible disinhibitory pathway via SST cells. If present in visual cortex, this circuitry may also provide input needed for shaping excitatory responses during the critical period during increased cholinergic drive to SST cells. Another possible pathway not investigated here is the interhemispheric pathway mediated by L1 interneurons, which drive dendritic inhibition through GABA-B receptors (Palmer et al., 2012; Wozny & Williams, 2011). The development of L1 interneurons, their modulation, and their inputs and outputs across maturation is not known.

On a broader level, it is not known if the microcircuitry described here drives other forms

of sensory-dependent plasticity during development. In general, there is a relationship between experience-dependent refinement and the complexity of the receptive field formation: simpler receptive fields are refined earlier in development, such as for scotopic and photopic spectral sensitivity, and the integration of multiple receptive fields occurs later on, as in binocular matching (Harwerth, Smith, Crawford, & von Noorden, 1990). Plasticity mechanisms for simple receptive fields likely deviate from the model proposed here, because they occur prior to PV cell innervation at the soma (Chattopadhyaya et al., 2004). However, SST cells are present in the cortex at birth (Gonchar et al., 2007). While the development of SST cell dendritic innervation is unknown, this favors a hypothesis in which dendritic inhibition is central to juvenile plasticity mechanisms. Furthermore, cortical sensory regions differ in their functional processing, and thus will have different demands in terms of cortical wiring. For example, the developing auditory cortex in ferret shows an opposite trend in bilateral integration, in which ipsilateral and contralateral inputs are similar in strength at the onset of hearing, but in older animals the contralateral input is stronger (Mrsic-Flogel, Versnel, & King, 2006). Intracortical connectivity also varies from region to region and layer to layer, and locomotion will not necessarily inform other sensory representations as it does in visual cortex. While our findings from layer 2/3 in the visual cortex may not be directly applicable to plasticity mechanisms of other sensory regions, it is plausible that circuit functions such as branch-specific inhibitory control, dendritic and somatic decoupling, and somatic disinhibition are common functional motifs in the cortex, evoked through various microcircuits to achieve plasticity.

6.4 Towards a cortical plasticity mechanism

It remains an outstanding challenge to define plasticity mechanisms *in vivo* at the single-cell level with circuit-level context. Hebbian-based plasticity models are inadequate to describe *in vivo* observations of the developing visual cortex: a weak input is strengthened in the presence of a strong input, correlated input is not required, and ocular dominance plasticity

occurs in the absence of somatic firing (Crair, Gillespie, & Stryker, 1998; Malach & Van Sluyters, 1989; Mioche & Singer, 1989). Based on the mapping of orientation-tuned inputs (Iacaruso, Gasler, & Hofer, 2017; D. E. Wilson, Whitney, Scholl, & Fitzpatrick, 2016), eye-specific inputs are expected to be intermixed within regions of the dendritic tree, forming functionally distinct compartments. Given that weak inputs cannot drive events at the soma, local dendritic activity will be a central component for plasticity of these compartments. Both cooperative and competitive plasticity rules are likely incorporated to selectively strengthen or weaken individual compartments while maintaining others. We find that binocular matching depends upon inhibition from SST cells, and in the presence of acetylcholine, SST cells can drive branch-specific inhibition and somatic disinhibition. These components provide traction to explore a more comprehensive plasticity mechanism within pyramidal neurons. In hippocampus, synaptic potentiation of weaker inputs cannot be achieved by increasing somatic firing alone, but the combination of local dendritic spikes, cholinergic modulation, and somatic spiking results in branch-specific potentiation (Losonczy, Makara, & Magee, 2008). A mechanism such as this has yet to be investigated in the cortex or within the context of the critical period.

Our data suggest that dendritic inhibition is spatially restricted and specific enough to locally alter thresholds and integration (Jadi, Polsky, Schiller, & Mel, 2012; Polsky, Mel, & Schiller, 2004). Positioned at the apical dendrite, SST cells have nuanced effects across the dendritic tree, with significant consequences for biophysical plasticity mechanisms. SST cells can locally silence synaptic activity, promote on and off-path inhibition, and decouple somatic and dendritic spikes (Gidon & Segev, 2012). These interneurons target the apical dendrite with increasing innervation towards the sealed ends of the neuron, suggesting that functionally their inhibition is powerful (Bloss et al., 2016). It is not known whether SST-mediated inhibition acts locally or globally across a single neuron; however, global inhibition will raise plasticity thresholds so that only the strongest inputs are maintained, and this cannot aide the strengthening of the ipsilateral input (Mel, Schiller, & Poirazi, 2017). Our data resonate with the

only other investigation of the role of SST cell inhibition on dendritic activity, in which the deletion of SST cells decreases independent activity within dendritic compartments (Cichon & Gan, 2015).

It is noteworthy that branch-specific modulation and disinhibition are not unique to the critical period, and may comprise of a fundamental mechanism for plasticity. In adult cortex, the same pattern of dendritic responses emerges during attention-mediated learning (Cichon & Gan, 2015; Kerlin et al., 2018). Therefore, the critical period may not be distinctive by its form of plasticity but by the engagement of cortical circuitry by neuromodulation. On the level of microcircuits, the loss of cholinergic input at SST cells may be a central component in the transition from arousal-based to attention-based plasticity that, respectively, distinguishes the critical period from adulthood. The disinhibition of PV neurons noted here is reminiscent of decreased feedforward inhibition after 1 day of monocular deprivation (Kuhlman et al., 2013), in which layer 2/3 PV cells lose excitation from layer 4, causing pyramidal neuron firing rates to double and ocular dominance to shift. Our data shows that this disinhibitory motif is engaged even when both eyes receive visual input, but via cholinergic circuitry and SST-mediated inhibition. Somatic disinhibition has also been implicated during adult plasticity (Froemke, Merzenich, & Schreiner, 2007; Letzkus et al., 2011). It remains an interesting question as to how somatic disinhibition and branch-specific dendritic activity evoked by SST cells permits the separation or interaction of inputs. Computational modeling suggests that an oscillation of dendritic inhibition at frequencies similar to that seen during cholinergic stimulation can couple dendritic and somatic activity (Li, Morita, Robinson, & Small, 2013), but this has yet to be tested *in vivo*. Our observations of branch-specific dendritic activity combined with increased somatic spiking could foster rapid synaptic potentiation and depotentiation within specific regions across the dendritic tree, characteristic of critical period plasticity.

It is unclear how SST cells are engaged during plasticity in adult cortex. This question is more apt for other cortical regions; in adult visual cortex, once the ipsilateral input has

strengthened, experience maintains these inputs and ocular dominance plasticity is generally more limited, barring the long-term occlusion or removal of an eye (Lehmann & Löwel, 2008). The contribution of SST cells to adult plasticity will depend on the cortical region, layer, and the type of task. In auditory cortex, SST cells increase their activity during passive exposure but are suppressed during the presentation of a salient cue (Abs et al., 2018; Kato, Gillet, & Isaacson, 2015). However, in primary motor cortex, SST cells are engaged during learning and promote branch-specific potentiation in a task without any salient cues (Cichon & Gan, 2015). While the functional circuitry of adult plasticity is still being uncovered within various cortical areas, in the visual cortex, juvenile and adult SST cells differ by their engagement during fluctuations in behavioral state. Without direct cholinergic input in adulthood, SST cells no longer actively contribute to top-down modulation during passive experience and instead appear to largely contribute to bottom-up processing.

6.5 Conclusion

In summary, this thesis defines a transient microcircuit engaged during normal visual experience to drive experience-dependent maturation of the binocular zone. During the critical period, SST cells are sensitive to fluctuations in behavioral state via the cholinergic system, which drives branch-specific dendritic activity as well as somatic disinhibition. Our findings are consistent with the idea that dendritic inhibition can determine plasticity rules locally and dictate the coupling of dendritic and somatic activity. Furthermore, if SST cells are suppressed, inputs which are most sensitive to visual experience are degraded and binocular matching does not develop, indicating that these cells mediate experience-dependent plasticity during the critical period. Our observations advance our understanding of the cell-specific inhibitory drive needed for critical period plasticity and further efforts toward a comprehensive biophysical plasticity mechanism in the developing visual cortex.

6.6 References

Abs, E., Poorthuis, R. B., Apelblat, D., Muhammad, K., Pardi, M. B., Enke, L., … Letzkus, J. J. (2018). Learning-Related Plasticity in Dendrite-Targeting Layer 1 Interneurons. *Neuron*, *100*(3), 684–699.e6. doi:10.1016/j.neuron.2018.09.001

Adesnik, H., Bruns, W., Taniguchi, H., Huang, Z. J., & Scanziani, M. (2012). A neural circuit for spatial summation in visual cortex. *Nature*, *490*(7419), 226–231. doi:10.1038/nature11526

Alitto, H. J., & Dan, Y. (2012). Cell-type-specific modulation of neocortical activity by basal forebrain input. *Frontiers in Systems Neuroscience*, *6*, 79. doi:10.3389/fnsys.2012.00079

Atallah, B. V., Bruns, W., Carandini, M., & Scanziani, M. (2012). Parvalbumin-expressing interneurons linearly transform cortical responses to visual stimuli. *Neuron*, *73*(1), 159–170. doi:10.1016/j.neuron.2011.12.013

Bear, M. F., & Singer, W. (1986). Modulation of visual cortical plasticity by acetylcholine and noradrenaline. *Nature*, *320*(6058), 172–176. doi:10.1038/320172a0

Beierlein, M., Gibson, J. R., & Connors, B. W. (2000). A network of electrically coupled interneurons drives synchronized inhibition in neocortex. *Nature Neuroscience*, *3*(9), 904–910. doi:10.1038/78809

Bloss, E. B., Cembrowski, M. S., Karsh, B., Colonell, J., Fetter, R. D., & Spruston, N. (2016). Structured Dendritic Inhibition Supports Branch-Selective Integration in CA1 Pyramidal Cells. *Neuron*, *89*(5), 1016–1030. doi:10.1016/j.neuron.2016.01.029

Cavanagh, M. E., & Parnavelas, J. G. (1988). Development of somatostatin immunoreactive neurons in the rat occipital cortex: a combined immunocytochemical-autoradiographic study. *The Journal of Comparative Neurology*, *268*(1), 1–12. doi:10.1002/cne.902680102

Chattopadhyaya, B., Di Cristo, G., Higashiyama, H., Knott, G. W., Kuhlman, S. J., Welker, E., & Huang, Z. J. (2004). Experience and activity-dependent maturation of perisomatic GABAergic innervation in primary visual cortex during a postnatal critical period. *The Journal of Neuroscience*, *24*(43), 9598–9611. doi:10.1523/JNEUROSCI.1851-04.2004

Chen, N., Sugihara, H., & Sur, M. (2015). An acetylcholine-activated microcircuit drives temporal dynamics of cortical activity. *Nature Neuroscience*, *18*(6), 892–902. doi:10.1038/nn.4002

Christophe, E., Roebuck, A., Staiger, J. F., Lavery, D. J., Charpak, S., & Audinat, E. (2002). Two types of nicotinic receptors mediate an excitation of neocortical layer I interneurons. *Journal of Neurophysiology*, *88*(3), 1318–1327. doi:10.1152/jn.2002.88.3.1318

Cichon, J., & Gan, W.-B. (2015). Branch-specific dendritic Ca(2+) spikes cause persistent synaptic plasticity. *Nature*, *520*(7546), 180–185. doi:10.1038/nature14251

Cottam, J. C. H., Smith, S. L., & Häusser, M. (2013). Target-specific effects of somatostatin-expressing interneurons on neocortical visual processing. *The Journal of Neuroscience*, *33*(50), 19567–19578. doi:10.1523/JNEUROSCI.2624-13.2013

Crair, M. C., Gillespie, D. C., & Stryker, M. P. (1998). The role of visual experience in the development of columns in cat visual cortex. *Science*, *279*(5350), 566–570. doi:10.1126/science.279.5350.566

Fanselow, E. E., Richardson, K. A., & Connors, B. W. (2008). Selective, state-dependent activation of somatostatin-expressing inhibitory interneurons in mouse neocortex. *Journal of Neurophysiology*, *100*(5), 2640–2652. doi:10.1152/jn.90691.2008

Froemke, R. C., Merzenich, M. M., & Schreiner, C. E. (2007). A synaptic memory trace for cortical receptive field plasticity. *Nature*, *450*(7168), 425–429. doi:10.1038/nature06289

Fu, Y., Tucciarone, J. M., Espinosa, J. S., Sheng, N., Darcy, D. P., Nicoll, R. A., … Stryker, M. P. (2014). A cortical circuit for gain control by behavioral state. *Cell*, *156*(6), 1139–1152. doi:10.1016/j.cell.2014.01.050

Gidon, A., & Segev, I. (2012). Principles governing the operation of synaptic inhibition in dendrites. *Neuron*, *75*(2), 330–341. doi:10.1016/j.neuron.2012.05.015

Goard, M., & Dan, Y. (2009). Basal forebrain activation enhances cortical coding of natural scenes. *Nature Neuroscience*, *12*(11), 1444–1449. doi:10.1038/nn.2402

Gonchar, Y., Wang, Q., & Burkhalter, A. (2007). Multiple distinct subtypes of GABAergic neurons in mouse visual cortex identified by triple immunostaining. *Frontiers in Neuroanatomy*, *1*, 3. doi:10.3389/neuro.05.003.2007

Harwerth, R. S., Smith, E. L., Crawford, M. L., & von Noorden, G. K. (1990). Behavioral studies of the sensitive periods of development of visual functions in monkeys. *Behavioural Brain Research*, *41*(3), 179–198. doi:10.1016/0166-4328(90)90107-P

Iacaruso, M. F., Gasler, I. T., & Hofer, S. B. (2017). Synaptic organization of visual space in primary visual cortex. *Nature*, *547*(7664), 449–452. doi:10.1038/nature23019

Jadi, M., Polsky, A., Schiller, J., & Mel, B. W. (2012). Location-dependent effects of inhibition on local spiking in pyramidal neuron dendrites. *PLoS Computational Biology*, *8*(6), e1002550. doi:10.1371/journal.pcbi.1002550

Kato, H. K., Gillet, S. N., & Isaacson, J. S. (2015). Flexible sensory representations in auditory cortex driven by behavioral relevance. *Neuron*, *88*(5), 1027–1039. doi:10.1016/j.neuron.2015.10.024

Kawaguchi, Y. (1997). Selective cholinergic modulation of cortical GABAergic cell subtypes. *Journal of Neurophysiology*, *78*(3), 1743–1747. doi:10.1152/jn.1997.78.3.1743

Kawaguchi, Y., & Shindou, T. (1998). Noradrenergic excitation and inhibition of GABAergic cell types in rat frontal cortex. *The Journal of Neuroscience*, *18*(17), 6963–6976.

Kerlin, A., Mohar, B., Flickinger, D., MacLennan, B. J., Davis, C., Spruston, N., & Svoboda, K. (2018). Functional clustering of dendritic activity during decision-making. *BioRxiv*. doi:10.1101/440396

Kruglikov, I., & Rudy, B. (2008). Perisomatic GABA release and thalamocortical integration onto neocortical excitatory cells are regulated by neuromodulators. *Neuron*, *58*(6), 911–924. doi:10.1016/j.neuron.2008.04.024

Kuhlman, S. J., Olivas, N. D., Tring, E., Ikrar, T., Xu, X., & Trachtenberg, J. T. (2013). A disinhibitory microcircuit initiates critical-period plasticity in the visual cortex. *Nature*, *501*(7468), 543–546. doi:10.1038/nature12485

Lee, A. M., Hoy, J. L., Bonci, A., Wilbrecht, L., Stryker, M. P., & Niell, C. M. (2014). Identification of a brainstem circuit regulating visual cortical state in parallel with locomotion. *Neuron*, *83*(2), 455–466. doi:10.1016/j.neuron.2014.06.031

Lee, S., Hjerling-Leffler, J., Zagha, E., Fishell, G., & Rudy, B. (2010). The largest group of superficial neocortical GABAergic interneurons expresses ionotropic serotonin receptors. *The Journal of Neuroscience*, *30*(50), 16796–16808. doi:10.1523/JNEUROSCI.1869-10.2010

Lehmann, K., & Löwel, S. (2008). Age-dependent ocular dominance plasticity in adult mice. *Plos One*, *3*(9), e3120. doi:10.1371/journal.pone.0003120

Letzkus, J. J., Wolff, S. B. E., Meyer, E. M. M., Tovote, P., Courtin, J., Herry, C., & Lüthi, A. (2011). A disinhibitory microcircuit for associative fear learning in the auditory cortex. *Nature*, *480*(7377), 331–335. doi:10.1038/nature10674

Levelt, C. N., & Hübener, M. (2012). Critical-period plasticity in the visual cortex. *Annual Review of Neuroscience*, *35*, 309–330. doi:10.1146/annurev-neuro-061010-113813

Li, X., Morita, K., Robinson, H. P. C., & Small, M. (2013). Control of layer 5 pyramidal cell spiking by oscillatory inhibition in the distal apical dendrites: a computational modeling study. *Journal of Neurophysiology*, *109*(11), 2739–2756. doi:10.1152/jn.00397.2012

Losonczy, A., Makara, J. K., & Magee, J. C. (2008). Compartmentalized dendritic plasticity and input feature storage in neurons. *Nature*, *452*(7186), 436–441. doi:10.1038/nature06725

Malach, R., & Van Sluyters, R. C. (1989). Strabismus does not prevent recovery from monocular deprivation: A challenge for simple Hebbian models of synaptic modification. *Visual Neuroscience*, *3*(03), 267–273. doi:10.1017/S0952523800010014

Mel, B.W., Schiller, J., & Poirazi, P. (2017). Synaptic plasticity in dendrites: complications and coping strategies. *Current Opinion in Neurobiology*, *43*, 177-186. doi:10.1016/j.conb.2017.03.012

Mineault, P. J., Tring, E., Trachtenberg, J. T., & Ringach, D. L. (2016). Enhanced spatial resolution during locomotion and heightened attention in mouse primary visual cortex. *The Journal of Neuroscience*, *36*(24), 6382–6392. doi:10.1523/JNEUROSCI.0430-16.2016

Mioche, L., & Singer, W. (1989). Chronic recordings from single sites of kitten striate cortex during experience-dependent modifications of receptive-field properties. *Journal of Neurophysiology*, *62*(1), 185–197. doi:10.1152/jn.1989.62.1.185

Morishita, H., Miwa, J. M., Heintz, N., & Hensch, T. K. (2010). Lynx1, a cholinergic brake, limits plasticity in adult visual cortex. *Science*, *330*(6008), 1238–1240. doi:10.1126/science.1195320

Mrsic-Flogel, T. D., Versnel, H., & King, A. J. (2006). Development of contralateral and ipsilateral frequency representations in ferret primary auditory cortex. *The European Journal of Neuroscience*, *23*(3), 780–792. doi:10.1111/j.1460-9568.2006.04609.x

Muñoz, W., Tremblay, R., Levenstein, D., & Rudy, B. (2017). Layer-specific modulation of neocortical dendritic inhibition during active wakefulness. *Science*, *355*(6328), 954–959. doi:10.1126/science.aag2599

Niell, C. M., & Stryker, M. P. (2010). Modulation of visual responses by behavioral state in mouse visual cortex. *Neuron*, *65*(4), 472–479. doi:10.1016/j.neuron.2010.01.033

Palmer, L. M., Schulz, J. M., Murphy, S. C., Ledergerber, D., Murayama, M., & Larkum, M. E. (2012). The cellular basis of GABA(B)-mediated interhemispheric inhibition. *Science*, *335*(6071), 989–993. doi:10.1126/science.1217276

Pecka, M., Han, Y., Sader, E., & Mrsic-Flogel, T. D. (2014). Experience-dependent specialization of receptive field surround for selective coding of natural scenes. *Neuron*, *84*(2), 457–469. doi:10.1016/j.neuron.2014.09.010

Pfeffer, C. K., Xue, M., He, M., Huang, Z. J., & Scanziani, M. (2013). Inhibition of inhibition in visual cortex: the logic of connections between molecularly distinct interneurons. *Nature Neuroscience*, *16*(8), 1068–1076. doi:10.1038/nn.3446

Pi, H.-J., Hangya, B., Kvitsiani, D., Sanders, J. I., Huang, Z. J., & Kepecs, A. (2013). Cortical interneurons that specialize in disinhibitory control. *Nature*, *503*(7477), 521–524. doi:10.1038/nature12676

Polsky, A., Mel, B. W., & Schiller, J. (2004). Computational subunits in thin dendrites of pyramidal cells. *Nature Neuroscience*, *7*(6), 621–627. doi:10.1038/nn1253

Rasmusson, D. D. (2000). The role of acetylcholine in cortical synaptic plasticity. *Behavioural Brain Research*, *115*(2), 205–218. doi:10.1016/S0166-4328(00)00259-X

Reimer, J., Froudarakis, E., Cadwell, C. R., Yatsenko, D., Denfield, G. H., & Tolias, A. S. (2014). Pupil fluctuations track fast switching of cortical states during quiet wakefulness. *Neuron*, *84*(2), 355–362. doi:10.1016/j.neuron.2014.09.033

Tremblay, R., Lee, S., & Rudy, B. (2016). Gabaergic interneurons in the neocortex: from cellular properties to circuits. *Neuron*, *91*(2), 260–292. doi:10.1016/j.neuron.2016.06.033

Trachtenberg, J. T. (2015). Competition, inhibition, and critical periods of cortical plasticity. *Current Opinion in Neurobiology*, *35*, 44–48. doi:10.1016/j.conb.2015.06.006

Urban-Ciecko, J., Jouhanneau, J.-S., Myal, S. E., Poulet, J. F. A., & Barth, A. L. (2018). Precisely timed nicotinic activation drives SST inhibition in neocortical circuits. *Neuron*, *97*(3), 611–625.e5. doi:10.1016/j.neuron.2018.01.037

Wilson, D. E., Whitney, D. E., Scholl, B., & Fitzpatrick, D. (2016). Orientation selectivity and the functional clustering of synaptic inputs in primary visual cortex. *Nature Neuroscience*, *19*(8), 1003–1009. doi:10.1038/nn.4323

Wilson, N. R., Runyan, C. A., Wang, F. L., & Sur, M. (2012). Division and subtraction by distinct cortical inhibitory networks in vivo. *Nature*, *488*(7411), 343–348. doi:10.1038/nature11347

Wozny, C., & Williams, S. R. (2011). Specificity of synaptic connectivity between layer 1 inhibitory interneurons and layer 2/3 pyramidal neurons in the rat neocortex. *Cerebral Cortex*, *21*(8), 1818–1826. doi:10.1093/cercor/bhq257

Yang, G. R., Murray, J. D., & Wang, X.-J. (2016). A dendritic disinhibitory circuit mechanism for pathway-specific gating. *Nature Communications*, *7*, 12815. doi:10.1038/ncomms12815